

**Polymeric System for Photochemical Generation of H<sub>2</sub>O<sub>2</sub> and Initiator for Photoreduction of Hexavalent Chromium**

by

PaviElle Marie Lockhart

A dissertation submitted to the Graduate Faculty of  
Auburn University  
in partial fulfillment of the  
requirements for the Degree of  
Doctor of Philosophy

Auburn, Alabama  
December 13, 2014

Keywords: photochemistry, peroxide, SPEEK, mechanism, chromium, photoreduction, polymer

Copyright 2014 by PaviElle Marie Lockhart

Approved by

German Mills, Professor of Chemistry  
Rik Blumenthal, Associate Professor of Chemistry  
Joseph V. Ortiz, Molette Professor Chemistry  
Vincenzo Cammarata, Associate Prof. of Chemistry and Associate Dean of Academic Affairs

## Abstract

Stimuli responsive polymers (SRPs) have become a technological advancement in areas of materials, pharmaceuticals, and biomedical applications because the polymers can respond to small changes in the environment which can be physical, chemical, or biochemical stimuli. By incorporating SRPs in fabrics, functions such as wound monitoring, skin-care capabilities, moisture/temperature management, and aesthetic appeal, to name a few, can be achieved. Utilizing light in the field of stimuli-responsive polymers has attracted great attention because of its renewable source of energy and its ability to be localized in time and space. The focus of this work is to show the chemistry of a polymeric system which can be used as a foundation to creating a potentially “smart” polymeric material. Presented in the dissertation is the potential use of a photochemical polymeric system that can utilize its redox reactivity as a means of providing personal and environmental protection.

Macromolecular systems containing reactive species are envisioned to function as protective barriers, such as reactive clothing, which chemically inactivate toxins and pathogens. Protective barriers based on polymeric sensitizers that generate reactive species photochemically are an attractive approach. An advantage of such barriers is their ability to regenerate reactive species by exposure to light. Presented in this dissertation are data obtained from photolysis experiments of crosslinked films from SPEEK/PVA blends. As in previous investigations dealing with photoreactions initiated in solid matrices, SPEEK/PVA films were immersed into air-saturated aqueous solutions during irradiations, because such an arrangement enabled the use

of conventional analytical methods for  $[H_2O_2]$  quantification. Interestingly, the efficiency of peroxide generation was found to be significantly higher than the quantum yield determined for solutions of the polymer blends.

Decontamination is not only a concern centered on the degradation of toxic chemical and biological agents on surfaces of materials and materials used for personal protection, but also for disinfection of water. The polymeric system explored in this dissertation has great potential to treat waste waters contaminated with hexavalent chromium as a filtering membrane. The reduction processes as well as the factors influencing the rates of reaction such as light intensity, buffer concentrations, effects of pH, and effects of initial chromium concentration have been studied in order to get a basic insight into the reduction process of the polymer-assisted photoreduction of hexavalent chromium.

## Acknowledgments

I would like to give all praise and honor to the most high, who has given me this great opportunity. A special thank you is given to Dr. German Mills who has guided me and assisted in this journey on becoming a scientist. Dr. J. V. Ortiz has been an influential inspiration and I am thankful to have had him as my mentor. I would like to also thank Dr. B. Lewis Slaten for his knowledge and advisement. Special thanks is given to my past lab mates; Dr. Brian Little and Dr. Dan Clary for their insight and guidance. I would also like to give special thank you to Dr. Eduardus Duin and Dr. Julie Howe for their time and expertise.

I would also like to thank my family and friends, more specifically; Angela Lockhart, Monique Baker, Phillip Lockhart, Patrice Johnson, Omotunde Dokun, Sharon Sales, and Devan Johnson for their love and never-ending encouragement.

## Table of Contents

Abstract .....	ii
Acknowledgments.....	iv
List of Tables .....	vii
List of Images and Figures.....	viii
List of Abbreviations .....	xii
I. Responsive Polymers .....	1
Introduction .....	1
Light Sensitive Polymers .....	2
Decontaminating Systems .....	3
SPEEK and PVA .....	8
Challenges and Benefits .....	10
References .....	13
II. Photogeneration of H <sub>2</sub> O <sub>2</sub> in Water-Swollen SPEEK/PVA Films .....	18
Introduction .....	18
Experimental .....	20
Results and Discussion .....	26
Conclusion .....	44
Reference .....	45

III. Photochemical Reduction of Hexavalent Chromium in Solutions of SPEEK/PVA .....	48
Introduction .....	48
Experimental .....	50
Results and Discussion .....	53
Conclusions .....	74
Reference .....	75
IV. Further Analysis of Reduction of Cr(VI) in Solutions of SPEEK/PVA .....	79
Introduction .....	79
Experimental .....	81
Results and Discussion .....	84
Conclusions .....	101
Reference .....	102
V. Conclusions .....	104

## List of Tables

Table 3.1 .....	28
-----------------	----

## List of Figures and Images

Figure 1.1 Schematic depiction of a multi-functional polymer that can detoxify chemical and biological warfare agents. ....	4
Figure 1.2 Schematic of SPEEK .....	8
Figure 2.1 Typical illumination vessel of borosilicate glass with a side arm for retrieval of samples. ....	23
Figure 2.2 Left panel: top view representation of the film location in the illumination vessel, where the glass tube served as boundary between the two regions of solution. Right panel: image of the photoreactor containing a solution of methylene blue. Films were located in the light-blue region beneath the top screw cap that is confined by the two meniscuses. ....	24
Figure 2.3 Molecular structure representing a PEEK monomer on the left as well as a sulfonated monomer on the right that includes the hydrogen atom H <sub>s</sub> next to the sulfonic group....	27
Figure 2.4 Plot of mass ratio versus thickness of dry films; swelling performed at neutral pH for films composed of: (◆) 30 wt% SPEEK and 70 wt% PVA, (●) PVA only. The inset shows the swell ratio as a function of the surface area before swelling. Data for films with a dry constant width of 2.4 cm, SPEEK was obtained from Evonik PEEK. ....	31
Figure 2.5 Comparison of the incorporated H <sub>2</sub> O mass versus the estimated volume after swelling for films composed of: (◆) 30 wt% SPEEK and 70 wt% PVA, (●) PVA only. The experimental parameters were described in Figure 2-4. ....	32
Figure 2.6 Optical spectra obtained after treatment with the iodide-molybdate method of samples from an air-saturated solution at pH = 5 in contact with a SPEEK/PVA film photolyzed with 350 nm light, I <sub>0</sub> = 1.4 x 10 <sup>-5</sup> M(hv)/s, for 0, 15, 30, 45, 60, 90 and 120 min. Solutions were diluted by a factor of 6 during the peroxide assay. Inset: plot of [H <sub>2</sub> O <sub>2</sub> ] versus illumination time, slope = 2.9 x 10 <sup>-9</sup> M/s, r <sup>2</sup> = 0.99; SPEEK sample obtained from Victrex PEEK. ....	34
Figure 2.7 Plot of H <sub>2</sub> O <sub>2</sub> formation rates as a function of light intensity from experiments with water-swollen SPEEK/PVA films containing polyketone derived from Evonik (■) and Victrek (●) PEEK. Films exposed to 350 nm photons in air saturated solutions with pH values in the range of 5.5-6. ....	35



Figure 2.8 Comparison of the corrected quantum yields of H <sub>2</sub> O <sub>2</sub> formation versus light intensity for SPEEK/PVA swollen in water with the efficiencies determined for solutions containing both the polyol and the polyketone. (◆) Solution results with Victrex PEEK; data from film experiments using SPEEK derived from Victrex (■), and Evonik PEEK (▲). Irradiations with 350 nm photons in neutral solutions saturated with air. ....	37
Figure 2.9 Dependence of r <sub>c</sub> (H <sub>2</sub> O <sub>2</sub> ) on the pH of air-saturated solution for swollen SPEEK/PVA photolyzed with 350 nm light with I <sub>0</sub> = 1.4 x 10 <sup>-5</sup> M(hv)/s. Experiments with SPEEK derived from Evonik (■) and (●) Victrex PEEK. ....	39
Figure 2.10 Plot of r <sub>c</sub> (H <sub>2</sub> O <sub>2</sub> ) as a function of water content in H <sub>2</sub> O/CH <sub>3</sub> CN mixtures for swollen, crosslinked SPEEK/PVA solid samples; (●) 30 μm thick films, SPEEK derived from Victrex precursor; (□) 30-40 μm thick films, SPEEK derived from Evonik PEEK; (◆) 40-50 μm thick films, SPEEK derived from Evonik precursor. Photolysis with 350 nm light, I <sub>0</sub> = 1.4 x 10 <sup>-5</sup> M(hv)/s. ....	41
Figure 3.1 Concentration of hexavalent chromium species as a function of solution pH of 1 mM total chromium concentration (adopted from reference 17). ....	49
Image 3.1 Illumination vessel used for the reduction of Cr(VI) in polymeric solutions. ....	51
Image 3.2 Illumination vessel for the reduction of Cr(VI) in SPEEK/PVA films. ....	52
Figure 3.2 Emission spectra of 0.7 mM SPEEK and 0.2 mM Cr(VI) in air-free, buffered solutions (pH 5.7). Excitation wavelength, λ= 350 nm and emission λ <sub>max</sub> ≈ 448 nm. ..	55
Figure 3.3 Optical spectra obtained after analysis with the 1,5-diphenylcarbazide (DPC) method on air-saturated, photolyzed solutions at pH = 5.7 containing 0.018 M SPEEK, 0.36 M PVA, and 2.8x10 <sup>-4</sup> M hexavalent chromium. Solution samples were diluted by a factor of 3 during the Cr(VI) assay. Top to bottom: samples irradiated with 350 nm light, where I <sub>0</sub> = 3.5 x 10 <sup>-5</sup> M(hv)/s, for 0 min, 1, 2, 3, 4, 5, 6, 7, 9 min, and no Cr(VI). Inset: Plot of absorbance at 545 nm divided by ε as a function of irradiation time (l = 0.2 cm). ....	57
Figure 3.4 Dependence of rate of reduction for Cr(VI) on phosphate buffer concentration in air-saturated solutions containing 0.018 M SPEEK, 0.36 M PVA, and 3.2 x 10 <sup>-4</sup> M Cr(VI) with pH = 5.6. Irradiations with 350 nm photons (I <sub>0</sub> = 3.5 x 10 <sup>-5</sup> M(hv)/s). ....	59
Figure 3.5 Plot of the reduction of Cr(VI) in buffered 0.36 M PVA solution containing 3.4 x 10 <sup>-4</sup> M Cr(VI) with pH = 5.7. Irradiations with 350 nm photons (I <sub>0</sub> = 3.5 x 10 <sup>-5</sup> M(hv)/s). Inset: first order plot. ....	61
Figure 3.6 Determinations of reduction of Cr(VI) in air saturated solutions of 0.018 M SPEEK/0.36 M PVA containing 2.1 x 10 <sup>-4</sup> M Cr(VI) and 5 mM phosphate buffer at pH 5.7. Irradiations are at various light intensities (I <sub>0</sub> ). Inset: plot of the rate of Cr (VI) reduction as a function of incident I <sub>0</sub> . ....	65

- Figure 3.7 Quantum yield of Cr(VI) reduction dependence on the solution pH. Determinations of reduction rates were carried out using air-saturated, buffered (5 mM) solutions containing: a) 0.018 M SPEEK/ 0.36 M PVA with initial Cr<sup>6+</sup> concentrations of 3.2 x 10<sup>-4</sup> M (◆) and 1 x 10<sup>-3</sup> M (●) and b) 0.36 M PVA with initial Cr<sup>6+</sup> concentrations of 3.2 x 10<sup>-4</sup> M (◆) and 1 x 10<sup>-3</sup> M (●). (I<sub>0</sub> = 3.0 x 10<sup>-5</sup> M(hv)/s). ..... 66
- Figure 3.8 Spectra of photoreduction of Cr(VI) in water-swollen SPEEK/PVA Film. Irradiation of film was conducted in buffered solution of 3.4 x 10<sup>-4</sup> M Cr(VI) with 350 nm photons with intensity of 3 x 10<sup>-5</sup> M(hv)/s and pH was 5.7. [Cr(VI)] was detected by direct analysis of solution (l = 1 cm). Film surface area was 24 cm<sup>2</sup>. *Inset*: Comparison plot of the abs spectra of chromium solution before irradiation and 5.5 hrs after irradiation. .. 71
- Figure 3.9 Photoreduction of Cr(VI) in swollen SPEEK/PVA Film. Irradiation of film was conducted in air-saturated, buffered solution of 3.4 x 10<sup>-4</sup> M Cr(VI) with 350 nm photons (I<sub>0</sub> = 3 x 10<sup>-5</sup> M(hv)/s, pH = 5.7). [Cr(VI)] was detected by direct analysis (l = 1 cm, ε = 1580 cm<sup>-1</sup>M<sup>-1</sup>). *Inset*: First order reduction plot. .... 72
- Image 4.1 Illumination vessel used for detection of Cr(III) formed in SPEEK/PVA solution (10cm cell). ..... 82
- Image 4.2 Illumination vessel used for degassed solutions of SPEEK/PVA and solutions absent of SPEEK. .... 83
- Figure 4.3 Optical spectra obtained after analysis with the 1,5-diphenylcarbazide (DPC) method on degassed, photolyzed solutions at pH = 5.7 containing 0.018 M SPEEK, 0.36 M PVA, and 3.2x10<sup>-4</sup> M hexavalent chromium. Solution samples were diluted by a factor of 3 during the Cr(VI) assay. Top to bottom: samples irradiated with 350 nm light, where I<sub>0</sub> = 3 x 10<sup>-5</sup> M(hv)/s, for 0 min, 0.5, 1, 1.5, 2, 2.5, 3 min, and no Cr(VI). *Inset*: Plot of absorbance at 545 nm divided by ε as a function of irradiation time (l = 0.2 cm). ..... 85
- Figure 4.4 Photoreduction of Cr(VI) in degassed solutions buffered at pH = 5.7 with 5 mM of the phosphate buffer also containing 0.018 M SPEEK and 0.36 M PVA with [Cr(VI)]: 2 x 10<sup>-4</sup> M (■), 4 x 10<sup>-4</sup> M (▲), and 7 x 10<sup>-4</sup> M (●). Photolysis with 350 nm light, and I<sub>0</sub> = 3 x 10<sup>-5</sup> M(hv)/s) ..... 86
- Figure 4.5 Initial rates of HCrO<sub>4</sub><sup>-</sup> photoreduction in degassed 0.36 M PVA solutions free of SPEEK at various Cr(VI) initial concentrations. Illumination of solutions buffered at pH 5.7 with [buffer] = 5 mM containing: ◆ [Cr(VI)] = 0.0179 mM; ■ [Cr(VI)] = 0.16 mM, ▲ [Cr(VI)] = 0.345 mM and ● [Cr(VI)] = 0.467 mM, with 350 nm photons, I<sub>0</sub> = 3 x 10<sup>-5</sup> M(hv)/s. [Cr(VI)] were determined using the DPC method. .... 88
- Figure 4.6 Comparison of quantum yield of Cr(VI) reduction in degassed solutions of 0.018 M SPEEK and 0.36 M PVA (◆), and solutions free of SPEEK with 0.36 M PVA (■) as a function of [Cr(VI)]. Irradiations conducted at pH = 5.7 with 350 nm light (I<sub>0</sub> = 3 x 10<sup>-5</sup> M(hv)/s); line is a guide to the eye. .... 89

- Figure 4.7 Photoreduction of  $\text{HCrO}_4^-$  in air-saturated, solutions of 0.018 M/0.36 M SPEEK/PVA buffered at pH = 5.7 with 5 mM phosphate buffer. a) ■ [Cr(VI)] = 0.28 mM, ◆ [Cr(VI)] = 0.0716 mM; b) ● [Cr(VI)] = 1.3 mM, ▲ [Cr(VI)] = 1.2 mM. Samples irradiated with 350 nm photons with  $I_0 = 3 \times 10^{-5} \text{ M(hv)/s}$ ; [Cr(VI)] determined using the DPC method. .... 91
- Figure 4.8 Determination of initial rates during the photoreduction of Cr(VI) in air-saturated solutions at pH = 5.7 with 0.36 M PVA with 5 mM buffer with 350 nm photons and  $I_0 = 3 \times 10^{-5} \text{ M(hv)/s}$ . [Cr(VI)] were determined by direct analysis. .... 92
- Figure 4.9 Comparison of quantum yield of Cr(VI) reduction in air-saturated solutions at pH = 5.7 of SPEEK/PVA (0.018 M/0.36 M) (◆) and solutions containing 0.36 M PVA but no SPEEK (○) as a function of [Cr(VI)]. Quantum yields for solutions without SPEEK were obtained from initial rates of reduction. Irradiations were conducted with 350 nm light,  $I_0 = 3 \times 10^{-5} \text{ M(hv)/s}$ . .... 92
- Figure 4.10 Double-reciprocal plot resulting from competition analysis of the yields of Cr (VI) reduction as a function of chromate concentration in air-saturated solutions buffered at pH = 5.7 with 0.018 M SPEEK and 0.36 M PVA. Illuminations were conducted with 350 nm light,  $I_0 = 3 \times 10^{-5} \text{ M(hv)/s}$ . .... 93
- Figure 4.11 EPR spectra of Cr(V) signal in degassed polymeric solutions with and without SPEEK (a), and air-saturated solutions with and without SPEEK (b). In degassed solutions, samples were irradiated for 5 minutes; air-saturated solutions were exposed to light for 20 minutes.  $[\text{Cr(VI)}]_i = 6 \times 10^{-4} \text{ M}$ ,  $I_0 = 3 \times 10^{-5} \text{ M(hv)/s}$ . .... 96
- Figure 4.12 Optical measurements of the formation of Cr(III) in air-saturated solutions of 0.018 M SPEEK/0.36 M PVA with initial [Cr(VI)] of  $3.2 \times 10^{-4} \text{ M}$  (pH = 5.7). Illumination times were 0, 1, 2, 3, 4, 5, 8, 12, 24, 27, 30, and 42 minutes ( $l = 10 \text{ cm}$ ,  $\epsilon = 144 \text{ M}^{-1} \text{ cm}^{-1}$ ).  $I_0 = 3 \times 10^{-5} \text{ M(hv)/s}$ . Inset: Plot of evolution of signal at 600 nm. .... 98

## List of Abbreviations

BP	benzophenone
BPK	benzophenylketyl
°C	degree Celsius
cm	centimeter
Cr(III)	chromium 3+ species
Cr(VI)	chromium 6+, $\text{HCrO}_4^-$
$\text{cm}^3$	cubic centimeter
DPC	1-5,diphenylcarbazide
EPR	electron paramagnetic resonance
$E^\circ$	energy potential
$\epsilon$	extinction coefficient
GA	glutaraldehyde
g	grams
h	hour
h $\nu$	photon
I	light intensity
ICP	inductively coupled plasma
L	liters
M	molar concentration
min	minute
$\mu\text{m}$	micrometer
mm	millimeter

nm	nanometer
O.D.	optical density or outer diameter
$\phi$	quantum yield
PVA	poly(vinyl alcohol)
$r_c$	corrected rate
$r_i$	initial rate
SPEEK	sulfonated poly(ether ether ketone)
UV	ultraviolet
Vis	visible
$\lambda$	wavelength

## I. Responsive Polymers

### 1.1 Introduction

Since the discovery of polymers, man has chemically altered the make-up of polymers by using different monomers in order to create a wide range of physical, mechanical, and chemical properties. Research lead by scientists and engineers has created or improved technologies by using newly developed polymers. These developments have been in the form of polymer solutions, gels, films, or hybrids. The replacement of liquid electrolytes with polymer gel electrolytes has been a means to extend the battery lifetimes.<sup>1</sup> Also with the high demand and every-changing advances in visual technology, polymer coatings that transmit light through optic surfaces to increase high contrast and brightness in display devices are materials of significant interest.<sup>2</sup> Even in drug delivery, polymeric nanohybrids are envisioned as systems capable of playing an important role in anti-cancer therapy treatments.<sup>3</sup> Synthetic polymer systems have been constructed to answer the demands for controlled and self-regulated drug delivery systems,<sup>4</sup> coatings that respond and interact with the environment,<sup>5</sup> fibers that mimic the action of muscles,<sup>6</sup> and thin films and nanoparticles for detection applications.<sup>7,8</sup> Stimuli responsive polymers (SRPs) have become a technological advancement in areas of materials, pharmaceuticals, and biomedical applications.

SRPs are polymers that respond to small changes in the environment which can be a) physical, b) chemical, or c) biochemical stimuli. Physical stimuli include the dependence on temperature, light, ionic strength, and electric field, whereas chemical stimuli are principles on pH and the presence of specific ions or solutes. Biochemical stimuli rely on effects from enzymes and metabolites. The potential versatility of polymers prompted researchers to develop smart materials with self-regulated structures and characteristics. Combining graphene with poly(N-isopropylacrylamide) produces a hydrogel that is thermal- and pH-responsive, which

makes them applicable to areas of chemical sensors and potentially in pharmaceutical applications.<sup>9</sup> This dual responsiveness is an example of a type of complexity within a system that provides multiple functions for one area of interest. The textile industry has found many ways to employ SRPs. By incorporating stimuli responsive polymers in fabrics, functions such as wound monitoring, skin-care capabilities, moisture/temperature management, and aesthetic appeal, to name a few, can be achieved.<sup>10</sup> Utilizing light in the field of stimuli-responsive polymers has attracted great attention because of its renewable source of energy and its characteristic to be localized in time and space.

## **1.2 Light Sensitive Polymers**

Polymers sensitive to light can undergo a variety of transformations including, but not limited to isomerization, ionization, homolytic fragmentation, hydrogen abstraction, and redox reactions. In order for polymers to be reactive to light, they must contain chromophores, groups consisting of pi-electron functions, and hetero-atoms having non-bonding, valence-shell electron pairs. In the field of electrochromic displays, light sensitive polymers are used for their redox reactivity. Polyaniline, used for its three distinct oxidation states with different colors and doping response, is an example of a light sensitive polymer that is also synthesized by a photopolymerization method.<sup>11</sup> Polymer synthesis can be a light-induced process, however light can also be used to better understand the redox processes taking place within these polymers. By combining spectroscopic techniques with the redox characteristics of such polymers, scientists are also able to observe the effects of counter ion pairs and defects as charged dopants in electrochromic polymers.<sup>12</sup> Incorporation of reactions of light sensitive polyelectrolytes with

their response to pH, ionic strength, and solvent properties can yield products that are useful to certain industries such as nanotechnology and surface engineering.<sup>13</sup> Although light-induced redox reactions are reversible and more conventional, irreversible photochemical reactions do exist.

The focus of this work is to show the chemistry of a polymeric system which can be used as a foundation to creating a potentially “smart” polymeric material, in other words materials that are able to respond to change in the environment as a stimuli. Presented in the dissertation is the potential use of a photochemical polymeric system that can utilize its redox reactivity as a means of providing personal and environmental protection.

### **1.3 Decontaminating Systems**

There has always been interest in achieving personal protection against exposures to biological and chemical hazards in areas of healthcare, agriculture production, emergency response and military personnel. Efforts have been made toward creating decontaminating materials by incorporating reactive compounds into fabrics.<sup>14,15</sup> These materials are usually made of filters, films, and membranes that inhibit contact with the potentially life-threatening substances. Depending on the hazards to which the personnel are subjected, most personal protective materials are expected to be fire-resistant, durable, light-weight, breathable, impermeable to water, and resistant to extreme temperatures. Scientists have researched and created systems with environmentally safe techniques that protect against biological and chemical agents by providing antimicrobial and decontaminating functions.<sup>14-19,21</sup>



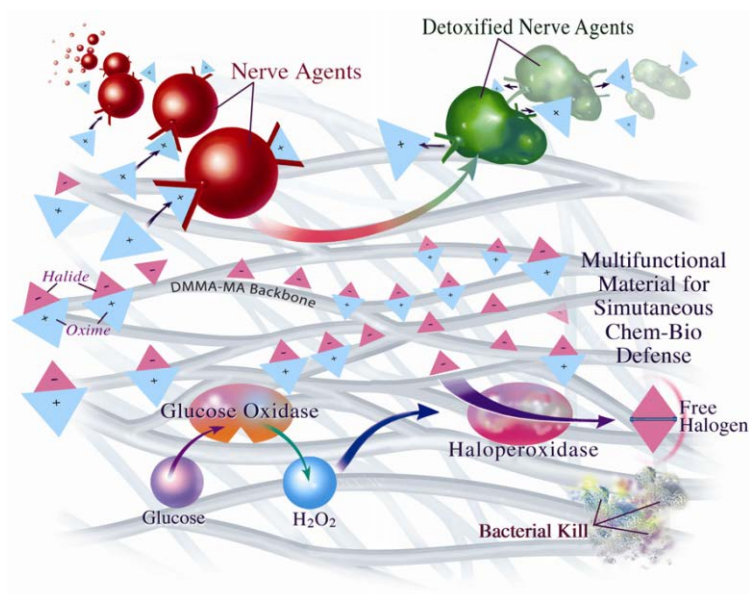


Figure 1.1 is adopted from [16]. Schematic depiction of a multi-functional polymer that can detoxify chemical and biological warfare agents.

Amitai *et al.* have created a material that is capable of deactivating toxic chemicals as well as generate biocidal activity in a multi-functional polymer<sup>16</sup>, illustrated in Figure 1. This work demonstrated that pyridinium aldoximes bound to a polymer backbone can act as a means to guard against organophosphate (OP) toxins, which are known to slowly detoxify OP directly.<sup>17</sup> Positively charged bromine and chlorine ions are used as biocidal halogens. Detoxification of diisopropylfluorophosphate (DFP), an example of an OP, reached a maximum of 85% in thirty minutes in solution. Although the system looks promising, the reactivity of the aldoximes is pH and dose-dependent. Without the additions of glucose, peroxidase, and buffered solutions, decontamination has proven to take hours. When the multi-functional polymers were electrospun with polyurethane to create a fibrous mat, it took over 7 hours for only 75% DFP to degrade. This showed a decrease in the rate of detoxification of DFP. Bringing together multiple

approaches in one material is a novel idea, however the complexity and restrictions of such systems usually outweigh the benefits resulting from the bactericidal and detoxification abilities. Interests are centered on systems that are stable, effective, inexpensive, and nontoxic to the environment.

Recyclability is one of the goals Gutch *et al* achieved in order to create a system that is able to decontaminate VX, a sulfur-containing organophosphate toxin, without producing toxic by-products.<sup>18</sup> They were able to overcome the drawbacks and limitations of decontaminating agents, such as long reactivity time and the use of hazardous solvents. Sulfonated poly(styrene-*co*-divinylbenzene) sulfonamide polymeric beads were used to decontaminate 100 % *O,S*-diethylmethyl phosphonothiate (OSDEMP), a simulant of VX, by oxidizing the bivalent sulfur atoms in a process of chlorination to produce nontoxic ethyl methylphosphonate. Gutch *et al* successfully detoxified OSDEMP by using polymeric beads after 15 minutes, and generated a technique that is recyclable, inexpensive, efficient, and easy to use.

Despite using functional groups on a polymer backbone to decontaminate chemical (CWA) and biological (BWA) warfare agents, chemically-generated reactive agents are another approach for decontamination. In this approach, the reactive species will help eliminate the spread of harmful agents by ensuring the surface of the material is constantly self-cleaning. Formulating a system capable of generating singlet oxygen ( $^1\text{O}_2$ ) by photosensitization of zinc octaphenoxypthalocyanine (ZnOPPC) bonded to polymer films and fibers resulted in systems that can degrade simulants of sulfur mustard gas (HD) and methylphosphonothioic acid (VX).<sup>19</sup> With  $^1\text{O}_2$  quantum yields between 0.6-0.78, these systems reacted to induce complete oxidative degradations and their performance lasted between 8 and 16 hours without damage to the polymer matrices. Singlet oxygen has also been proven to be a potent antibacterial agent.<sup>20</sup> The

ability to integrate highly reactive functionalities into a material for self-decontamination could also eliminate the need for post-contamination cleaning. However application and compatibility challenges arise when different formulations (i.e., liquids, and foams) and surfaces (ex. concrete, glass, steel, and polymer) are considered.<sup>21</sup> More importantly the relevant question is, are these self-decontaminating materials efficient enough to be worn as personal protection?

A common problem with personal protective barriers is that the materials are not “breathable”, that is, they do not enable diffusion of gases and water. Even though the main objective is to impair free passage of biological threats and toxic chemicals through the protective membranes, the lack of exchange of water vapor can lead to heat exhaustion by the user after extended times.<sup>22</sup> A possible solution is to consider a reactive composite film containing hydrophilic, hydroxylated, ionic liquid polymers and a basic zeolite; such combination should allow free motion of water vapor while, at the same time, block the transport of a chemical agent through the protective barrier.<sup>23</sup> Although this film composite shows promise in degrading toxic chemicals, a complete mechanistic study has not been possible due to the heterogeneous nature of the organic liquid polymer. The problem lies within the characteristics of the water molecules transported within the film. The nucleophilic oxygen atoms on the polymer groups undergo hydrogen bonding with the transported water molecules leading to a suppression of the degradation reactions of the targeted toxic chemical.<sup>24</sup> As it is important to have water diffuse through the membrane, it is equally imperative to gain understanding about the influence that the diffusion process has on the chemistry within the film.

Decontamination is not only a concern centered on the degradation of toxic chemical and biological agents on surfaces of materials and materials used for personal protection, but also for disinfection of water. The need for adequate access to clean water and sanitation is one of the

world's most persistent problems. Toxic metal ions, such as Hg(II), Pb(II), Cd(II), Ag(I), Ni(II), and Cr(VI) are released into the environment in large quantities by an array of industrial activities. However, recovery and removal of waste metals can potentially resolve issues of resource conservation and metal pollution prevention. Chemical oxidative treatments and advanced oxidative processes (AOPs), including photolysis with UV light, reactions with hydrogen peroxide, Fenton reactions, ozonation, heterogeneous catalysis, and any combination of these, are known for their ability to produce reactive oxygen species (ROS) that oxidize and mineralize nearly any organic contaminant.<sup>25-27</sup> Semiconductor photocatalysis, one method for water treatment, has proven to have synergism between photocatalytic oxidation and reduction processes in water contaminated with metals and organic chemicals.<sup>28</sup> However for these processes, it is important to be aware of the influence of pH, and the concentrations of metal ions, catalysts, and organic species because the degradation efficiencies are affected within the treated water.<sup>29,30</sup> As a potential electron acceptor, even the presence of dissolved oxygen can inhibit the photocatalytic reduction of certain metal ions.<sup>31</sup>

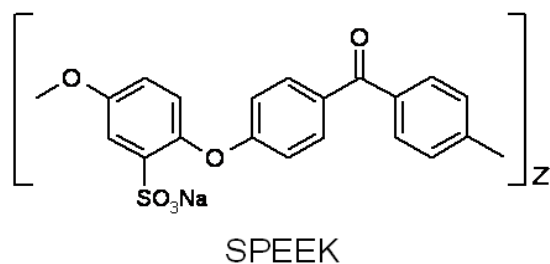
The polymeric system explored in this dissertation can be used as a means of personal protection by photochemically generating hydrogen peroxide in films, serving as a self-decontaminating polymer, and has great potential to treat waste waters contaminated with heavy metals. The films would contain benzophenone (BP) moieties, and can be used as a photo-induced anti-bacterial agent on polymeric materials and fabrics, in addition to decomposing certain chemicals.<sup>14,32</sup> Through irradiation with UVA light, the excited BP ( $n \rightarrow \pi^*$ ) transitions to triplet state through intersystem crossing, and forms a radical by hydrogen-abstracting from a neighboring polymer or from the bacteria membrane. In the presence of oxygen, BP radicals produce ROS, such as superoxide radical ( $O_2^{\bullet-}$ ), hydroperoxyl radical ( $HO_2^{\bullet}$ ), and hydrogen

peroxide ( $\text{H}_2\text{O}_2$ ), therefore oxidizing a variety of pollutants. Hydrogen peroxide is used as a biocide for disinfection, sterilization, and antiseptics.<sup>33</sup> Hence, incorporation of these properties into films will enable the surface to become “self-cleaning” and allow for degradation of toxic chemicals and heavy metals.

#### 1.4 SPEEK and PVA

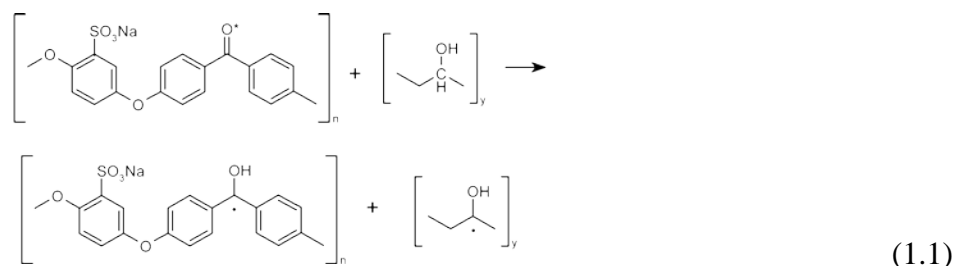
Poly(ether ether ketone) (PEEK) is an insoluble polymer that exhibits high chemical, thermal, and mechanical stabilities. Adding sulfonate groups to PEEK alters its chain conformation and reduces available crystalline domains; however, the additions increase molecular bulkiness.<sup>34</sup> Sulfonated poly(ether ether ketone) (SPEEK) is water-soluble when fully sulfonated. Figure 2 illustrates the molecular structure of SPEEK.

Figure 2



SPEEK is known for its proton conducting capabilities<sup>35</sup>, however few have reported on its light-induced reactivity. In our research group, SPEEK has been utilized as a photoinitiator for photochemical redox reactions. Poly(vinyl alcohol) (PVA) has characteristics, such as optical transparency and flexibility as a solid, that are critical for the photoreactions in the material. SPEEK paired with PVA is analogous to their monomeric counterparts, benzophenone and isopropyl alcohol. Upon absorption of 350 nm photons, an excited state of SPEEK has been

proven to react with poly(vinyl alcohol), PVA, to generate reducing  $\alpha$ -hydroxy radicals (also known as benzophenyl ketyl radicals) along the backbone of SPEEK polymer chains.<sup>36</sup>



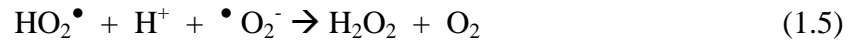
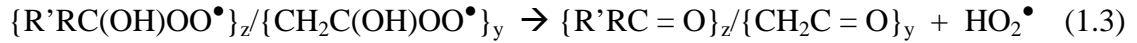
Reaction 1 illustrates the reaction after excitation of SPEEK polymer chain to its triplet state,  $\{^3\text{SPEEK}^*\}$ , which subsequently abstracts a hydrogen from PVA to produce  $\alpha$ -hydroxy radicals in SPEEK/PVA systems. With oxidation potentials of -1.3 V, similar to its analog benzophenone, the SPEEK radicals are capable of reducing  $\text{Ag}^+$ ,  $\text{Au}^{3+}$ , and  $\text{Cu}^{2+}$  and forming crystallites in both solutions and films.<sup>36</sup> This polymeric system shows possible use in areas demanding synthesis of metal nanoparticles. SPEEK/PVA solutions were also used to prove dehalogenation of carbon tetrachloride by reactions with generated radicals.<sup>37</sup> The system has demonstrated great potential to be used in decontamination methods appropriate for personal protection against exposure to toxic chemicals. With intentions to be used as a “self-cleaning system”, irradiated solutions of SPEEK/PVA have been discovered to also produce hydrogen peroxide as a by-product in the formation of SPEEK radicals in the presence of air.<sup>38</sup> Films of SPEEK/PVA have been previously produced and are capable of redox reactions<sup>39</sup>, however a detailed look into the effects of environmental factors on the formation of hydrogen peroxide will be discussed further in this dissertation.

## 1.5 Challenges and Benefits for Dissertation

Deactivating toxic organic chemicals is an area of constant interest which has been driven due to the sense of urgency created by world events. Photochemical reactivity in chemical degradation is a very useful and efficient technique for organic pollutants which can be a simple and cost efficient process<sup>40</sup>; it also can produce safer products from the degradation of toxic compounds, remove trace elements, and destroy viruses and bacteria.<sup>41</sup> TiO<sub>2</sub> and ZnO are known for their photocatalytic reactivity involving photogenerated reactive oxygen species by using UV light.<sup>42,43</sup> Also, carbonyl-containing macromolecules that photochemically produce singlet oxygen, <sup>1</sup>O<sub>2</sub>, have yielded polymeric photooxidizers (O<sub>2</sub><sup>•-</sup> and H<sub>2</sub>O<sub>2</sub>) useful for degrading undesired chemicals,<sup>44</sup> and for inactivation of pathogens.<sup>45</sup>

In systems containing ketones, alcohol, water, and air, hydrogen peroxide can form by photochemical reactions producing ketyl radicals. Ketones exhibit high quantum yields of intersystem crossing to excited triplet states and then abstract hydrogen atoms from neighboring alcohols creating alcohol radicals and ketyl radicals.<sup>46-48</sup> Oxygen scavenges these radicals and photochemically generates superoxide radicals (O<sub>2</sub><sup>•-</sup>) eventually leading to H<sub>2</sub>O<sub>2</sub> formation. Photoinduced oxygen uptake was measured in solutions containing benzophenone in air-saturated 2-propanol/water (1:100 vol.) with yields (φ<sub>-O<sub>2</sub></sub>) of 0.6.<sup>49</sup> SPEEK/PVA solutions have produced hydrogen peroxide in a synchronous fashion with the consumption of oxygen, and with no formation of stable organic peroxides.<sup>38</sup> The proposed mechanism for the reduction of oxygen by SPEEK<sup>•</sup> and PVA<sup>•</sup>, and the formation of H<sub>2</sub>O<sub>2</sub> in air-saturated solution is:





where  $\{CH_2C^\bullet OH\}_y$  and  $\{R'RC^\bullet OH\}_z$  represents the  $\alpha$ -hydroxy radicals of PVA and SPEEK, respectively. Oxygen reacts with PVA radicals by formation of peroxy radicals thereby decaying through elimination of hydroperoxyl radicals ( $HO_2^\bullet$ ,  $k = 700 \text{ s}^{-1}$ ) or superoxide ( $\bullet O_2^-$ ).<sup>50</sup> Reactions are to occur likewise with  $\alpha$ -hydroxy radicals of SPEEK. Hydrogen peroxide was produced by disproportionation reactions with  $HO_2^\bullet$  and  $\bullet O_2^-$ , yet aided by the fast deprotonation of the hydroperoxyl radicals ( $pK_a = 4.8$ ).<sup>51</sup> The measurements for  $H_2O_2$  formation in solution have proved to be an easy task compared to the measured peroxide generated within polymer films.

There is one challenge associated with measuring photochemically generated  $H_2O_2$  in SPEEK/PVA films. This challenge was to quantitatively measure the formation of peroxide produced within the film without altering the photochemical reactions occurring during illumination. The most reasonable idea was to conduct the illuminations in a water-swollen state since PVA is known to absorb water from air as a function of ambient temperature. Preparations of SPEEK films and membranes have been performed predominantly by casting of the solution on a glass plate and crosslinking by thermal treatment.<sup>52,53</sup> Films of blended SPEEK and PVA chains will be expected to swell as a function of water uptake due to the PVA chains.<sup>54</sup> To the



best of our knowledge, hydrogen peroxide measurements have not been conducted in water-swollen polymeric films however; Shiraishi *et al* have quantitatively measured  $H_2O_2$  photocatalytically-generated by  $TiO_2$  substrates in water by using peroxidase enzyme while taking into account the effect of film-diffusional resistance.<sup>55</sup> Therefore, this study allows for a new way to measure peroxide generated within water-swollen polymeric films.

In fact, this polymeric system will prove beneficial in several ways. Primarily, films comprised of SPEEK/PVA will have more SPEEK radicals to produce  $H_2O_2$  because the decay rate of the radicals is more than three orders of magnitude smaller than that in solution.<sup>36,39</sup> In solid state, the radicals have low mobility and disproportionation products are reduced, thereby increasing the longevity of the radicals within a film as opposed to solution. Secondly, the formation of peroxide will increase, and a highly concentrated presence of peroxide in an area of film will be utilized as a secondary means of protection against harmful compounds with SPEEK radicals being primary in direct sunlight. Incorporation of this film into fabrics will allow for self-decontamination as a means of personal protection. Finally, a technique is presented which enables extraction of peroxide from films as a standard in a spectrophotometric measurement.

As stated before, the polymeric system explored in this dissertation can be used as a means of personal protection by photochemically generating hydrogen peroxide in films, and thereby serve as a self-decontaminating polymer. Also, the reduction potential of SPEEK radicals produced in polymeric solution and films will be used to reduce hexavalent chromium, and eliminate its presence from contaminated waters.

## References

- 1) Li, G.; Li, Z.; Zhang, P.; Zhang, H.; Wu, Y. Research on a Gel Polymer Electrolyte for Li-ion Batteries. *Pure Appl. Chem.* **2008**, *80* (11) 2553-2563.
- 2) Li, X.; Gao, J.; Xue, L.; Han, Y. Porous Polymer Films with Gradient-Refractive-Index Structure for Broadband and Omnidirectional Antireflection Coatings. *Adv. Funct. Mater.* **2010**, *20*, 259-265.
- 3) Prakash, S.; Malhotra, M.; Shao, W.; Tomaro-Duchesneau, C.; Abbasi, S. Polymeric Nanohybrids and Functionalized Carbon Nanotubes as Drug Delivery Carriers for Cancer Therapy. *Adv. Drug Delivery Rev.* **2011**, *63*, 1340-1351.
- 4) Bawa, P.; Pillay, V.; Choonara, Y.E.; du Toit, L.C. Stimuli-Responsive Polymers and Their Applications in Drug Delivery. *Biomed. Mater.* **2009**, *4*, 1-15.
- 5) Feng, W.; Patel, S.H.; Young, M-Y.; Xanthos, M. Smart Polymeric Coatings: Recent Advances. *Adv. in Polym. Technol.* **2007**, *25* (1) 1-13.
- 6) Takashima, Y.; Hatanaka, S.; Otsubo, M.; Nakahata, M.; Kakuta, T.; Hashidzume, A.; Yamaguchi, H.; Harada, A. Expansion- Contraction of Photoresponsive Artificial Muscle Regulated by host-Guest Interactions. *Nat. Commun.* **2012**, *3*, 1270.
- 7) Barrett, C.; Mermut, O.; Yager, K. Thin Films of Light- Responsive Polymers for Sensing and Surface Patterning. *Proc. SPIE.* **2003**, *5053*, 51-60.
- 8) Hu, J.; Liu, S. Responsive Polymers for Detections and Sensing Applications: Current Status and Future Developments. *Macromol.* **2010**, *43* (20) 8315-8330.
- 9) Sun, S.; Wu, P. A One-Step Strategy for Thermal- and pH-Responsive Graphene Oxide Interpenetrating Polymer Hydrogel Networks. *J. Mater. Chem.* **2011**, *21*, 4095-4097.
- 10) Hu, J.; Meng, H.; Li, G.; Ibekwe, S.I. A Review of Stimuli-Responsive Polymers for Smart Textile Applications. *Smart Mater. Struct.* **2012**, *21*, 1-23.
- 11) de Barros, R.A.; Areias, M.C.C.; de Azevedo, W.M. Conduction Polymer Photopolymerization Mechanism; The Role of Nitrate Ions (NO<sub>3</sub><sup>-</sup>). *Synth. Met.* **2010**, *160*, 61-64.
- 12) Domagala, W.; Palutkiewicz, D.; Cortizo-Lacalle, D.; Kanibolotsky, A.L.; Skabara, P.J. Redox Doping Behaviour of Poly(3,4-ethylenedithiophene)- The Counterion Effect. *Opt. Mater.* **2011**, *33*, 1405-1409.
- 13) Xu, F.J.; Su, F.B.; Deng, S.B.; Yang, W.T. Novel Stimuli-Responsive Polyelectrolyte Brushes. *Macromol.* **2010**, *43*, 2630-2633.

- 14) Sun, G.; Hong, K.H. Photo-Induced Antimicrobial and Decontamination Agents: Recent Progress in Polymer and Textile Applications. *Text. Res. J.* **2013**, *83*(5), 532-542.
- 15) Zhu, J.; Bahramian, Q.; Gibson, P.; Schreuder-Gibson, H.; Sun, G. Chemical and Biological Decontamination Functions of Nanofibrous Membranes. *J. Mater. Chem.*, **2012**, *22*, 8532-8540.
- 16) Amitai, G.; Murata, H.; Anderson, J.D.; Koepsel, R.R.; Russell, A.J. Decontamination of Chemical and Biological Warfare Agents with a Single Multi-functional Material. *Biomater.*, **2010**, *31*, 4417-4425.
- 17) Terrier, F.; Rodriguez, D.P.; Le Guevel, E.; Moutiers, G. Revisiting the Reactivity of Oximate Alpha -Nucleophiles with Electrophilic Phosphorus Centers. Relevance to Detoxification of Sarin, Soman and DFP Under Mild Conditions. *Org. Biomol. Chem.*, **2006**, *4* (23), 4352-63.
- 18) Gutch, P.K.; Singh, R.; Acharya, J. *N,N*-Dichloro Poly(styrene-*co*-divinyl benzene) Sulfonamide Polymeric Beads: An Efficient and Recyclable Decontaminating Reagent for *O,S*-Diethyl Methyl Phosphonothiolate, a Simulant of VX. *J. Appl. Polym. Sci.*, **2011**, *121*, 2250-2256.
- 19) Gephart, III, R.T.; Coneski, P.N.; Wynne, J.H. Decontamination of Chemical-Warfare Agent Simulant by Polymer Surfaces Doped with the Singlet Oxygen Generator Zinc Octaphenoxyphthalocyanine. *Appl. Mater. Interfaces*, **2013**, *5*, 10191-10200.
- 20) McCluskey, D.M.; Smith, T.N.; Madasu, P.K.; Coumbe, C.E.; Mackey, M.A.; Fulmer, P.A.; Wynne, J.H.; Stevenson, S.; Phillips, J.P. Evidence for Singlet-Oxygen Generation and Biocidal Activity in Photoresponsive Metallic Nitride Fullerene- Polymer Adhesive Films. *Appl. Mater. Interfaces*, **2009**, *1* (4), 882-887.
- 21) Love, A.H.; Bailey, C.G.; Hanna, M.L.; Hok, S.; Vu, A.K.; Reutter, D.J.; Raber, E. Efficacy of Liquid and Foam Decontamination Technologies for Chemical Warfare Agents on Indoor Surface. *J. Hazard. Mater.*, **2011**, *196*, 115-122.
- 22) Smith, N.; Roberson, C. Chemical/Biological Protective Garments and Laminates. US Patent 7,937,772, May 10, 2011; *Scifinder Scholar*.
- 23) Hudiono, Y.C.; Miller, II, A.L.; Gibson, P.W.; LaFrate, A.L.; Noble, R.D.; Gin, D.L. A Highly Breathable Organic/Inorganic Barrier Material that Blocks the Passage of Mustard Agent Simulants. *Ind. Eng. Chem. Res.*, **2012**, *51*, 7453-7456.
- 24) Kanyi, C.W.; Doetschman, D.C.; Schulte, J.T. Nucleophilic Chemistry of X-Type Faujasite Zeolites with 2-Chloroethyl Sulfide (CEES), a Simulant of Common Mustard Gas. *Microporous Mesoporous Mater.*, **2009**, *124*, 232-235.
- 25) a) Malato, S.; Fernandez-Ibanez, P.; Maldonado, M.I.; Blanco, J.; Gernjak, W. Decontamination and Disinfection of Water by Solar Photocatalysis: Recent Overview and

Trends. *Catal. Today*, **2009**, *147*, 1-59. b) Malato, S.; Blanco, J.; Caceres, J.; Fernandez-Alba, A.R.; Aquera, A.; Rodriguez, A. Photocatalytic Treatment of Water-soluble Pesticides by Photo-Fenton and TiO<sub>2</sub> Using Solar Energy. *Catal. Today*, **2002**, *76*, 209-220. c) Robert, D.; Malato, S. Solar Photocatalysis: A Clean Process for Water Detoxification. *Sci. Total Environ.*, **2002**, *291*, 85-97. d) Malato, S.; Blanco, J.; Vidal, A.; Alarcon, D.; Maldonado, M.I.; Caceres, J.; Gernjak, W. Applied Studies in Solar Photocatalytic Detoxification: An Overview. *Solar Energy*, **2003**, *75*, 329-336.

26) Pera-Titus, M.; Garcia-Molina, V.; Banos, M.A.; Gimenez, J.; Esplugas, S. Degradation of Chlorophenols by Means of Advanced Oxidative Processes: A General Review. *Appl. Catal. B: Environ.*, **2004**, *47*, 219-256.

27) Legrini, O.; Oliveros, E.; Braun, A.M. Photochemical Processes for Water Treatment. *Chem. Rev.*, **1993**, *93*, 671-698.

28) Prairie M.R.; Evans, L.R.; Stange, B.M.; Martinez, S.L. An Investigation of TiO<sub>2</sub> Photocatalysis for the Treatment of Water Contaminated with Metals and Organic Chemicals. *Environ. Sci. Technol.*, **1993**, *27*, 1776-1782.

29) Liu, Y.; Deng, L.; Chen, Y.; Wu, F.; Deng, N. Simultaneous Photocatalytic Reduction of Cr(VI) and Oxidation of Bisphenol A Induced by Fe(III)-OH Complexes in Water. *J. Hazard. Mater. B*, **2007**, *139*, 399-402.

30) Chong, M.N.; Jin, B.; Chow, C.W.K.; Saint, C. Recent Developments in Photocatalytic Water Treatment Technology: A Review. *Water Res.*, **2010**, *44*, 2997-3027.

31) Chen, D.; Ray, A.K. Removal of Toxic Metal Ions from Wastewater by Semiconductor Photocatalysis. *Chem. Eng. Sci.*, **2001**, *56*, 1561-1570.

32) Hong, K.H.; Gang, S. Photocatalytic Functional Cotton Fabrics Containing Benzophenone Chromophoric Groups. *J. Appl. Polym. Sci.*, **2007**, *106*, 2661-2667.

33) McDonnell, G.; Denver, R. Antiseptics and Disinfectants: Activity, Action, and Resistance. *Clin. Microbiol. Rev.*, **1999**, *12* (1), 147-179.

34) Jin, X.; Bishop, M.T.; Ellis, T.S.; Karasz, F.E. A Sulfonated Poly(aryl Ether Ketone). *Br. Polym. J.* **1985**, *17* (1), 4-10.

35) a) Padmavathi, R.; Sangeetha, D. Design of Novel SPEEK-based Proton Exchange Membranes by Self-Assembly Method for Fuel Cells. *Ionics*. **2013**, *19*, 1423-1436. b) An Efficient Proton Conducting Electrolyte Membrane for High Temperature Fuel Cell in Aqueous-Free Medium. *J. Membr. Sci.* **2014**, *450*, 389-396. c) Zhao, Y.; Tsuchida, E.; Choe, Y.K.; Ikesholi, T.; Barique, M.A.; Ohira, A. Ab Initio Studies on the Proton Dissociation and Infrared Spectra of Sulfonated Poly(ether ether ketone) (SPEEK) Membranes. *Phys. Chem. Chem. Phys.* **2014**, *16*, 1041-1049.

- 36) Korchev, A.S; Shulyak, T.S.; Slaten, B.L.; Mills, G. Sulfonated Poly(Ether Ether Ketone)/Poly(Vinyl Alcohol) Sensitizing System for Solution Photogeneration of Small Ag, Au, and Cu Crystallites. *J. Phys. Chem. B.* **2005**, *109*, 7733-7745.
- 37) Black II, J.R. Redox Reactions in Polymeric Systems. Ph.D. Dissertation, Auburn University, State University, AL, May 2011.
- 38) Little, B.K.; Lockhart, P.; Slaten, B.L.; Mills, G. Photogeneration of H<sub>2</sub>O<sub>2</sub> in SPEEK/PVA Aqueous Polymer Solutions. *J. Phys. Chem. A.* **2013**, *117*, 4148-4157.
- 39) Korchev, A.S.; Konovalova, T.; Cammarata, V.; Kispert, L.; Slaten, L.; Mills, G. Radical-Induced Generation of Small Silver Particles in SPEEK/PVA Polymer Films and Solutions: UV-Vis, EPR, and FT-IR Studies. *Langmuir*, **2006**, *22*, 375-384.
- 40) Dwivedi, A.H.; Pande, U.C. Photochemical Degradation of Halogenated Compounds. *Sci. Rev. Chem. Commun.*, **2012**, *2* (1), 41-65.
- 41) Gaya, U.I.; Abdullah, A.H. Heterogeneous Photocatalytic Degradation of Organic Contaminants over Titanium Dioxide: A Review of Fundamentals, Progress, and Problems. *J. Photochem. Photobiol. C: Photochem. Rev.*, **2008**, *9*, 1-12.
- 42) Pal, B.; Sharon, M. Photocatalytic Formation of Hydrogen Peroxide Over Highly Porous Illuminated ZnO and TiO<sub>2</sub> Thin Film. *Toxicol. Environ. Chem.*, **2000**, *78*, 233-241.
- 43) Yan, G.; Chen, J.; Hua, Z. Roles of H<sub>2</sub>O<sub>2</sub> and OH radical in Bactericidal Action of Immobilized TiO<sub>2</sub> Thin-Film Reactor: An ESR Study. *J. Photochem. Photobiol. A: Chem.*, **2009**, *207*, 153-159.
- 44) (a) Nowakoska, M.; Kepczynski, M.; Szczubialka, K. New Polymeric Photosensitizers. *Pure Appl. Chem.* **2001**, *73*, 491-495. (b) Nowakoska, M.; White, B.; Guillet, J. E. Studies of the Antenna Effect in Polymer Molecules. 12. Photochemical Reactions of Several Polynuclear Aromatic Compounds Solubilized in Aqueous Solutions of Poly(sodium styrenesulfonate-co-2-vinylnaphthalen). *Macromol.*, **1989**, *22*, 2317-2324.
- 45) Ji, E.; Corbitt, T. S.; Parthasarathy, A.; Schanze, K. S.; Whitten, D. G. Light and Dark-Activated Biocidal Activity of Conjugated Polyelectrolytes. *ACS Appl. Mater. Interfaces*, **2011**, *3*, 2820-2829.
- 46) Testa, A.C. The Effect of Light Intensity at 318 nm on the Photochemical Disappearance of Benzophenone in Isopropyl Alcohol. *J. Phys. Chem.*, **1963**, *67*, 1341-1343.
- 47) Schuster, D.I.; Karp, P.B. Photochemistry of Ketones in Solution LVIII: Mechanism of Photoreduction of Benzophenone by Benzhydrol. *J. Photochem.*, **1980**, *12*, 333-344.
- 48) Akiyama, K.; Sekiguchi, S.; Tero-Kubota, S. Origin of an Absorptive Electron Spin Polarization Observed in Photochemical Hydrogen Abstraction Reaction by Benzophenone Derivatives. CW and Pulsed EPR Studies. *J. Phys. Chem.*, **1996**, *100*, 180-183.

- 49) Gorner, H. Oxygen Uptake and Involvement of Superoxide Radicals upon Photolysis of Ketones in Air-saturated Aqueous Alcohol, Formate, Amine or Ascorbic Acid Solutions. *Photochem. Photobiol.*, **2008**, 82, 801-808.
- 50) Ulanski, P.; Bothe, K.; Rosiak, J.M.; von Sonntag, C. OH-Induced Crosslinking and Strand Breaking of Poly(vinyl alcohol) in Aqueous Solution in the Absence and Presence of Oxygen. A Pulse Radiolysis and Product Study. *Macromol. Chem. Phys.* **1994**, 195, 1443-1461.
- 51) Bielski, B.H.; Cabelli, D.E.; Arudi, R.L.; Ross, A.B. Reactivity of  $\text{OH}_2/\text{O}_2^-$  Radicals in Aqueous Solution. *J. Phys. Chem. Ref. Data*, **1985**, 14, 1041-1100.
- 52) Huang, R.Y.M.; Shao, P.; Feng, X.; Burns, C.M. Pervaporation Separation of Water/Isopropanol Mixture Using Sulfonated Poly(ether ether ketone) (SPEEK) Membranes: Transport Mechanism and Separation Performance. *J. Membr. Sci.*, **2001**, 192, 115-127.
- 53) Mikhailenko, S.D.; Wang, K.; Kaliaguine, S.; Xing, P.; Robertson, G.P.; Guiver, M.D. Proton Conducting Membranes based on Cross-linked Sulfonated Poly(ether ether ketone) (SPEEK). *J. Membr. Sci.*, **2004**, 233, 93-99.
- 54) Hodge, R.M.; Edward, G.H.; Simon, G.P. Water Absorption and States of Water in Semicrystalline Poly(vinyl alcohol) Films. *Polym.*, **1996**, 37(8), 1371-1376.
- 55) Shiraishi, F.; Kawanishi, C. Effect of Diffusional Film on Formation of Hydrogen Peroxide in Photocatalytic Reactions. *J. Phys. Chem. A*, **2004**, 108, 10491-10496.

## II. Photogeneration of H<sub>2</sub>O<sub>2</sub> in Water-Swollen SPEEK/PVA Polymer Films

### 2.1 Introduction

Photosensitive polymers remain a subject of investigation in view of their capacity to employ light as an energy source for initiating reactions. Much of the available knowledge pertains the ability of these polymers to transform themselves via photoprocesses, which have resulted in important scientific and technological advances.<sup>1-3</sup> Macromolecules able to initiate transformations of other compounds are of interest because polymeric sensitizers can, in principle, be made compatible with both fluid and solid matrices. For instance, polymers containing benzophenone (BP) as a sensitizer can generate singlet oxygen, <sup>1</sup>O<sub>2</sub>, and enable to incorporate oxygen-containing functionalities into organic compounds in solution.<sup>4</sup> Solid-state initiators of various photoreactions including oxidations have been obtained through binding of BP to polystyrene beads.<sup>5</sup> Polymeric sensitizers that generate <sup>1</sup>O<sub>2</sub> have been used to induce oxidation of toxic chemicals.<sup>6</sup> Macromolecular systems containing reactive species are envisioned to function as protective barriers, such as reactive clothing, which chemically inactivate toxins and pathogens.<sup>7</sup> “Self-cleaning fabrics” that utilize enzymes to degrade organophosphorus compounds are examples of reactive clothing.<sup>8</sup> Protective barriers based on polymeric sensitizers that generate reactive species photochemically are an attractive alternative approach. An advantage of such barriers is their ability to regenerate the reactive species by exposure to light. Macromolecular systems containing sensitizers that photogenerate <sup>1</sup>O<sub>2</sub> as the reactive species have been proven to be effective for the inactivation of pathogens;<sup>9</sup> fabrics and fibers containing crosslinked BP have also been reported to exhibit antibacterial capabilities upon irradiation.<sup>10</sup>

Utilization of  $\text{H}_2\text{O}_2$  as a reactive species in protective barriers seems worth considering given that several chemical warfare agents can be degraded efficiently by means of methodologies based on the peroxide as the active ingredient.<sup>11</sup> Furthermore,  $\text{H}_2\text{O}_2$  exhibits an effective biocidal activity against a wide spectrum of organisms and spores.<sup>12</sup> Generation of hydrogen peroxide has been demonstrated upon exposing solutions of flavins to light in the presence of air but these photosensitizers degraded during the photoreactions.<sup>13</sup>  $\text{H}_2\text{O}_2$  was generated with a quantum yield efficiency of 0.01 during illumination of porphyrins deposited on polymer films in contact with aqueous solutions containing oxygen.<sup>14</sup> While a higher quantum yield of 0.08 was obtained in analogous studies performed with swollen methacrylates containing anthraquinone (AQ) as a photosensitizer,  $\text{H}_2\text{O}_2$  formed mainly via a slow post-irradiation process.<sup>15</sup> Photolysis of swollen iminodiacetic acid resins containing adsorbed tris(2,2'-bipyridine)ruthenium(II) ions as sensitizers were also investigated but the efficiency of  $\text{H}_2\text{O}_2$  generation was not reported.<sup>16</sup> Recently, blends of poly(vinyl alcohol), PVA, and the sodium salt of sulfonated poly(ether etherketone), SPEEK, have been shown to produce  $\text{H}_2\text{O}_2$  with an initial quantum yield ( $\phi_i(\text{H}_2\text{O}_2) = 0.02$  upon exposure to 350 nm light in air-saturated aqueous solutions.<sup>17</sup> The blends were conceived to function as polymeric analogues of the well-known BP/2-propanol photosystem in which a benzophenone triplet ( $n, \pi^*$ ) excited state forms  $\alpha$ -hydroxy radicals (or benzophenyl ketyl, BPK, radical) via H-atom abstraction from alcohol molecules.<sup>18</sup> Earlier results supported such an interpretation since illumination of the blends generated  $\alpha$ -hydroxy radicals of SPEEK (or SPEEK $\bullet$ ).<sup>19</sup> These strongly reducing radicals (oxidation potential between -1.2 and -1.4 V<sup>19b</sup>) were involved in the  $\text{O}_2$  reduction that photogenerated  $\text{H}_2\text{O}_2$ .

The previous study on peroxide photogeneration was carried out utilizing solutions of the polymer blends to avoid the problems associated with product quantification from reactions



taking place in solid samples such as films.<sup>17</sup> Although useful mechanistic information on the peroxide formation was obtained, a more realistic evaluation of the ability of SPEEK/PVA blends to serve as protective barriers necessitated quantitative information about the ability of blend films to photogenerate H<sub>2</sub>O<sub>2</sub>. Presented in this chapter are data obtained from photolysis experiments of crosslinked films from SPEEK/PVA blends. As in previous investigations dealing with photoreactions initiated in solid matrices,<sup>13-16</sup> SPEEK/PVA films were immersed into air-saturated aqueous solutions during irradiations, because such an arrangement enabled the use of conventional analytical methods for [H<sub>2</sub>O<sub>2</sub>] quantification. Interestingly, the efficiency of peroxide generation was found to be significantly higher than the quantum yield determined for solutions of the polymer blends.

## 2.2 Experimental

Poly(vinyl alcohol), 99+% hydrolyzed with an average molar mass of  $8.9-9.8 \times 10^4$  g/mol as well as ammonium molybdate (VI) tetrahydrate, dimethyl sulfoxide (d<sub>6</sub>) and glutaraldehyde (GA, 25% wt solution) were obtained from Sigma Aldrich. Potassium iodide, potassium hydrogen phthalate, potassium dihydrogen phosphate, sodium tetraborate (decahydrate), sodium hydroxide, methanol (HPLC Grade), sulfuric acid, perchloric acid, acetonitrile (HPLC Grade) and hydrogen peroxide (30% v/v) were purchased from Fisher Scientific. All solutions were prepared with water purified using a Millipore Milli-Q Biocel system. Samples of poly(ether ether ketone), PEEK, with an average molar mass of  $4.5 \times 10^4$  g/mol were provided as gifts by Evonik and Victrex, or acquired from Polysciences. PEEK from Evonik or Victrex was received as sheets, which were cut into strips, followed by grinding into a powder and then drying under vacuum at 100 °C for 6 h. The Polysciences material consisted of pellets coated with 0.01% of

calcium stearate that needed cleaning before processing. After grinding the pellets, the resulting powder was soaked in deionized water for one hour, washed three times by vacuum filtration with THF and also with hexanes, followed by drying as described before.<sup>19</sup> Unless stated otherwise, most experiments were performed at room temperature.

Large batches (~ 150 g) of Victrex PEEK were sulfonated using the method described earlier,<sup>19b</sup> which consisted of heating at 50 °C under stirring a suspension of the polymer powder in concentrated H<sub>2</sub>SO<sub>4</sub> for several days. These suspensions were further stirred at room temperature until complete dissolution of the polymeric material was achieved. Sulfonation of PEEK from Evonik or Polysciences used smaller batches (~10 g) dispersed in H<sub>2</sub>SO<sub>4</sub> at a concentration of 30% w/v of the dried powders. These dispersions were heated at 50-55 °C under constant stirring for up to 10 days; the resulting product was a sodium salt of sulfonated PEEK (called SPEEK) that was isolated as before.<sup>19b</sup> Due to the smaller amount of PEEK treated, complete dissolution (indicating substantial sulfonation) was noticed after a few days of reaction. Characterization of the SPEEK samples via standard <sup>1</sup>H and <sup>13</sup>C NMR methods used DMSO-*d*<sub>6</sub> solutions containing 3-8% w/w of SPEEK with tetramethylsilane (TMS) as an internal standard. FTIR measurements were carried out with SPEEK powder in KBr pellets; elemental analysis on SPEEK sodium salt was performed by Atlantic Microlab, Atlanta, GA.

Crosslinked SPEEK/PVA films were prepared using glutaraldehyde (GA) as the crosslinking agent following a slight modification of the previous casting method.<sup>19a</sup> SPEEK and PVA aqueous solutions with concentrations of 1.5 and 3.6% w/v, respectively, together with a 1% (0.1 M) GA yielded films consisting of 30/70 SPEEK/PVA wt% (after neglecting the small amount of glutaraldehyde incorporated). The lower reactant concentrations enabled preparation of films with a more reproducible and uniform thickness while also allowing accessing a wider

range of thicknesses. Unless otherwise stated, irradiations were performed on films with a thickness of 50 ( $\pm 6$ )  $\mu\text{m}$ . The dimensions and weight of the dry films were determined by means of a ruler, a digital micrometer (Mitutoyo 0-1”), and a balance (Pioneer), respectively.

Experiments were carried out to measure the uptake of water during swelling of crosslinked films in the absence of light. For that purpose, individual films were immersed in petri dishes containing  $\text{H}_2\text{O}$ ; equilibration swelling was reaching in less than 1 h. The swollen films were then collected on a filter paper and the increase in mass was determined gravimetrically. Water uptakes were expressed in terms of the mass ratio (MR) defined as:

$$\text{MR} = (W_s - W_d) / W_d \quad (2.1)$$

where  $W_s$  is the weight of swollen films and  $W_d$  is the weight of dried films determined before swelling. The length and width of the swollen films were measured with a ruler. Thicknesses of swollen films were estimated based on the increase in surface areas of films.

Photolyses took place in a Rayonet 100 circular illuminator that used sixteen RPR-3500Å lamps to produce photons with  $\lambda = 350 \pm 15 \text{ nm}$ . The light intensity ( $I_0$ ) was determined with the Amberchrome 540 chemical actinometer.<sup>20</sup> All illuminations were performed in duplicate under constant stirring; uniform exposure of the samples was achieved by placing a photoreactor at the center mid-height position within of the cavity of the illuminator, where the temperature was 29 °C. Shown in Figure 2-1 is an image of an irradiation vessel made from borosilicate glass. The overall length of the photoreactor (from base to top of glass opening)



**Figure 2-1.** Typical illumination vessel of borosilicate glass with a side arm for retrieval of samples.

amounts to 140 mm with a width at the base of 55 mm. Fitted on top of the vessel is an Ace-Thread glass adaptor # 25 with an outer diameter of 31.5 mm, which includes a nylon bushing cap (inner diameter = 26 mm). Screwing this cap serves to secure inside the photoreactor a glass tube (outer diameter = 25 mm, length = 100 mm) with the aid of an o-ring. The top of the glass tube was terminated in a small opening. A side arm with an Ace-Thread glass adaptor # 7, equipped with a cap possessing a small opening sealed with a rubber septum, serve to retrieve aliquots of the solutions. SPEEK/PVA films were placed between the inner surface of the vessel and the outer surface of the vertically secured glass tube. In this way the films were held in a fully extended position without applying excessive pressure on them. The films were subsequently swollen (1 h) with aqueous solutions to ensure their equilibrium volume was reached. This procedure avoided extensive manipulation of the somewhat fragile swollen films.

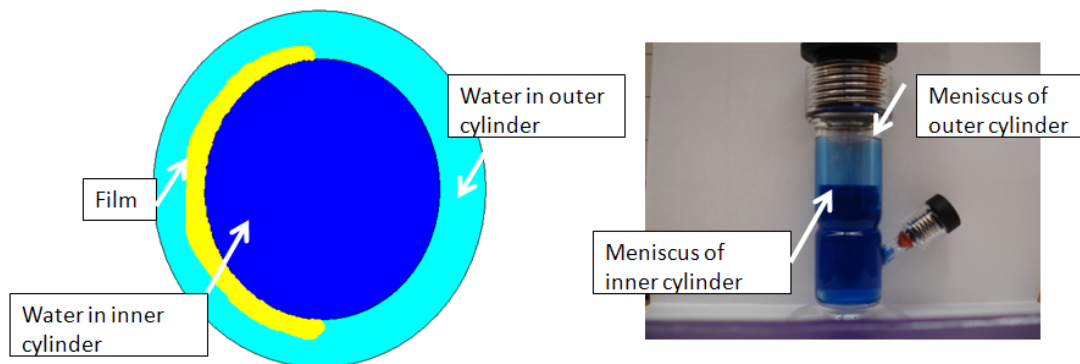


**Figure 2-2.** Left panel: top view representation of the film location in the illumination vessel, where the glass tube served as boundary between the two regions of solution. Right panel: image of the photoreactor containing a solution of methylene blue. Films were located in the light-blue region beneath the top screw cap that is confined by the two menisci.

The left panel of Figure 2-2 is a top view representation of the film position inside the photochemical reactor. Presented in the right panel is an image of a vessel with a film immersed in a methylene blue (MB) solution. The light blue region on the photoreactor top identifies the film location since the path length there is smaller than below the tube held vertically inside the vessel. Tests with MB solutions showed that diffusion of the dye to SPEEK/PVA films occurred in about 3 s under constant stirring. These results ensured that any  $\text{H}_2\text{O}_2$  photogenerated inside the swollen films quickly diffused into the solution present in the photochemical vessel. The photochemical reactor was closed prior to illumination and the pressure was equilibrated against air by means of needle punctured through the septum located top opening. Small aliquots of the photolyzed solutions were retrieved during illumination through the side arm using gas-tight syringes (Hamilton) for subsequent  $\text{H}_2\text{O}_2$  analysis.

Optical spectra were recorded on a Shimadzu UV-Vis 2501PC spectrophotometer. NMR data were collected on a Bruker Avance 400 MHz instrument whereas FTIR spectra were

acquired by means of a Shimadzu IR-Prestige-21 spectrometer.  $[H^+]$  was determined via a Radiometer PHM95 pH/ion meter equipped with an Accumet pH electrode. The following buffer solutions ( $\sim 10^{-3}$  M) were employed to maintain a desired  $[H^+]$  during illuminations: potassium hydrogen phthalate and NaOH (pH 5), potassium dihydrogen phosphate and NaOH (pH 6 and 7), and finally sodium tetraborate and HCl (pH 9 and 10). To achieve a value of pH 4, a solution of perchloric acid and NaOH was prepared ( $\sim 10^{-3}$  M). Hydrogen peroxide concentrations were quantified by means of the spectrophotometric molybdenum-triiodide method.<sup>21</sup> Aliquots of the illuminated solutions were mixed with 1 mL of a potassium biphthalate solution and 1 mL of a mixture containing KI,  $(NH_4)_2MoO_4$  and NaOH in a 1 cm quartz optical cell, followed by dilution to 3 mL. A small correction of the optically determined  $[H_2O_2]$ , that accounted for the decrease in solution volume due to the sample withdrawal from the photochemical reactor, yielded the formation rate,  $r(H_2O_2)$ . Evaluation of the rates of peroxide photogeneration *inside* the films used the dilution factor,  $D_c$ , which corrects for the dilution resulting when  $H_2O_2$  diffused from the swollen solids into the solution. This modification used the equation:

$$r_c(H_2O_2) = D_c \times r(H_2O_2) \quad (2.2)$$

where  $r_c(H_2O_2)$  corresponds to the corrected rate of peroxide formation within the film and  $D_c = V(\text{solution})/V(\text{film})$ , where  $V(\text{solution})$  is the solution volume (33 mL) and  $V(\text{film})$  represents the volume of the swollen film. Quantifications of  $[H_2O_2]$  via the  $I_3^-$  procedure exhibited a typical error of < 10% in water but deviations of 35% were noticed during photolysis of the SPEEK/PVA films. Such large deviations were also observed during the peroxide photogeneration in SPEEK/PVA solutions and are probably a result of the heterogeneous nature of the polymeric photochemical systems. Estimation of quantum yields of  $H_2O_2$  formation,

$\phi(\text{H}_2\text{O}_2)$ , was considered useful in order to compare the photochemical efficiency of the films with that of SPEEK/PVA solutions determine previously.<sup>17</sup> However, efforts to determine  $\phi(\text{H}_2\text{O}_2)$  were complicated by uncertainties concerning the amount of photons absorbed by the polymer films. While the chemical actinometer accounts for the photon flux entering the photoreactor, the polymer films covered only a fraction of the internal surface area of the vessel. Thus, the flux of photons absorbed by the films was estimated using the equation:

$$I_c = I_o \times SA_f \quad (2.3)$$

where  $I_c$  is the corrected intensity of photons absorbed by the films and  $SA_f$  corresponds to the ratio of surface area of swollen film and vessel. Evaluation of the corrected quantum efficiencies of peroxide generation were obtained from the relationship  $\phi_c(\text{H}_2\text{O}_2) = r_c(\text{H}_2\text{O}_2) / I_c$ . The resulting values are just rough estimates (probably lower limits) given the difficulties associated with determining precisely the surface area and volume of the swollen films, and also because losses of photons due to scattering at the interfaces of the polymeric solids were not accounted for.

### 2.3 Results and Discussion

Sulfonation of PEEK samples from Evonik and Polysciences was carried out at a smaller scale than the procedure employed previously for the poly(ether etherketone) material from Victrex. The reason for this change was the long processing times, of several weeks, required by the original procedure. Treatment of PEEK samples in sulfuric acid as described in the Experimental section lasted between 1 and 10 days. Samples treated for only 24 hours did not

completely dissolve in hot water indicating that very little sulfonation took place. The degree of sulfonation (D.S.) was determined via elemental analysis and also utilizing NMR determinations as proposed recently.<sup>21</sup> This method uses the signal intensity due to the H atom next to the sulfonic group, denoted as H<sub>s</sub> and centered at 7.5 ppm vs TMS).

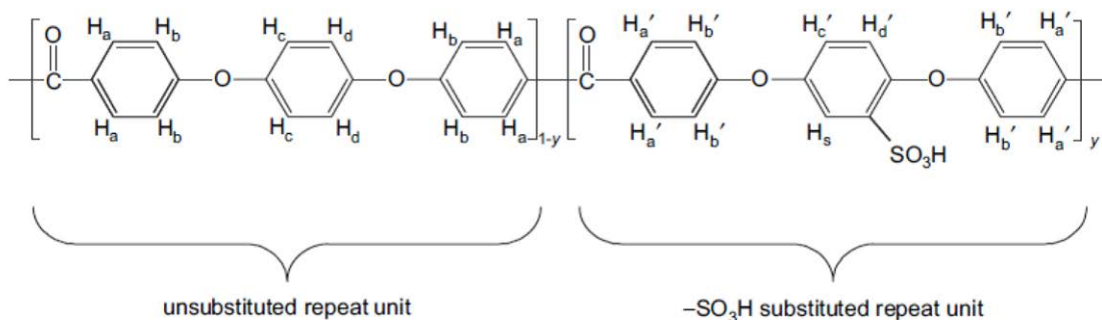


**Figure 2-3.** Molecular structure representing a PEEK monomer on the left as well as a sulfonated monomer on the right that includes the hydrogen atom H<sub>s</sub> next to the sulfonic group.

Figure 2-3 shows a molecular structure identifying the position of such H atom in the SPEEK chain. Approximate D.S. values can be obtained from analysis of the <sup>1</sup>H NMR spectra using the following equation:

$$\frac{\text{Peak area (H}_s\text{)}}{\Sigma \text{Peak area (H}_x\text{)}} = \frac{y}{12-2y} \quad (2.4)$$

where the term  $\Sigma \text{Peak area (H}_x\text{)}$  corresponds to the summation of the integrated areas of all the H signals. D.S. is then obtained via multiplication of  $y$  by 100. More accurate D.S. values were obtained via elemental analysis of the C, H and S composition of the polymer samples. D.S. based on the elemental analysis was calculated using the equation:  $\text{D.S.} = (S_E \times 100) / S_T$ , where  $S_E$  and  $S_T$  are the experimental and theoretical values for the sulfur content per monomer of SPEEK.



Summarized in Table 3-1 are the results obtained from the different analytical methods, and includes theoretical compositions for dry SPEEK sodium salt as well as for polymers containing one and two water molecules per monomer, denoted as SPEEK•H<sub>2</sub>O and SPEEK•2H<sub>2</sub>O, respectively in the table.

**Table 3-1 Elementary Compositions and Degree of Sulfonation of SPEEK Samples**

Sample	Days of Sulfonation	Carbon %	Hydrogen %	Sulfur %	D.S. <sup>1</sup> H NMR	D.S. Elemen. Analysis
PEEK	0	79.2	4.2	0	---	0
100% SPEEK*	---	58.2	2.8	8.2	---	100
SPEEK•H <sub>2</sub> O*	---	55.9	3.2	7.8	---	95.1
SPEEK•2H <sub>2</sub> O*	---	53.5	3.5	7.5	---	91.5
1	1	---	---	---	47	---
2	3	---	---	---	74.2	---
3	4	54	3.6	7.4	83.5	90.2
4	5	---	---	---	80.56	---
5	7	54	3.4	7.4	88.7	90.2
6	10	---	---	---	84.83	---

\*Theoretical values

The experimental data for a PEEK sample coincided exactly with the theoretical composition. Elemental analysis was also performed for PEEK samples sulfonated for 4 and 7 days. The results of Table 3-1 indicate that the experimental compositions matched well the one predicted for SPEEK•2H<sub>2</sub>O.

A D.S. value of 90.2 % was determined for both samples, indicating that sulfonation was essentially completed in about 4 days. Somewhat lower D.S. values (83.5 and 88.7%) resulted from the NMR determinations of the PEEK samples treated for 4 and 7 days. Nevertheless, these results support the conclusion that about 4 days were required to complete the sulfonation process. The NMR and FTIR results for PEEK samples treated for up to 7 days were in good agreement with the characterization data reported in earlier studies.<sup>22,23</sup> However, some of the characteristic NMR signals of SPEEK were no longer detected in the case of PEEK samples sulfonated for 10 days, indicating that polymer decomposition took place due to such extensive exposure to H<sub>2</sub>SO<sub>4</sub> at the higher temperature.

Investigation of photochemical reactions taking place on solid matrices is made difficult by the problems associated with quantification of the reactions products. A procedure employed frequently involves carrying illuminations of films in contact with aqueous solutions. H<sub>2</sub>O can then transport products into the solution, enabling the use of conventional analytical methods.<sup>14-</sup>  
<sup>16</sup> An analogous method was adopted in the present investigation that took advantage of the swelling behavior of crosslinked SPEEK/PVA films in aqueous systems. Photolysis of the dry films yields SPEEK radicals that remain stable inside the solid matrices for hours even in the presence of air.<sup>19</sup> One reason for the unusual stability of the highly reducing  $\alpha$ -hydroxy SPEEK• is because their fast decay via radical-radical reactions is inhibited due to chain crosslinking in the solid substrates. Another reason is that the O<sub>2</sub> solubility in solid polymers depends on the

amount of H<sub>2</sub>O present, which is very low in the case of PVA.<sup>24</sup> In contrast, no SPEEK• was detected during irradiation of air-saturated SPEEK/PVA solutions as reaction of the radicals with O<sub>2</sub> formed H<sub>2</sub>O<sub>2</sub>.<sup>17</sup> Utilization of swollen crosslinked SPEEK/PVA films was anticipated to allow fast O<sub>2</sub> transport into the polymer matrices. This, in turn, was expected to enable photogeneration of H<sub>2</sub>O<sub>2</sub> and then peroxide diffusion to the solution bulk. Also, film dimensions increased during swelling, allowing them to cover a larger area of the photochemical reactor and, therefore, to absorb a greater fraction of the impinging photon flux.

Efforts were made to characterize the swelling behavior of the films given that incorporation of water into the polymeric solids was anticipated to play a role in the photochemical processes. Figure 2-4 depicts the amount of water incorporated as a function of the thickness determined for SPEEK/PVA solid materials before swelling. An increase in mass by a factor of 3 was noticed for the thinnest films (20-30 μm) together with a slight decrease to about 2.5 as the thickness increased to 70 μm. Blank experiments performed with films containing PVA also seemed to follow the same trend although only data for the high end of thickness was available. These results are in agreement with the mass increases of 300% reported for films of PVA and for PVA blends with poly(acrylic acid), PAA, that were lightly crosslinked with GA.<sup>25,26</sup> The inset shows the swell ratio, that is the quotient of areas for the swollen dry states, is plotted versus the film surface area prior to swelling. A fairly constant ratio of 2 persists in the range of surface areas between 6 and 9 cm<sup>2</sup> but falls to 1.7 for the largest films. The limited data available for films containing only PVA seem to follow a trend analogous as that for the SPEEK/PVA blend. Overall, the results depicted in Figure 2-4 guarantee that water was absorbed by the film when they were located in the illumination vessel. The data indicates that swelling of the SPEEK/PVA films is controlled mainly by the ability of PVA to uptake water since the polyol is the main

component of the solid blends. In addition, swelling of SPEEK/PVA films decreases slightly as the surface area and thickness of the films increases.

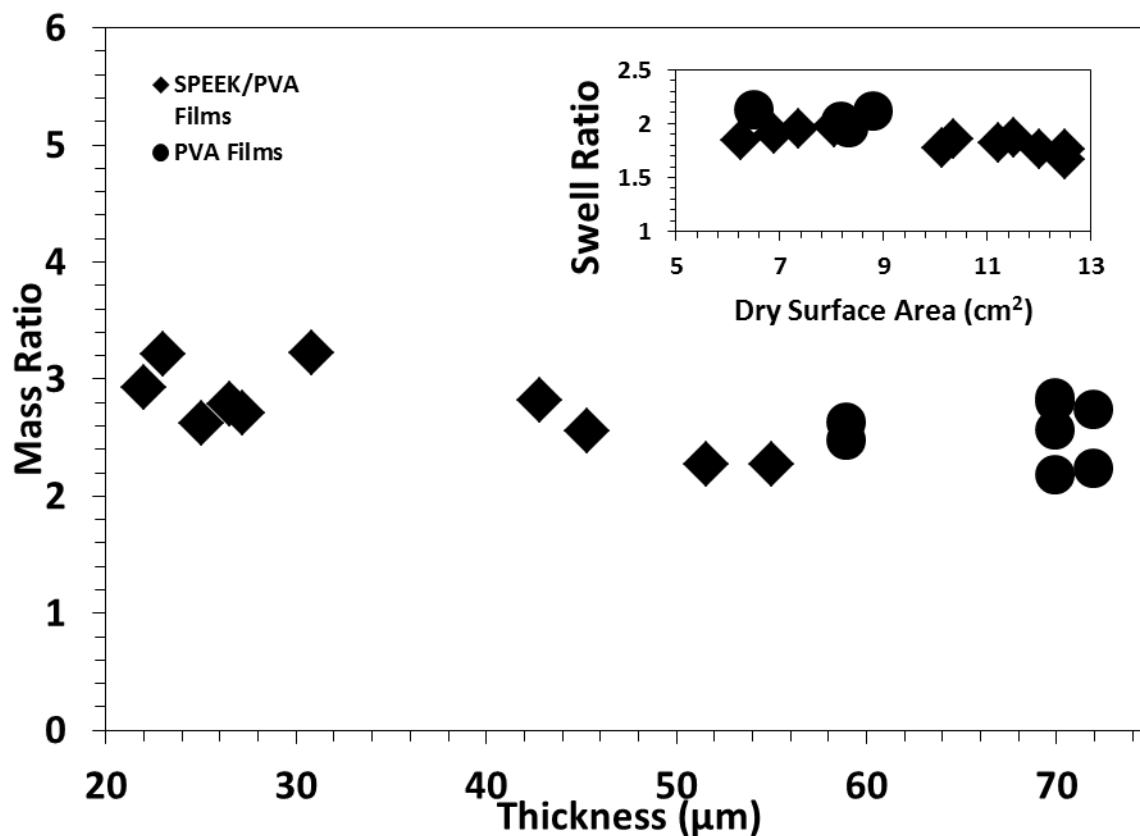


**Figure 2-4.** Plot of mass ratio versus thickness of dry films; swelling performed at neutral pH for films composed of: (◆) 30 wt% SPEEK and 70 wt% PVA, (●) PVA only. The inset shows the swell ratio as a function of the surface area before swelling. Data for films with a dry constant width of 2.4 cm, SPEEK was obtained from Evonik PEEK.

An interesting question related to the swelling experiments concerns the volume change that resulted from the uptake of H<sub>2</sub>O. Although determination of the surface area of swollen films was straightforward, evaluation of the thickness change was quite difficult. In most cases the thickness increased by a factor of approximately  $\sqrt{2}$ . Thus, a volume change by a factor of  $2\sqrt{2}$

is obtained under the assumption that the surface area also increased by a factor of two, a reasonable approximation based on the results included in the inset of Figure 2-4. Since the density of water equals to  $1 \text{ g/cm}^3$ , a 1:1 relationship between the amount of  $\text{H}_2\text{O}$  incorporated and the estimated film volume was anticipated. Such expectation was based on the apparently reasonable supposition that the film volume corresponded basically to the volume of water incorporated. Presented in Figure 2-5 is a plot of the mass of water incorporated during swelling as a function of the estimated volume for films containing only PVA and for SPEEK/PVA films.

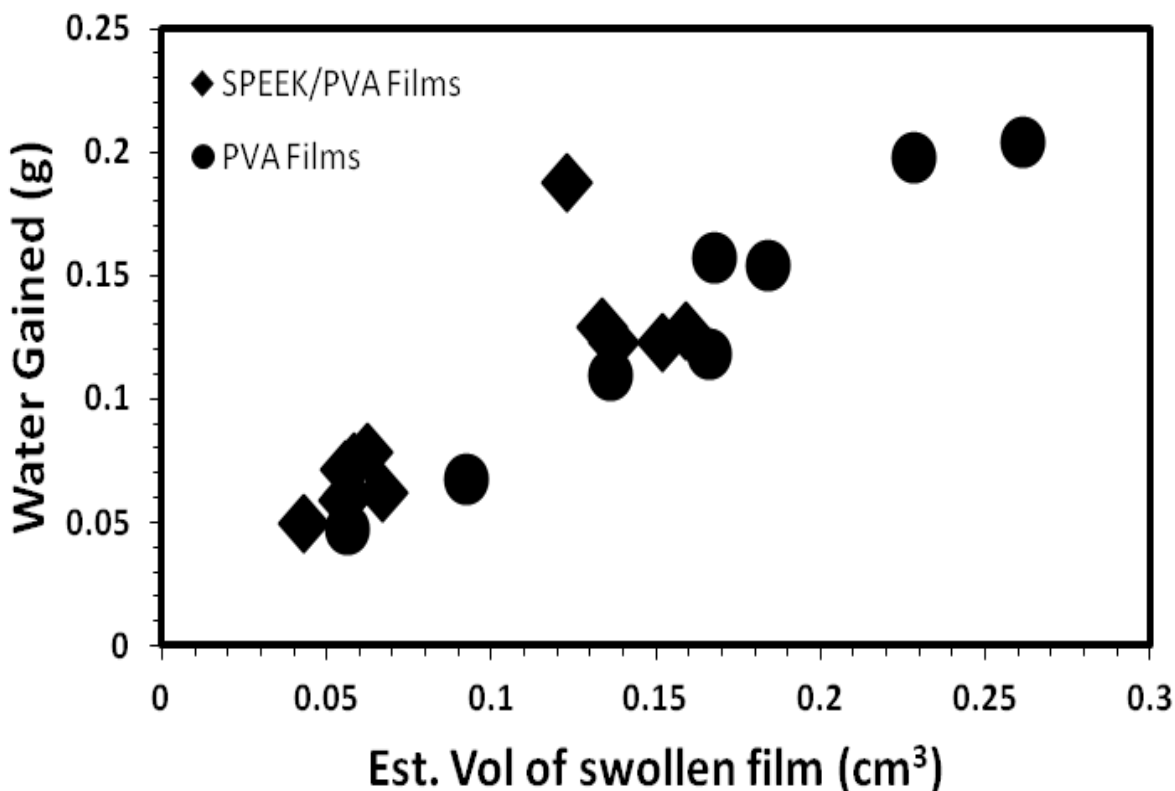


**Figure 2-5.** Comparison of the incorporated  $\text{H}_2\text{O}$  mass versus the estimated volume after swelling for films composed of: (◆) 30 wt% SPEEK and 70 wt% PVA, (●) PVA only. The experimental parameters were described in Figure 2-4.

As mentioned before, the volume of the swollen films was estimated based on the increases in surface area and thickness determined after incorporation of water. In all cases, the 1:1 relationship between mass of H<sub>2</sub>O incorporated and film volume was not observed, which is not surprising given that the water volume is a partial molar fraction that depends on the composition of the mixture.<sup>27</sup> For films consisting of PVA the estimated volume was always more than anticipated (density < 1) but a linear relationship between the mass of incorporated H<sub>2</sub>O and film volume was noticed. Such observations indicate that strong hydrogen bonding between H<sub>2</sub>O and the polyol chains in conjunction with the elastic properties of the films increased their expansion when water was incorporated. Similarly, the volumes of the swollen SPEEK/PVA films were always larger than anticipated based on the amount of H<sub>2</sub>O incorporated (density < 1). This means that the presence of the Na<sup>+</sup> cations and of the anionic sulfonic groups from SPEEK do not play a major role in the volume changes during water absorption. SPEEK/PVA films achieved the same volume expansion via incorporation of the water quantity absorbed by PVA within the films. This trend is slightly more pronounced for thicker SPEEK/PVA films as, according to Figure 2-4, they absorbed less water (per unit mass) than thinner films.

Illustrated in Figure 2-6 are spectra that resulted when the molybdenum-iodide procedure for quantification of [H<sub>2</sub>O<sub>2</sub>] was applied to samples obtained during illumination of a SPEEK/PVA film in contact with an air-saturated aqueous solution at pH 5. An absorption centered at the wavelength of maximum intensity ( $\lambda_{\text{max}}$ ) of 350 nm was noticed that increased in intensity as illumination progressed. This signal corresponds to the well-known absorption of I<sub>3</sub><sup>-</sup> with  $\lambda_{\text{max}} = 350$  in water and an extinction coefficient ( $\epsilon$ ) of  $2.64 \times 10^4 \text{ M}^{-1} \text{ cm}^{-1}$ .<sup>21</sup> In contrast, the absorption was centered at 370 in solutions containing SPEEK and PVA used in our earlier study because red-shifts of the triiodide spectrum and decreases in  $\epsilon$  are known to occur when alcohols

are present at high concentrations.<sup>17</sup> Given that PVA is confined to the films and no longer dissolved in the solution, the  $I_3^-$  signals shown in Figure 2-6 exhibit

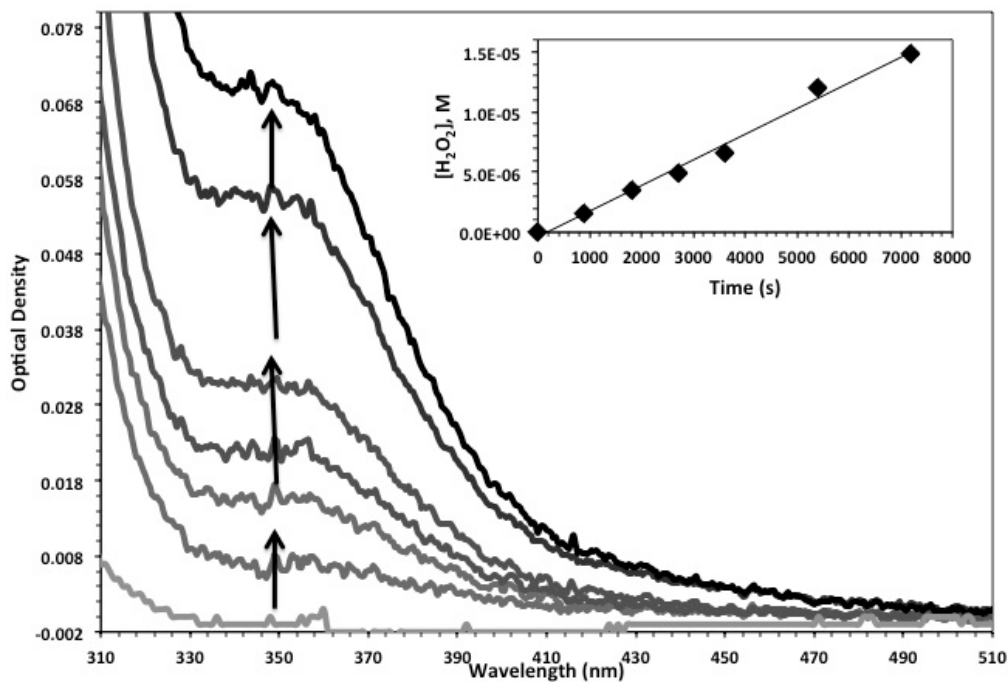


**Figure 2-6.** Optical spectra obtained after treatment with the iodide-molybdate method of samples from an air-saturated solution at pH = 5 in contact with a SPEEK/PVA film photolyzed with 350 nm light,  $I_0 = 1.4 \times 10^{-5} \text{ M}(h\nu)/\text{s}$ , for 0, 15, 30, 45, 60, 90 and 120 min. Solutions were diluted by a factor of 6 during the peroxide assay. Inset: plot of  $[H_2O_2]$  versus illumination time, slope =  $2.9 \times 10^{-9} \text{ M/s}$ ,  $r^2 = 0.99$ ; SPEEK sample obtained from Victrex PEEK.

the characteristic  $\lambda_{\text{max}}$  found in water, allowing determination of  $[H_2O_2]$  with the  $\epsilon$  value measured in  $H_2O$ . These results clearly demonstrated that photolysis of SPEEK/PVA films in contact with an air-saturated solution yielded hydrogen peroxide as a product. In contrast, no  $H_2O_2$  was detected upon illumination of films containing only PVA. Included in the inset is a plot of the  $[H_2O_2]$  evolution with increasing irradiation time, indicating that the rate of peroxide formation follows a zero-order process. Thus, the slope of such a plot corresponds to the rate of peroxide formation,  $r(H_2O_2)$ , which amounted to  $2.9 \times 10^{-9} \text{ M/s}$  for the data shown in Figure 2-6.

Similar zero-order increases in  $[H_2O_2]$  with irradiation time were observed for SPEEK/PVA films immersed in neutral solutions irrespective of the origin of the PEEK material used in the preparation of the polyketone. SPEEK/PVA films containing polyketone prepared from Evonik and Victrex PEEK were tested in terms of their efficiency of generating peroxide at different light intensities. According to the results presented in Figure 2-7 the  $r_c(H_2O_2)$  values increased linearly with  $I_0$  in both cases. The slopes of the resulting straight lines correspond to the quantum yields of  $H_2O_2$  formation. Comparable  $\phi(H_2O_2)$  values were obtained of 0.11 and 0.15 for polyketones derived from the Victrex and Evonik PEEK polymers, respectively.

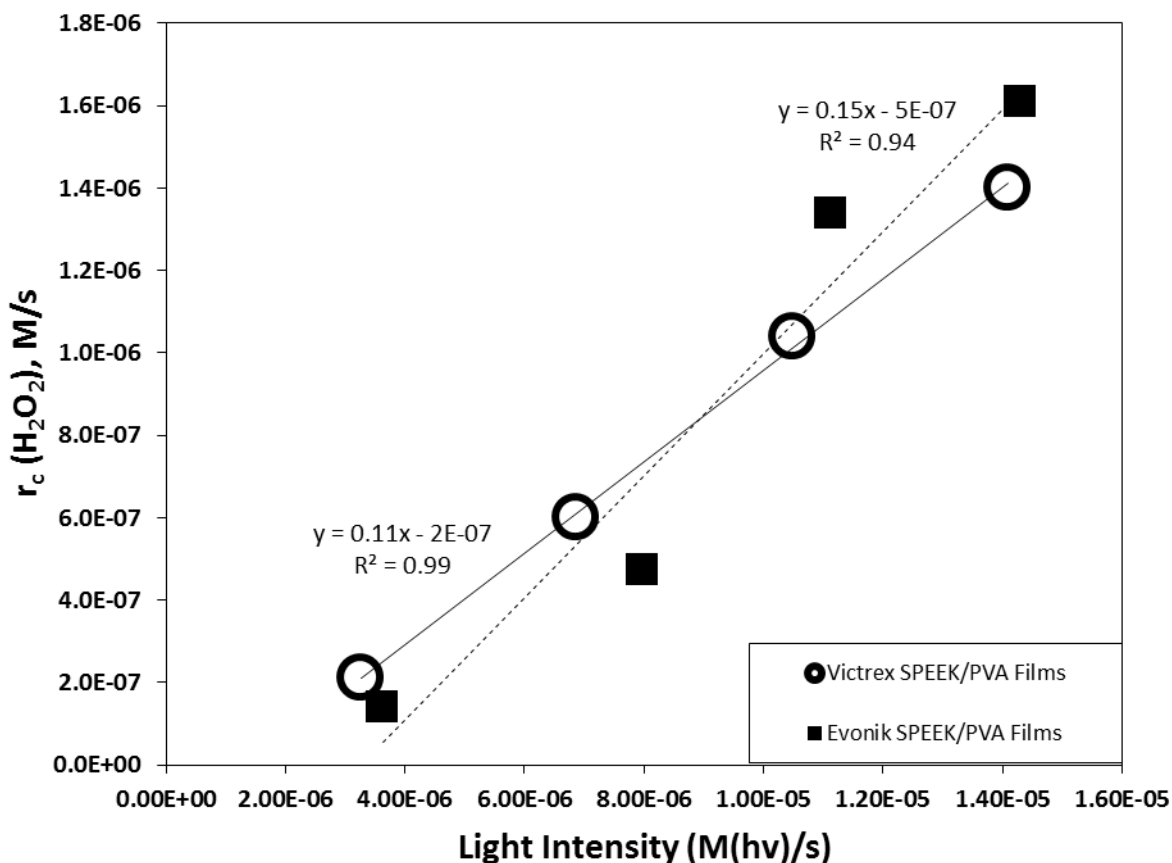


**Figure 2-7.** Plot of  $H_2O_2$  formation rates as a function of light intensity from experiments with water-swollen SPEEK/PVA films containing polyketone derived from Evonik (■) and Victrex (○) PEEK. Films exposed to 350 nm photons in air saturated solutions with pH values in the range of 5.5-6.



The linear dependence of  $r_c(\text{H}_2\text{O}_2)$  with light intensity indicates that the reaction rate is first-order with respect to  $I_0$ . This means that the speed of peroxide formation is controlled by the intensity of photons entering the irradiation vessel which agrees well with the findings from experiments with SPEEK/PVA solutions.<sup>17</sup>

However, the previous analysis of the data underestimates the true quantum yields given that the films only absorbed a fraction of the incident photon flux. Therefore, efforts were made to introduce a correction, using equation 2.3, for the incomplete absorption of the photon flux. Presented in Figure 2-8 are the corrected quantum yields together with the values obtained previously for experiments with SPEEK/PVA solutions from reference 17. Obviously, the quantum yields derived directly from the slopes of the straight lines shown in Figure 2-7 are, at least, 5 times higher than the  $\phi(\text{H}_2\text{O}_2)$  value of 0.02 obtained previously for experiments with solutions of the polymer blend. As is obvious from Figure 2-8, the values of corrected quantum yields scatter considerably because estimation of the amount of light absorbed by the films is not precise. One of the difficulties is to determine accurately the dimensions of the swollen films, particularly the thickness. For instance, the correction given by equation 2-2 employs the volume of the swollen film, which was estimated to be twice that of the dry state, but significant uncertainty remains concerning such an estimate. Furthermore, decreases in the light intensity that impinges on the films due to losses induced by light scattering at the polymer-water interfaces are also related to the film dimensions.

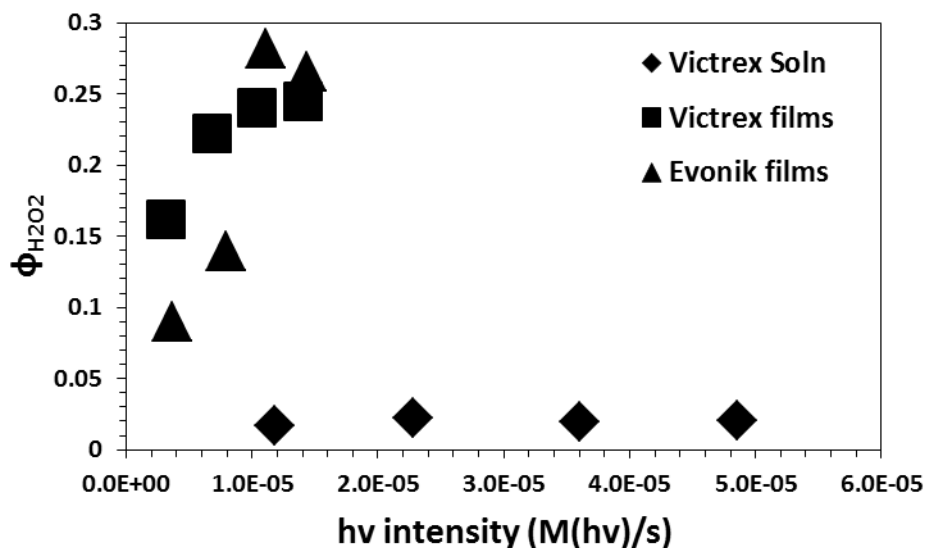


**Figure 2-8.** Comparison of the corrected quantum yields of  $H_2O_2$  formation versus light intensity for SPEEK/PVA swollen in water with the efficiencies determined for solutions containing both the polyol and the polyketone. (◆) Solution results with Victrex PEEK; data from film experiments using SPEEK derived from Victrex (■), and evonik PEEK (▲). Irradiations with 350 nm photons in neutral solutions saturated with air.

However, estimation of such losses is not a straightforward task. Using the average value of the quantum yields of Figure 2-8 results in  $\phi_c(H_2O_2) = 0.2$ , that is 10 times the efficiency for peroxide formation in the SPEEK/PVA solution system. A plausible explanation is that most of the SPEEK radicals are lost in solution via radical-radical combination and disproportionation reactions that usually occur via diffusion controlled processes in the case of  $\alpha$ -hydroxy radicals. In the case of SPEEK radicals the equivalent reaction is:



To simplify the notation  $\{R'RC\bullet OH\}_z$  was employed to represent the  $\alpha$ -hydroxy radical of SPEEK and the meaning of this formula is that, on average, one unpaired electron is present per

polymer radical chain. Motion of SPEEK chains is restricted in crosslinked films and such restriction enables the radicals to survive for a time long enough to undergo reaction with  $O_2$ . Hence, a much higher number of SPEEK radicals is scavenged by oxygen in the swollen polymer films, resulting in a higher yield of hydrogen peroxide.

Several experiments were performed in which the rate of peroxide formation was determined as a function of the temperature. Essentially the same rates were obtained in the temperature range of 5-35 °C but larger  $r(H_2O_2)$  values, by a factor of 2-7, were determined at  $40 \leq T \leq 60$  °C. However, the results were not reproducible at  $T \geq 40$  °C; DSC experiments revealed that endothermic transitions take place for water-swollen SPEEK/PVA or PVA films, but not for dry solid samples. Swelling of crosslinked PVA/PAA films was noticed to increase with increasing temperatures.<sup>26</sup> An analogous behavior could explain the increases of  $r(H_2O_2)$  at higher temperatures. If such an explanation is correct then the calorimetric results pertain to some transition that enables further water absorption by the SPEEK/PVA films.

Illustrated in Figure 2-9 is the dependence of the rate of  $H_2O_2$  photogeneration for SPEEK/PVA films illuminated in solutions with different pH values. Films containing SPEEK derived from the Victrex precursor exhibited a maximum rate in the pH range of 7 to 8 resembling the results obtained in solution experiments.<sup>17</sup> The steep decrease in the  $H_2O_2$  formation rate in solution was explained in terms of the deprotonation of SPEEK radicals, with a  $pK_a$  of about 9,<sup>17</sup> which is the value for benzophenone radicals in water.<sup>28</sup> The BP radical anion reacts much faster with a neutral benzophenone radical than the combination of two neutral radicals. A similar reaction involving  $\{R'RC\bullet OH\}_z$  and the corresponding anionic radical explained the sharp decay in  $H_2O_2$  formation at  $pH > 8$  for SPEEK/PVA solution systems.<sup>17</sup>

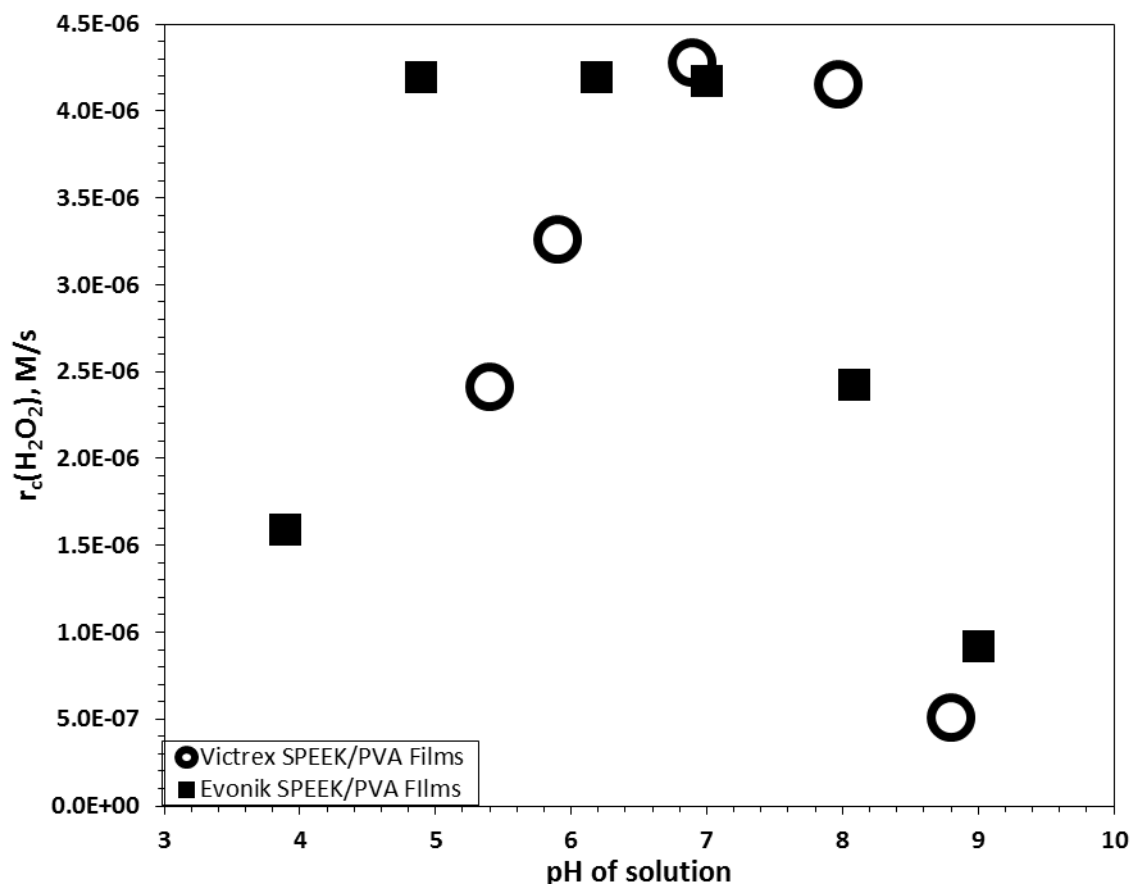


**Figure 2-9.** Dependence of  $r_c(\text{H}_2\text{O}_2)$  on the pH of air-saturated solution for swollen SPEEK/PVA photolyzed with 350 nm light with  $I_0 = 1.4 \times 10^{-5} \text{ M}(\text{h}\nu)/\text{s}$ . Experiments with SPEEK derived from Evonik (■) and (○) Victrex PEEK.

However, radical-radical reactions involving SPEEK species are not a reasonable explanation for the results shown at  $\text{pH} > 8$  in Figure 2-9 due to the restricted mobility of polymer chains in crosslinked films. Hydroxide ions quench the triplet excited state of BP that is the precursor of the benzophenone radicals but with a rate constant of only  $4.9 \times 10^6 \text{ M}^{-1} \text{ s}^{-1}$ .<sup>29</sup> A similar process may have contributed to the decrease in  $r_c(\text{H}_2\text{O}_2)$  for films with SPEEK derived from both Evonik and Victrex precursors.

The sharp decrease in  $r_c(\text{H}_2\text{O}_2)$  for films with SPEEK derived from Victrex PEEK is consistent with the results gained in the solution study using the same polyketone.  $\text{H}_3\text{O}^+$  ions are efficient

quenchers of the BP triplet excited state with a rate constant of  $3.8 \times 10^8 \text{ M}^{-1} \text{ s}^{-1}$ .<sup>30</sup> An analogous quenching of the triplet excited state of SPEEK is anticipated, which explains the lower efficiency of peroxide photogeneration noticed at  $\text{pH} < 7$ . Surprisingly, no drastic drop in  $r_c(\text{H}_2\text{O}_2)$  was noticed for SPEEK/PVA films containing the polyketone prepared from the Evonik precursor. Only at pH values below 5 was  $\text{H}_2\text{O}_2$  produced in a less efficient fashion than in neutral solutions. The reason for such higher photochemical efficiency in mildly acidic medium is not understood.

Studies were also performed on the efficiency of SPEEK/PVA films to generate peroxide when in contact with solutions containing water and an organic solvent that is not an H-atom donor toward excited BP groups. The purpose of such experiments was to ascertain if the films were able to generate peroxide in the absence of liquid  $\text{H}_2\text{O}$ .  $\text{CH}_3\text{CN}$  was considered an ideal co-solvent for these experiments given the good miscibility of acetonitrile with water and the fact that this solvent is relatively inert toward the triplet state of BP.<sup>18</sup>

Shown in Figure 2-10 are the rates of peroxide formation for SPEEK/PVA films prepared with polyketone samples from both Evonik and Victrex precursors. Similar trends are observed for thin films containing SPEEK made from both suppliers of PEEK, in which  $r_c(\text{H}_2\text{O}_2)$  increases with decreasing mol fraction of water. Although no swelling experiments were performed with the solvent mixtures, significant expansion of the films was detected in the range of water mole fractions of 0.4 and 1. Although  $[\text{O}_2]$  has not been determined for the  $\text{H}_2\text{O}/\text{CH}_3\text{CN}$  mixtures employed in the present study, the oxygen solubility from air in acetonitrile is 1 mM,<sup>31</sup> as compared with the value of 0.26 mM for water.<sup>17</sup> Thus, the steady increase in  $r_c(\text{H}_2\text{O}_2)$  with increasing  $\text{CH}_3\text{CN}$  concentration can be related to the higher  $[\text{O}_2]$  that is present in the mixtures with increasing acetonitrile content

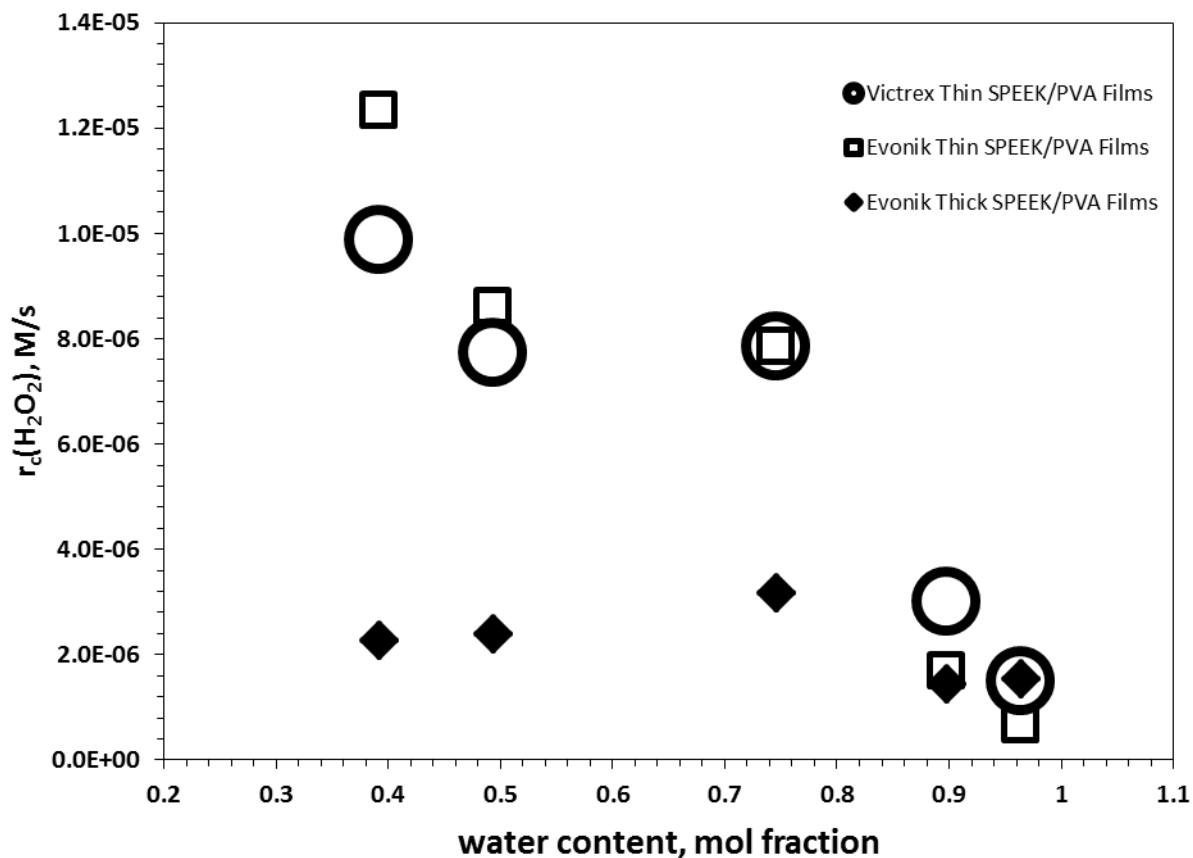
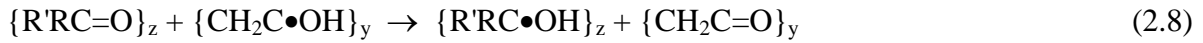


**Figure 2-10.** Plot of  $r_c(\text{H}_2\text{O}_2)$  as a function of water content in  $\text{H}_2\text{O}/\text{CH}_3\text{CN}$  mixtures for swollen, crosslinked SPEEK/PVA solid samples; ( $\odot$ ) 30  $\mu\text{m}$  thick films, SPEEK derived from Victrex precursor; ( $\square$ ) 30-40  $\mu\text{m}$  thick films, SPEEK derived from Evonik PEEK; ( $\blacklozenge$ ) 40-50  $\mu\text{m}$  thick films, SPEEK derived from Evonik precursor. Photolysis with 350 nm light,  $I_0 = 1.4 \times 10^{-5} \text{ M}(\text{h}\nu)/\text{s}$ .

Estimates of  $\phi_c(\text{H}_2\text{O}_2)$  based on the results depicted in Figure 2-10 indicate that the corrected quantum yields approach a value of 1 with increasing  $\text{CH}_3\text{CN}$  concentration. In contrast,  $r_c(\text{H}_2\text{O}_2)$  remains small and fairly constant when slightly thicker SPEEK/PVA films were exposed to light. These somewhat unexpected results may reflect the tendency of thicker films to absorb less  $\text{H}_2\text{O}$  as noted previously when discussing the swelling results. The apparent difficulty of thick SPEEK/PVA films to absorb water may be exacerbated by the presence of

acetonitrile. An observation that seems to support this assumption is that mixtures containing acetonitrile mole fractions  $> 0.6$  inhibited swelling of the films. No  $\text{H}_2\text{O}_2$  was detected when such collapsed films were photolyzed, indicating that efficient peroxide generation requires the presence of liquid water in the solid polymer matrices.

The results presented thus far indicate that the formation of hydrogen peroxide in the swollen SPEEK/PVA films shares numerous analogies with the results obtained in solutions containing both polymers.<sup>17</sup> For this reason the film data were rationalized in terms of the mechanism proposed earlier for the photoreduction of  $\text{O}_2$  in air-saturated SPEEK/PVA solutions, which consists of the following steps:



For simplicity  $\{\text{CH}_2\text{C}\bullet\text{OH}\}_y$  was employed to represent the  $\alpha$ -hydroxy radical of PVA meaning that, on average, one unpaired electron exists per polymer radical chain. The  $\alpha$ -hydroxy radical of PVA is expected to reduce SPEEK via step 2.7, which should be favored by the high

concentration of SPEEK carbonyl groups present in the films. Steps 2.10 and 2.11 represent the contributions of both PVA and SPEEK radicals to the  $O_2$  reduction in the SPEEK/PVA system. Several reactions involving  $HO_2\bullet$  and/or  $\bullet O_2^-$  produce  $H_2O_2$  but step 2.13 is the fastest of such processes and is aided by the deprotonation ( $pK_a = 4.8$ ) of the perhydroxyl radical, step 2.12.<sup>32</sup> The disproportionations of  $HO_2\bullet$  and  $\bullet O_2^-$  is frequently summarized by step 2.13, which is the reason that this step is also used here.



## 2.4 Conclusions

The results gathered in the present investigation demonstrate that  $\text{H}_2\text{O}_2$  is produced via illumination of SPEEK/PVA films swollen when in contact with aqueous solutions containing air. The kinetic data support a mechanism in which a photochemical process that forms  $\alpha$ -hydroxy radicals of SPEEK dictates the rate of the peroxide formation. Photolysis of such systems results in quantum yields at least 5 times higher than previously found from analogous studies with solutions containing SPEEK and PVA. Additional corrections for the absorbed intensity of photons indicate that the quantum efficiencies are in the order of 0.2 in neutral solutions. Films containing SPEEK prepared from PEEK polymers made by Evonik are more efficient than films containing polyketone derived from a Victrex precursor, which was employed in the previous solution studies.<sup>17</sup> Increases in the  $[\text{O}_2]$  induced by the presence of acetonitrile in the aqueous phase increases the efficiency of peroxide formation reaching quantum yields close to one. However, experiments with mixed solvents highlighted the role that film swelling by  $\text{H}_2\text{O}$  plays in the formation of peroxide since negligible peroxide photogeneration takes place for films free of liquid water. Therefore, preparation of SPEEK-based films useful as light-activated protective barriers will require the presence of a polymer component significantly more hygroscopic than PVA. In this way, swelling of the films could be accomplished via absorption of humidity from air.

## References

- 1) Ishimura, K. In *Organic Photochromic and Thermochromic Compounds*; Crano, J. A.; Guglielmetti, R. J., Eds.; Kluwer/Plenum: New York, 1999, Vol. 2, Chapter 1.
- 2) Reiser, A. *Photoreactive Polymers: The Science and Technology of Resists*; Wiley-Interscience: New York, 1989.
- 3) Guillet, J. *Polymer Photophysics and Photochemistry*; Cambridge University Press: Cambridge, 1985; Chapters 9 and 10.
- 4) (a) Koizume, H.; Shiraishi, Y.; Hirai, T. Temperature-Controlled Photosensitization Properties of Benzophenone-Conjugated Thermoresponsive Copolymers. *J. Phys. Chem. B* **2008**, *112*, 13238-13244. (b) Koizume, H.; Shiraishi, Tojo, S.; Fujitsuka, M.; Majima, T.; Y.; Hirai, T. Temperature-Driven Oxygenation Rate Control by Polymeric Photosensitizer. *J. Am. Chem. Soc.* **2006**, *128*, 8751-8753.
- 5) (a) Nishikubo, T.; Kondo, T.; Inomata, K. Study of Polymeric Photosensitizers. 5. Synthesis of Multifunctional Photosensitizers Bonded on Cross-Linked Polymer Beads and Their Application for Photoisomerization of Potassium Sorbate. *Macromolecules* **1989**, *22*, 3827-3833. (b) Bourdelande, J. L.; Font, J.; Sánchez-Ferrando, F. The use of insoluble benzoylated polystyrene beads (polymeric benzophenone) in photochemical reactions. *Can. J. Chem.* **1983**, *61*, 1007-1016.
- 6) (a) Nowakoska, M.; Kepczynski, M.; Szczubialka, K. New Polymeric Sensitizers. *Pure Appl. Chem.* **2001**, *73*, 491-495. (b) Nowakoska, M.; White, B.; Guillet, J. E. Studies of the Antenna Effect in Polymer Molecules. 12. Photochemical Reactions of Several Polynuclear Aromatic Compounds Solubilized in Aqueous Solutions of Poly(sodium styrenesulfonate-co-2-vinylnaphthlene). *Macromolecules* **1989**, *22*, 2317-2324.
- 7) Schreuder-Gibson, H.; Truong, Q.; Walker, J. E.; Owens, J. R.; Wander, J. D.; Jones, Jr., W. E. Chemical and Biological Protection and Detection in Fabrics for Protective Clothing. *MRS Bulletin* **2003**, 574-578.
- 8) Singh, A.; Lee, Y.; Dressick, W. J. Self-Cleaning Fabrics for Decontamination of Organophosphorous Pesticides and Related Chemical Agents. *Adv. Mater.* **2004**, *16*, 212-215.
- (9) Ji, E.; Corbitt, T. S.; Parthasarathy, A.; Schanze, K. S.; Whitten, D. G. Light and Dark-Activated Biocidal Activity of Conjugated Polyelectrolytes. *ACS Appl. Mater. Interfaces* **2011**, *3*, 2820-2829.
- 10) Sun, G.; Hong, K. H. Photo-induced antimicrobial and decontaminating agents: recent progress in polymer and textile applications. *Text. Res. J.* **2013**, *83*, 532-542.
- 11) (a) Wagner, G. W.; Sorrick, D. C.; Procell, L. R.; Brickhouse, M. D.; Mcvey, I. F.; Schwartz, L. I. Decontamination of VX, GD, and HD on a Surface Using Modified Vaporized Hydrogen Peroxide. *Langmuir* **2007**, *23*, 1178-1186. (b) Wagner, G. W.; Yang, Y.-C. Rapid Nucleophilic/Oxidative Decontamination of Chemical Warfare Agents. *Ind. Eng. Chem. Res.* **2002**, *41*, 1925-1928.

- 12) McDonnell, G.; Russell, D. Antiseptics and Disinfectants: Activity, Action and Resistance. *Clinical Microbiol. Rev.* **1999**, *12*, 147-179.
- 13) De la Rosa, M. A.; Navarro, J. A.; De la Rosa, F. F.; Losada, M. Stabilization by high pH of hydrogen peroxide production with flavin photosystems. *Photobiochem. Photobiophys.* **1983**, *5*, 93-103.
- 14) Schlettwein, D.; Kaneko, M.; Yamada, A.; Wöhrle, D.; Jaeger, N. I. Light-Induced Dioxygen Reduction at Thin Films Electrodes of Various Porphyrins. *J. Phys. Chem.* **1991**, *95*, 1748-1755.
- 15) Foyle, V. P.; Takahashi, Y.; Guillet, J. A. Photocatalytic Production of Hydrogen Peroxide Using Polymer Bound Anthraquinone. I. Photoproducts in 2-Hydroxyethyl Methacrylate Hydrogels Swollen with Water and 2-Propanol. *J. Polym. Sci. A* **1992**, *39*, 257-268.
- 16) Kurimura, Y.; Nagashima, M.; Takato, K.; Tsuchida, E.; Kaneko, M.; Yamada, A. Photoredox Reactions Using Ion-Exchange Resin-Adsorbed Ru(bpy)<sub>3</sub><sup>2+</sup>. Photosensitized Reductions of Methyl Viologen and Molecular Oxygen Using Ion-Exchange Resin-Adsorbed Tris(2,2'-bipyridine)ruthenium(II). *J. Phys. Chem.* **1982**, *86*, 2432-2437.
- 17) Little, B. K.; Lockhart, P.; Slaten, B. L.; Mills, G. Photogeneration of H<sub>2</sub>O<sub>2</sub> in SPEEK/PVA Aqueous Polymer Solutions. *J. Phys. Chem. A* **2013**, *117*, 4148-4157.
- 18) Gilbert, A.; Baggott, J. *Essentials of Molecular Photochemistry*; CRC Press: Boca Raton, 1991; Chapter 7.
- 19) (a) Korchev, A. S.; Konovalova, T.; Cammarata, V.; Kispert, L.; Slaten, B. L.; Mills, G. Radical-Induced Generation of Small Silver Particles in SPEEK/PVA Polymer Films and Solutions: UV-Vis, EPR, and FT-IR Studies. *Langmuir* **2006**, *22*, 375-384. (b) Korchev, A. S.; Shulyak, T. S.; Slaten, B. L.; Gale, W. F.; Mills, G. Sulfonated Poly(Ether Ether Ketone)/Poly(Vinyl Alcohol) Sensitizing System for Solution Photogeneration of Small Ag, Au, and Cu Crystallites. *J. Phys. Chem. B* **2005**, *109*, 7733-7745. (c) Korchev, A. S.; Sartin, M.; Mills, G.; B. L. Slaten, B. L.; Gale, W. F. In *Clusters and Nano-Assemblies: Physical and Biological Systems*; Jena, P.; Khanna, S. N.; Rao, B. K.; Eds, World Scientific Publishing Co.: Singapore, 2005; 371-377. (d) Korchev, A. S.; Bozak, M. J.; Slaten, B. L.; Mills, G. Polymer-Initiated Photogeneration of Silver Nanoparticles in SPEEK/PVA Films: Direct Metal Photopatterning. *J. Am. Chem. Soc.* **2004**, *126*, 10-11.
- 20) Heller, H. G.; Langan, J. R. Photochromic Heterocyclic Fulgides. Part 3. The Use of (E)-a-(2,5-Dimethyl-3-furylethylidene) (isopropylidene)succinic Anhydride as a Simple Convenient Chemical Actinometer. *J. Chem. Soc., Perkin Trans. 2* **1981**, 341-343.
- 21) Stefanic, I.; Asmus, K.-D.; Bonifacic, M. Quantification of iodide oxidation by trichloromethyl peroxy radicals and  $I^- + I_2 \rightleftharpoons I_3^-$  equilibrium in alcohol/water mixtures. *Phys. Chem. Chem. Phys.* **2003**, *5*, 2783-2789.
- 22) (a) Muthu Lakshmi, R. T. S.; Choudhary, V.; Varma, I. K. Sulfonated Poly(ether ether ketone): Synthesis and Characterisation. *J. Mater. Sci.* **2005**, *40*, 629-636. (b) Xing, P.; Robertson, G. P.; Guiver, M. D.; Mikhailenko, S. D.; Wang, K.; Kaliaguine, S. Synthesis and

Characterization of Sulfonated Poly(ether ether ketone) for Proton Exchange Membrane. *J. Mater. Sci.* **2004**, 29, 95-106.

23) Jin, X., Bishop, M.T., Ellis, T.S., Karasz, F.E. A Sulfonated Poly(aryl Ether Ketone). *British Polym. J.* **1985**, 17, 4-10.

24) Lien, L.; Fellows, C. M.; Copeland, L.; Hawkett, B. S.; Gilbert, R, G. Water Binding and Oxygen Permeability in Poly(vinyl alcohol) Films. *Aust. J. Chem.* **2002**, 55, 507-512.

25) Kim, K.-J.; Lee, S.-B.; Han, H.-W., Effects of the Degree of Crosslinking on Properties of Poly(vinyl alcohol) Membranes, *Polym. J.* **1993**, 25, 1295-1302.

26) Gudeman, L. F.; Peppas, N. A., Preparation and Characterization of pH-Sensitive Interpenetrating Networks of Poly(vinyl alcohol) and Poly(acrylic acid), *J. Appl. Polym. Sci.* **1995**, 55, 919 – 928.

27) Levine, I. N. *Physical Chemistry*, 6<sup>th</sup> ed.; McGraw-Hill: New York, 2009; pp. 264-268.

28) Porter, G.; Wilkinson, F. Primary Photochemical Processes in Aromatic Molecules. Part 5. Flash Photolysis of Benzophenone in Solution. *Trans. Faraday Soc.* **1961**, 57, 1686-1691.

29) Shizuka, H.; Obuchi, H. Anion-Induced Triplet Quenching of Aromatic Ketones by Nanosecond Laser Photolysis. *J. Phys. Chem.* **1982**, 86, 1297-1302.

30) Ledger, M. B.; Porter, G. Primary Photochemical Processes in Aromatic Molecules. Part 15.—The Photochemistry of Aromatic Carbonyl Compounds in Aqueous Solution *J. Chem. Soc., Faraday Trans. 1* **1972**, 68, 539-553.

31) Horstmann, S.; Grybat, A.; Kato, R. Experimental determination and prediction of gas solubility data for oxygen in acetonitrile. *J. Chem. Thermodynamics* **2004**, 36, 1015-1018.

32) Bielski, B. H.; Cabelli, D. E.; Arudi, R. L.; Ross, A. B. Reactivity of HO<sub>2</sub>/O<sub>2</sub><sup>-</sup> Radicals in Aqueous Solution. *J. Phys. Chem. Ref. Data* **1985**, 14, 1041-1100.

### III. Photochemical Reduction of Hexavalent Chromium in Solutions of SPEEK/PVA

#### 3.1 Introduction

Hexavalent chromium ( $\text{Cr}^{6+}$ ), present in many compounds, is a well-known toxic ion with demonstrated carcinogenic and mutagenic characteristics.<sup>1</sup> Among the effects induced by  $\text{Cr}^{6+}$  is a mismatch replication of the DNA strand that leads to instability in the formation of double-stranded DNA.<sup>2</sup> However, not all Cr ions are toxic and  $\text{Cr}^{3+}$  is an essential species used for supplementing weight loss, increasing muscle mass, and alleviating symptoms of type 2 diabetes.<sup>3,4</sup>  $\text{Cr}^{6+}$  is frequently released into the environment from different sources such as leather industries, chromium plating, textile operations and mining, ultimately contaminating surrounding waters, surface waters, and soils.<sup>5-9</sup> Because of the toxic nature of Cr(VI), studies have been conducted to decrease the presence of this ion via reduction to the nontoxic trivalent oxidation state. In chemical treatment of contaminated waters procedures based on oxidative degradation are usually employed to eliminate toxic organics and enhancements are achieved by applying photochemical methods that can induce hydroxyl radical generation, as well as electron-transfer and energy-transfer processes.<sup>10</sup> Photochemical reduction of chromium by organic compounds,<sup>11</sup> metal oxides,<sup>12</sup> alcohols,<sup>13</sup> and  $\text{TiO}_2$  suspensions<sup>14</sup> have proven that solution pH and initial concentration of chromium influence the photoreduction process.

In dilute solutions, hexavalent chromium is present in a number of species, which are dependent on Cr(VI) concentration, buffering materials and solution pH. These species include  $\text{H}_2\text{CrO}_4$ ,  $\text{HCrO}_4^-$ ,  $\text{CrO}_4^{2-}$ , and  $\text{Cr}_2\text{O}_7^{2-}$ , that are involved in the following set of equilibria;<sup>15, 16</sup>



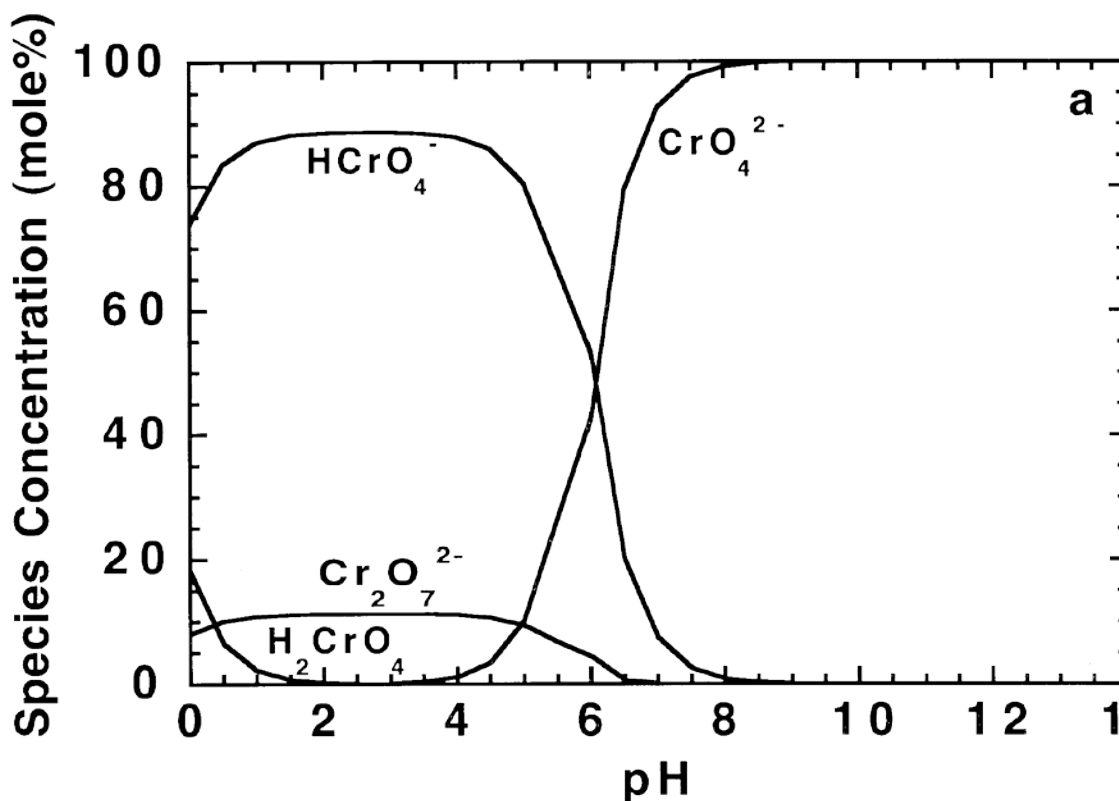


Figure 3-1. Concentration of hexavalent chromium species as a function of solution pH of 1 mM total chromium concentration (adopted from reference 17).



The concentrations of Cr(VI) species as a function of solution pH are presented in Figure 3-1.<sup>17</sup> In the pH range of 2 to 6, the  $\text{HCrO}_4^{2-}$  and  $\text{Cr}_2\text{O}_7^{2-}$  anions are predominant. The  $\text{H}_2\text{CrO}_4$  acid is present at  $\text{pH} < 1$ , and  $\text{CrO}_4^{2-}$  predominates above  $\text{pH} 8$ . The dimerization of chromium occurs when the concentration of  $\text{Cr}_2\text{O}_7^{2-}$  is higher than  $10^{-3} \text{ M}$ .<sup>18</sup> In the majority of this work, a  $[\text{Cr}^{6+}] < 1 \text{ mM}$  was employed, meaning that monomeric oxyanion species predominated which will be further referred to as Cr(VI).

Results presented in this chapter demonstrate that Cr(VI) can be reduced effectively via photolysis in aqueous solutions containing poly(vinyl alcohol), PVA, and sulfonated poly(ether

ether ketone), referred to as SPEEK. The present research will show that Cr(VI) is reduced with higher yields in solutions of SPEEK/PVA than in systems containing only PVA. The reduction is initiated by reaction of Cr(VI) with polymeric ketyl radicals, photogenerated when excited ( $n, \pi^*$ ) triplet states of SPEEK carbonyls abstract a H-atom from neighboring PVA chains. Cr(VI) reduction in the polymeric systems has been followed with UV-Vis spectrophotometric techniques. Also, the reduction processes as well as the factors influencing the rates of reaction such as light intensity, buffer concentrations, and effects of pH have been studied in order to get a basic insight into the reduction process of the polymer-assisted photoreduction of hexavalent chromium. Experiments will be conducted in air-saturated solutions to simulate environmental effects in polymeric system.

### 3.2 Experimental

Poly (vinyl alcohol), (PVA) 99+% hydrolyzed with an average molar mass of  $8.9-9.8 \times 10^4$  g/mol and potassium phosphate monobasic were purchased from Sigma Aldrich. Potassium dichromate, potassium phosphate dibasic, and 1, 5-diphenylcarbazide was obtained from Fisher. Poly(ether ether ketone) (PEEK) was a gift from Evonik with an average molar mass of  $4.5 \times 10^4$  g/mol. PEEK was received in sheets that were cut into strips, further ground into a powder, and later dried in a vacuum oven at 100 °C for about 6 hours. Solutions of 30% w/v were prepared with the dried PEEK and H<sub>2</sub>SO<sub>4</sub>, and were stirred constantly at a temperature between 50-55 °C for several days. Collection of sulfonated PEEK used the same procedure as described before.<sup>19</sup> Solution preparations for SPEEK/PVA solutions were conducted as stated previously,<sup>19</sup> and the molarity for solutions containing PVA with no SPEEK was the same as that for solutions of SPEEK/PVA. Films preparations were conducted the same as in Chapter 2.



Image 3-1. Illumination vessel used for the reduction of Cr(VI) in polymeric solutions.

Stock solutions of  $2 \times 10^{-3}$  M and 0.125 M Cr(VI) were used to obtain the desired concentration of Cr(VI) via dilution. Phosphate buffer solutions were prepared at the pH needed for the photochemical reduction experiments. Chromium concentrations were determined by optical measurements performed on a Shimadzu UV-Vis 2501PC spectrophotometer. The two methods used for collecting optical data of Cr(VI) concentrations were direct optical density determinations and also by means of the 1,5-diphenylcarbazide (DPC) method. Data from direct analysis were obtained from buffered SPEEK/PVA solutions containing Cr(VI) in a 1 cm cell. The second method was a sensitive spectrophotometric method for determining hexavalent chromium which required DPC to react with Cr(VI) in acidic medium (pH 1) producing a chromium (III)-diphenylcarbazone complex, which results in violet solutions with the wavelength of maximum absorption ( $\lambda_{\max}$ ) being at 545 nm.<sup>20</sup> DPC solutions were prepared by dissolving 0.2 g in acetone with 1 mL of concentrated sulfuric acid followed by raising the volume to 100 mL. Such solutions were not kept for more than 2 days. In experiments that



investigated the effects of initial [Cr(VI)] and buffer concentrations on the metal ion reduction, the [Cr(VI)] were measured by means of the DPC method. All other measurements, such as determinations of the light intensity ( $I_0$ ) dependency, and reactions in solutions containing only PVA were conducted using direct analysis. Standard polymer solutions for the reduction of Cr(VI) contained 0.018 M SPEEK, 0.036 M PVA, 5 mM phosphate buffer, and approximately  $3.2 \times 10^{-4}$  M Cr(VI).



Image 3-2. Illumination vessel for the reduction of Cr(VI) in SPEEK/PVA films.

Illuminations of air-saturated solutions were conducted under stirring in a 3 mL optical vessel (Image 3-1). The height was 4.9 cm with a base width of 2 cm. Illumination of SPEEK/PVA films was conducted in a glass vessel constructed to specific dimensions (Image 3-2). The top of the vessel was fitted with a “Giant” glass adapter #25 purchased from Ace-Thred with outer diameter of 31.5 mm which includes a nylon bushing cap whose inner diameter is 26 mm. The

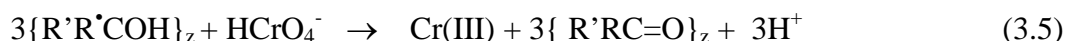
inner tube is fitted with an o-ring and secured by screwing on the nylon brushing cap. The outer diameter of the inner glass tube is 25 mm with a length of 100 mm. At the top of the tube, a small open has a standard wall length of 8 mm. Length of the overall vessel is 140 mm with a base width of 55 mm. The side arm has a small glass adapter #7 from Ace-Thred with a small electrode-fitting hole in cap and secured with a rubber seal. Aliquots of solution are taken from side arm by using Hamilton 1 mL gas syringe. Gas-tight syringes, purchased from Hamilton, were used to extract aliquots from the photolyzed solutions. Optical data were collected on a Shimadzu UV-Vis 2501PC spectrophotometer and the illuminations were carried out inside a Rayonet 100 circular illuminator that generated photons with  $\lambda = 350 \pm 15$  nm by means of 16 RPR-3500A lamps; the light intensity was determined by means of the Aberchrome 540 actinometer.<sup>21</sup> A Perkin Elmer LS 55 luminescence spectrophotometer was used to conduct emission measurements. MINTEQA2 4.03, a speciation program was used to determine the predominant chromate ion in the buffered polymeric solution to be  $\text{HCrO}_4^-$ , when the total concentration is less than  $10^{-3}$  M. In film experiments, chromium remaining in solution was analyzed directly with inductively coupled plasma spectrometry ICP (CIROS CCD model; Spectro Analytical Instruments, Mass Analysis). Quantification of  $[\text{Cr(VI)}]$  via DPC spectrophotometric method and direct analysis exhibited typical error of  $< 10\%$ , but deviations of 30% were observed in SPEEK/PVA solutions.

### **3.3 Results and Discussion**

#### **3.3.1 Photochemical reduction of hexavalent Chromium**

Air-saturated buffered solutions of SPEEK/PVA containing hexavalent chromium were irradiated with 350 nm photons in order to reduce Cr(VI) to the trivalent oxidation state.

Irradiations of air-saturated SPEEK/PVA solutions have produced measurable amounts of H<sub>2</sub>O<sub>2</sub> due to the photochemical generation of SPEEK radicals.<sup>22</sup> Since SPEEK• is a strong reducing agent with an estimated oxidation potential in the range of -1.2 to -1.4 V,<sup>19</sup> and the redox potential of Cr(VI) to Cr(III) in acidic medium is 1.3 V,<sup>23</sup> the reduction of hexavalent chromium by SPEEK radicals is to be represented by the overall reaction provided by eq. 3.5.



Here  $\{R'R^{\bullet}COH\}_z$  represents the SPEEK radicals, and the implicit assumption is that only one unpaired electron is present per radical chain. Thus, the net result is the reduction of Cr(VI) to Cr(III) with reformation of the carbonyl group present on the SPEEK chains, which are the sensitizing chromophores.

Chromium is known to absorb 350 nm light, which is the wavelength of the photons that are used to excite SPEEK to the triplet excited state that forms radicals via hydrogen abstraction from PVA. The polymeric solutions contained 0.018 M SPEEK, which exhibits an extinction coefficient ( $\epsilon$ ) of 900 M<sup>-1</sup>cm<sup>-1</sup> at 350 nm whereas the  $\epsilon$  value for Cr(VI) at that wavelength amounts to 3500 M<sup>-1</sup>cm<sup>-1</sup>.<sup>19,20</sup> Thus, the absorbance at 350 nm due to SPEEK was 16 times greater than that due to Cr(VI) at a standard [HCrO<sub>4</sub><sup>-</sup>] of 3 x 10<sup>-4</sup> M. Emission measurements of degassed solutions containing Cr(VI); SPEEK; and Cr(VI) together with SPEEK were conducted to determine the quenching abilities of Cr(VI).

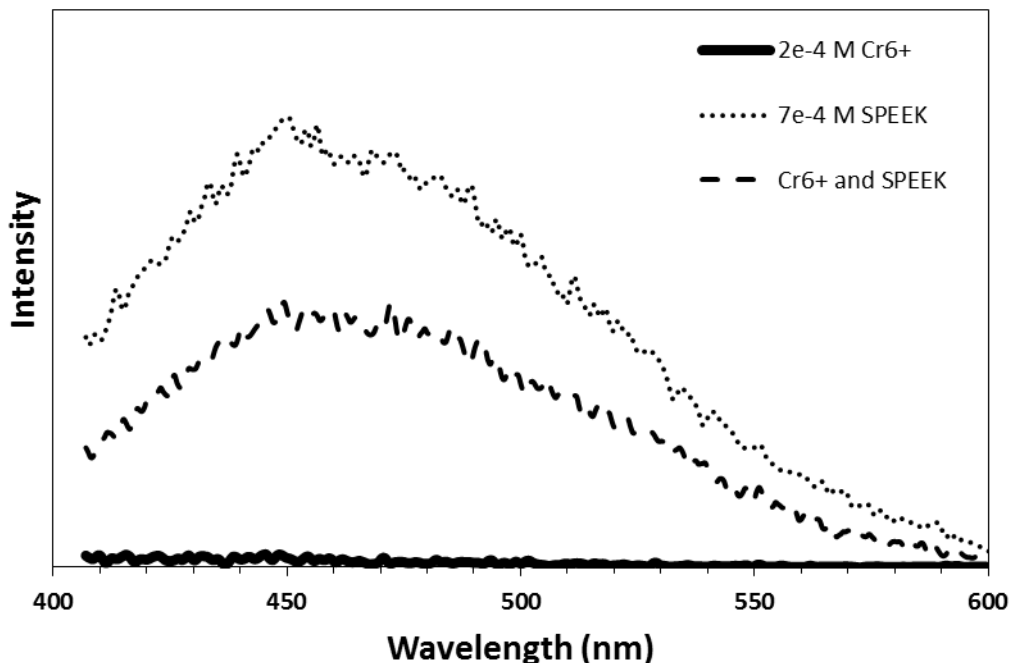


Figure 3-2. Emission spectra of 0.7 mM SPEEK and 0.2 mM Cr(VI) in air-free, buffered solutions (pH 5.7). Excitation wavelength,  $\lambda = 350$  nm and emission  $\lambda_{\text{max}} \approx 448$  nm.

Shown in Figure 3-2 are the emission spectra resulting from excitation by 350 nm photons. A broad emission peak centered at  $\lambda_{\text{max}} = 448$  nm was observed for a solution containing only SPEEK. The overall spectral characteristics are similar to the known phosphorescence spectrum of BP at room temperature with a maximum at 450 nm.<sup>24</sup> In fact, the emission spectrum of SPEEK is broader than that of BP but resembles closely the phosphorescence signals of poly(p-vinylbenzophenone), pVB. Such a result is not surprising since pVB polymer is another macromolecular analogue of BP that is not water-soluble. Given the close resemblance of the emission spectra a logical conclusion is that the SPEEK spectrum shown in Fig. 3-2 corresponds to the room-temperature phosphorescence resulting from the radiative decay experienced by triplet excited state of the sulfonated polyketone.

Also included in Fig. 3-2 are the results from an experiment in which Cr(VI) ions were excited with 350 nm light. The absence of any emission signals indicates that relaxation of the excited metal ions occurred in a radiationless fashion. On the other hand, excitation of SPEEK in the presence of Cr(VI) resulted in a broad signal also centered at about 448 nm but with an intensity that was only 56% of that recorded in the absence of the Cr(VI) ions. An estimate of the fraction of photons absorbed by SPEEK in the presence of the Cr(VI) ions was performed using the extinction coefficients of both species at 350 nm together with their respective concentrations in the emission experiment. By using Beer-Lambert's Law, calculations show about 50% of the excitation light was absorbed by the Cr(VI) ions, indicating that the decrease in phosphorescence intensity depicted in Fig. 3-2 was not a result of quenching of the SPEEK excited state by the Cr species. This means that the photochemical reactions of SPEEK that yield reducing polymeric phenylketyl radicals reported in previous studies are not hindered by the presence of Cr(VI). The conclusion that Cr<sup>6+</sup> oxyanions are not quenchers of the triplet excited state of SPEEK is at odds with claims that an unidentified excited state of carbonyl groups generated by oxidation of PVA to form "polyvinyl alcohol ketone-derivative nanoparticles" can be quenched by Cr(VI).<sup>25</sup> The validity of such claims remains questionable in the absence of an analysis of the fraction of photons absorbed by Cr(VI) during the emission experiments with the oxidized PVA compounds.

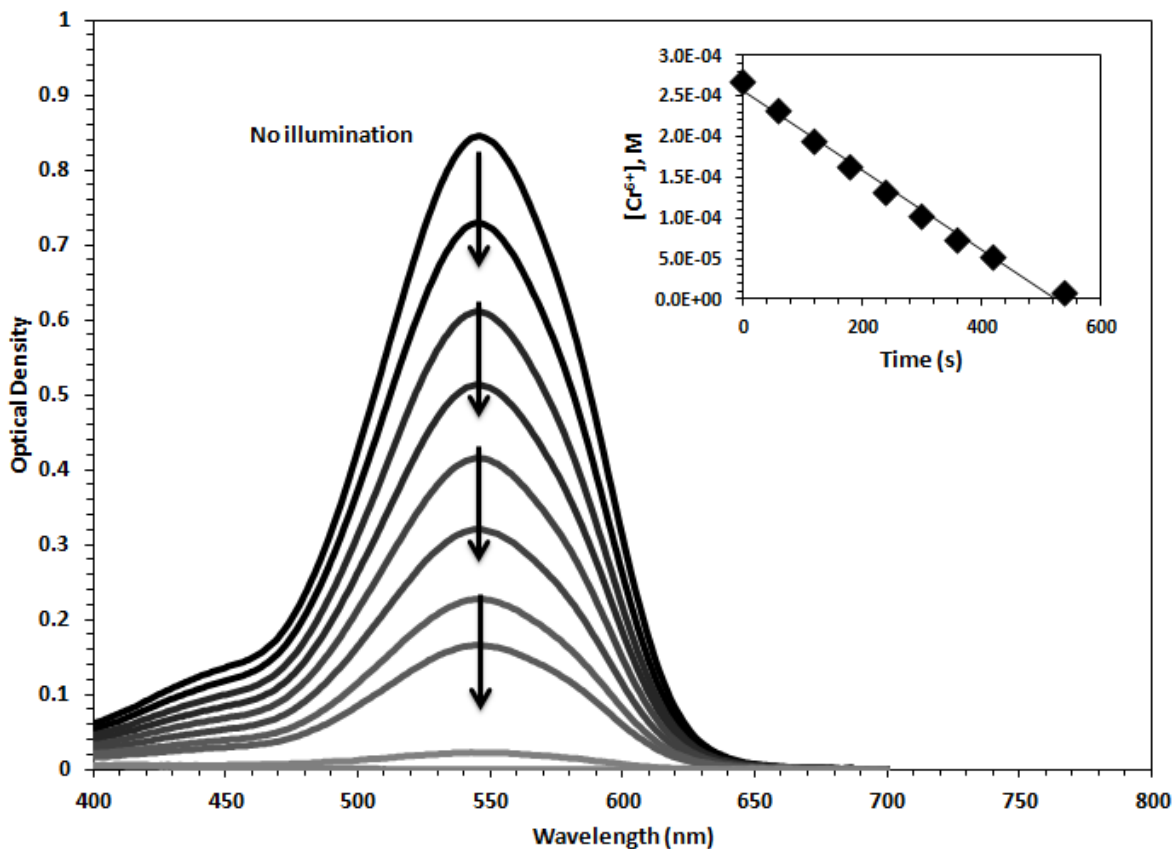


Figure 3-3. Optical spectra obtained after analysis with the 1,5-diphenylcarbazide (DPC) method on air-saturated, photolyzed solutions at pH = 5.7 containing 0.018 M SPEEK, 0.36 M PVA, and  $2.8 \times 10^{-4}$  M hexavalent chromium. Solution samples were diluted by a factor of 3 during the Cr(VI) assay. Top to bottom: samples irradiated with 350 nm light,  $I_0 = 3.5 \times 10^{-5}$  M(hv)/s, for 0 min, 1, 2, 3, 4, 5, 6, 7, 9 min, and no Cr(VI). Inset: Plot of absorbance at 545 nm divided by  $\epsilon$  as a function of irradiation time ( $l = 0.2$  cm).

Quantifications of the [Cr(VI)] remaining in solution after illumination were carried out by the DPC spectrophotometric method; the extinction coefficient for the resulting colored Cr(III) complex was determined in SPEEK/PVA solution to be  $4.71 \times 10^4 \text{ M}^{-1}\text{cm}^{-1}$  at the 545 nm. This  $\epsilon$  value is 8% higher than the extinction coefficient reported previously,<sup>26</sup> which is possibly due to the presence of polymers in the detection solution. Figure 3.3 shows optical spectra recorded after mixing the DPC reagent with aliquots from an solution containing Cr(VI), SPEEK

and PVA that was illuminated for different times. The absorption signal centered at  $\lambda_{\text{max}} = 545$  nm was found to decrease in intensity as the illumination progressed.

Consequently, the concentration of hexavalent chromium decreased during photolysis in the presence of air; the corresponding kinetic data are presented in the inset of Figure 3-3. As shown in the inset, [Cr(VI)] decreased linearly with irradiation time throughout the transformation, implying that the reaction is zero-order with respect to the metal ion concentration. Therefore, the rate of the Cr(VI) reduction,  $r(-\text{Cr(VI)})$ , was obtained from the slope of zero-order plots. This rate was useful to evaluate the quantum yield of Cr(VI) reduction using the equation  $\phi(-\text{Cr(VI)}) = r(-\text{Cr(VI)})/I_0$ , which will be discussed later in this chapter. In systems devoid of SPEEK, where the Cr(VI) reduction was not a linear function of time  $\phi(-\text{Cr(VI)})$  was calculated from the initial rate of reaction,  $r_i(-\text{Cr(VI)})$ , evaluated via extrapolation to  $t = 0$ .

The photochemical reduction of Cr(VI) in SPEEK/PVA solutions is initiated by the photogeneration of SPEEK<sup>•</sup> radicals, a product of <sup>3</sup>SPEEK\* H-atom abstraction from PVA, which is similar to the light-induced transformations of benzophenone with isopropyl alcohol.<sup>27</sup>

Reduction of hexavalent chromium to the trivalent state will involve protons in aqueous media as represented by the following overall equation:



As shown in Chapter 2, each  $\alpha$ -hydroxy radical of SPEEK produces a proton upon reducing an electron acceptor. However, equation 3.6 indicates that the  $\text{HCrO}_4^-$  reduction requires 7  $\text{H}^+$  ions but the SPEEK radicals involved in the reduction can provide only 3 protons. Thus, a pH increase is anticipated in the absence of a species capable to donate  $\text{H}^+$ . To avoid pH increases,

which will alter the thermodynamics of the Cr(VI) reduction, the photochemical transformations were investigated in solutions containing inert buffers able to function as a source of H<sup>+</sup> ions.

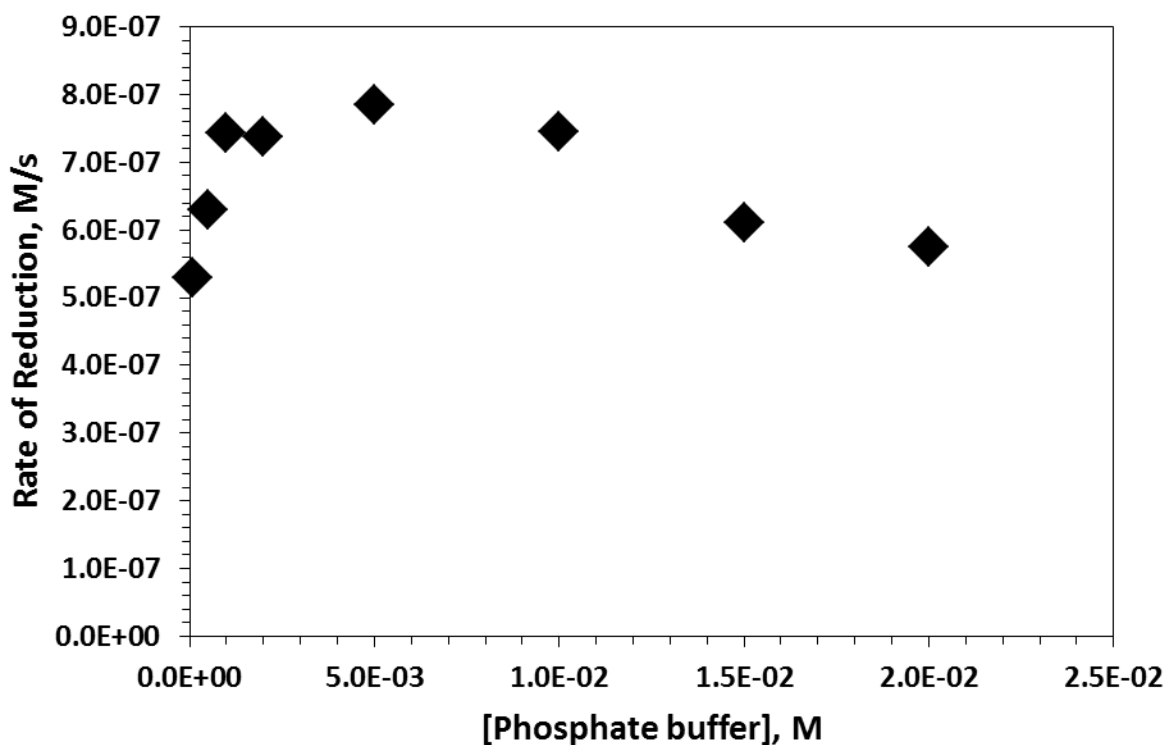


Figure 3-4. Dependence of rate of reduction for Cr(VI) on phosphate buffer concentration in air-saturated solutions containing 0.018 M SPEEK, 0.36 M PVA, and  $3.2 \times 10^{-4}$  M Cr(VI) with pH = 5.6. Irradiations with 350 nm photons ( $I_0 = 3.5 \times 10^{-5}$  M(hv)/s).

The dependency of rates of Cr(VI) reduction in SPEEK/PVA solutions on phosphate buffer concentrations at a constant pH of 5.7 is shown in Figure 3-4. An immediate increase in reduction rates is noticed with solutions containing up to 5 mM of phosphate buffer, but a gradually decrease in reduction rate is apparent at higher concentrations.

Numerous studies using a variety of polyelectrolytes, most notably sodium polystyrene sulfonate (NaPSS) as a model compound, have shown that polyions experience changes in conformation and also in aggregation when the ionic strength is raised using inert



electrolytes.<sup>28,29</sup> The effect of electrolytes on SPEEK chains has not been investigated but, given the structural analogies of this material with NaPSS, a logical expectation is that increases in the phosphate buffer concentration will induce changes in the aggregation and conformation of the polyketone chains. The initial increase in  $r(-\text{Cr(VI)})$  to reach a maximum rate at 5 mM buffer shown in Figure 3.4 can be understood in terms of reaction 3.6 since  $\text{H}^+$  ions provided by the buffer enabled the reduction to occur efficiently. Unraveling the causes that induce the decrease in  $r(-\text{Cr(VI)})$  at higher [buffer] is not possible as the concomitant ionic strength increases affect both the conformation and aggregation of the SPEEK chains and the effects of such alterations in the photochemical reactivity of the polyketone are not easy to predict. In fact, both polymer aggregation and formation of more compact chain conformations could reduce the photochemical reactivity of SPEEK. Such expectation arises because both alterations could bring the BP groups of SPEEK closer to each other. BP is known to quench benzophenone molecules in their triplet excited state with a quenching rate constant of  $k_Q = 1.6 \times 10^8 \text{ M}^{-1} \text{ s}^{-1}$ .<sup>30</sup> Factors that facilitate proximity of the BP groups in SPEEK will enhance quenching of the triplet excited state and lower the efficiency of radical photogeneration, thereby decreasing the rate of Cr(VI) reduction.

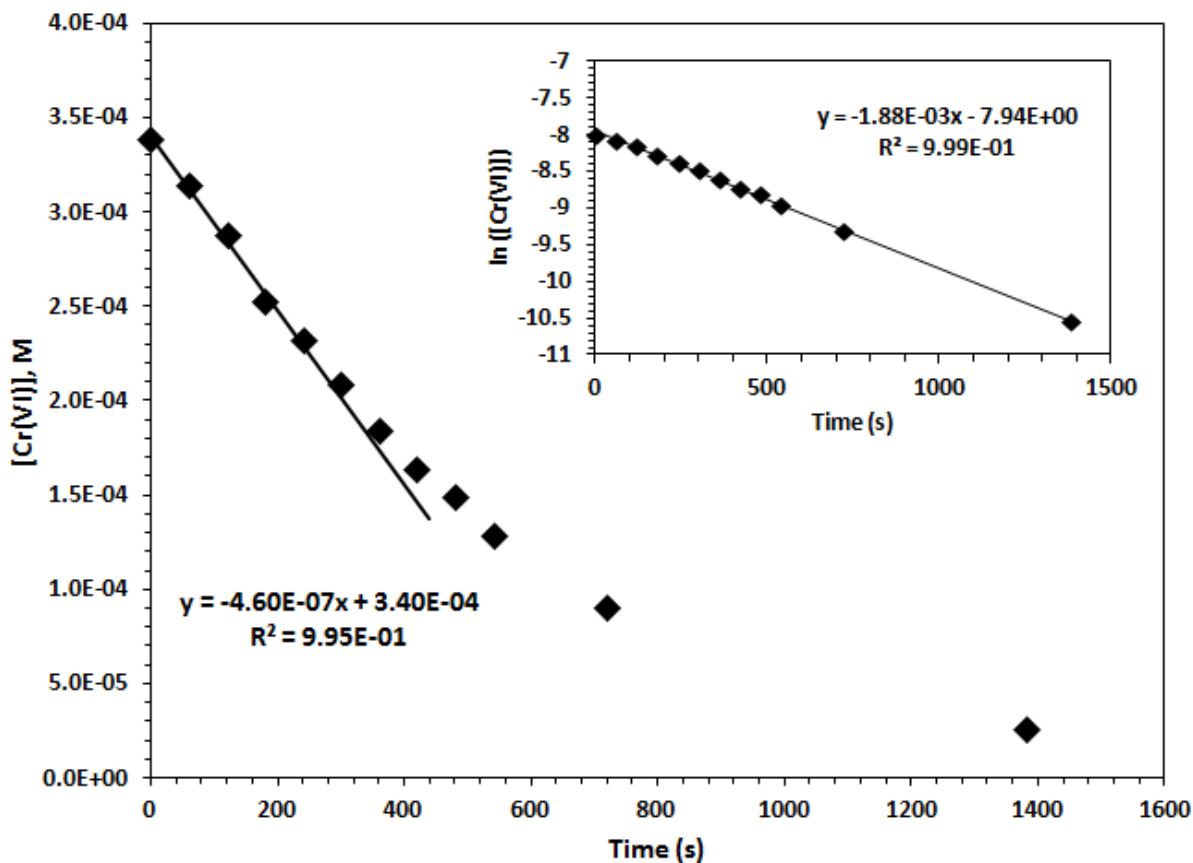


Figure 3-5. Plot of the reduction of Cr(VI) in buffered 0.36 M PVA solution containing  $3.4 \times 10^{-4}$  M Cr(VI) with pH = 5.7. Irradiations with 350 nm photons ( $I_0 = 3.5 \times 10^{-5}$  M(h $\nu$ )/s). Inset: first order plot.

Cr(VI) is known to undergo photochemical reduction in the presence of an alcohol in aqueous, acidic solutions without an additional photosensitizer.<sup>31, 32</sup> By comparing the reduction of Cr(VI) in solutions free of SPEEK with results obtained in the presence of the polyketone, a better understanding of the role of the photosensitizer will be obtained in order to formulate a simple mechanism for Cr(VI) reduction in the polymeric system. Polymeric solutions free of SPEEK were prepared as previously stated, however without the addition of SPEEK. Figure 3-5 shows the photo-induced reduction of Cr(VI) in phosphate buffer solution containing PVA, where [Cr(VI)] was measured spectrophotometrically by direct analysis of the irradiated sample.

Obviously, the results showed that the zero-order dependence observed for the SPEEK-induced photoreduction (Figure 3-3) was not followed when  $\text{HCrO}_4^-$  ions were exposed to 350 nm photons. The data shown in the inset confirm that direct excitation of Cr(VI) ions induced a photoreduction that is first-order with respect to  $[\text{Cr(VI)}]$ . Comparisons of the reduction rates in the presence and absence of SPEEK can be made from the results shown in Figure 3-4 and the  $r_i(-\text{Cr(VI)})$  value presented in Figure 3-5. In the presence of SPEEK and in a solution with 5 mM phosphate buffer  $r(-\text{Cr(VI)}) = 7.8 \times 10^{-7} \text{ M s}^{-1}$ , that is close to 2 times the initial rate evaluated without the polyketone,  $4.8 \times 10^{-7} \text{ M s}^{-1}$ . However, the initial reaction rate decreases in the absence of SPEEK because less photons are absorbed as the reaction progresses due to the consumption of the Cr(VI) chromophore. Hence, this is the reason for the first-order rate law observed under such conditions. In the presence of SPEEK the rate is independent of  $[\text{Cr(VI)}]$  because the polyketone acts as a sensitizer that is not consumed during the photoreaction. The results presented in Figure 3-5 suggested that the Cr(VI) reduction in the presence of SPEEK could, in principle, operate via two reaction channels: one involving the photochemistry initiated via excitation of the polyketone, and another involving absorption of photons directly by  $\text{HCrO}_4^-$  ions. However, the experimental conditions selected ( $[\text{SPEEK}] \gg [\text{Cr(VI)}]$ ) favored the first reaction channel given that under such conditions most of the photons were anticipated to be absorbed by the polymeric ketone. The faster Cr(VI) reduction in the presence of SPEEK together with the different rate law for this process support the conclusion that the reaction channel involving absorption of photons directly by the metal ions played no important role when the polyketone was present.

Westheimer *et. al.* were able to prove that the primary step of chromate reduction by 2-propanol to acetone (or the oxidation of 2-propanol by chromate) in acidic aqueous solution was proceeded by an ester complex<sup>31</sup>,



Any dichromate in solution (<1%) is inactive during the reduction process. Klaning also, found the dichromate ion to interact weakly with 2-propanol in aqueous solution of  $10^{-3}$  M perchloric acid, and ultimately determined the equilibrium constant of 1:1 ester complexes of acid chromate ion ( $10^{-4}$  M Cr(VI)) with alcohols or acetaldehyde which was analyzed by spectrophotometric determinations.<sup>32</sup> The equilibrium constant he obtained was measured to be  $0.078 \text{ M}^{-1}$  at  $25^\circ\text{C}$  for Cr(VI) in aqueous solutions containing 2-propanol. Because 2-propanol is analogous to PVA, the concentration of Cr(VI):PVA complex can be estimated by using the mentioned equilibrium constant with the concentration of the PVA in the system (0.36 M) and the calculated concentration of  $\text{HCrO}_4^-$  from the Minteqa2 speciation program ( $2.4 \times 10^{-4}$  M). The value obtained for the [Cr(VI):PVA] complex is  $6.7 \times 10^{-6}$  M, which is a ratio of 36:1 of Cr(VI) oxyanions to one Cr(VI):PVA complex in the standard system. These rough estimates suggest that the [Cr(VI):PVA] is not a species that played an important role during the photoreduction of  $\text{HCrO}_4^-$  ions.

### 3.3.2 Effect of Light Intensity

The fact that Cr(VI) was photoreduced via a zero-order rate law suggested that the overall process was controlled by the initial light-initiated formation of polymer radicals as was found during the conversion of  $\text{O}_2$  into  $\text{H}_2\text{O}_2$ .<sup>22</sup> Confirmation of such interpretation was provide by tests on the effect that systematic variations of  $I_0$  exerted on the reaction rate for solutions of

SPEEK/PVA. Presented in Figure 3-6 are kinetic plots obtained using different light intensities for SPEEK/PVA solutions with an initial Cr(VI) concentrations of about  $2.1 \times 10^{-4}$  M. Reasonable zero order processes were observed; as shown in the inset of Figure 3-6,  $r(-\text{Cr(VI)})$  increased in a linear fashion with  $I_0$  ( $r^2 = 0.98$ ). The slope of the straight line corresponded to the quantum yield for the reduction of Cr(VI) in the presence of SPEEK, amounting to  $\phi(-\text{Cr(VI)}) = 0.012$ . These observations imply that the light intensity was the factor controlling the speed of the Cr(VI) photoreduction and that the reaction rate was first-order with respect to  $I_0$ . Consequently, the rate of the Cr(VI) reduction was dictated by the speed at which SPEEK radicals were generated; since SPEEK $\bullet$  is formed with a constant rate under continuous photolysis the result being a zero-order consumption of  $\text{HCrO}_4^-$  ions. Photogeneration of hydrogen peroxide in air-saturated SPEEK/PVA solution of the same polymer concentrations as used in the present study resulted in  $\phi(\text{H}_2\text{O}_2) = 0.02$ .<sup>22</sup> The previous study yielded a  $[\text{O}_2]$  in SPEEK/PVA solutions equal to  $2.6 \times 10^{-4}$  M, which is close to the  $[\text{Cr(VI)}]$  employed in the experiments of Figure 3-6. Under such conditions  $\text{O}_2$  is anticipated to compete with Cr(VI) for SPEEK $\bullet$ . As was shown earlier,<sup>22</sup>  $\text{H}_2\text{O}_2$  is formed when SPEEK radicals are scavenged by  $\text{O}_2$  but the peroxide generated is 2 orders of magnitude less than the presence of chromium. Also, the  $\text{H}_2\text{O}_2$  formed is not an effective reductant of Cr(VI) at  $\text{pH} > 5$ .<sup>33</sup> This means that the photogenerated  $\text{H}_2\text{O}_2$  was not a contributor to the photoreduction of Cr(VI). Hence, the loss of some SPEEK $\bullet$  due to scavenging by  $\text{O}_2$  is the reason for  $\phi(-\text{Cr(VI)})$  being lower than the quantum yield for  $\text{H}_2\text{O}_2$  formation determined previously in the absence of Cr(VI). Support for this interpretation is provided below by the larger  $\phi(-\text{Cr(VI)})$  values determined in solutions with higher  $[\text{Cr(VI)}]$ .

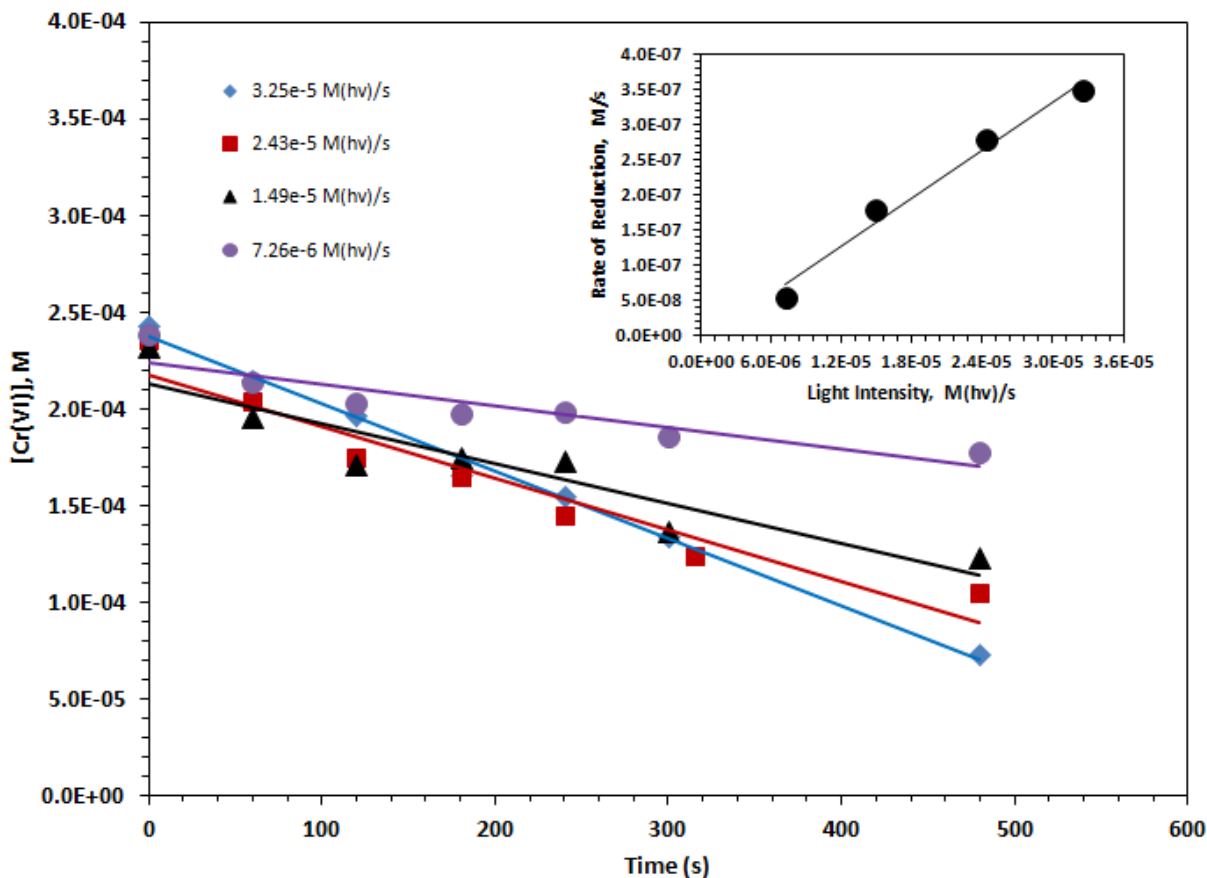


Figure 3-6. Determinations of reduction of Cr(VI) in air saturated solutions of 0.018 M SPEEK/0.36 M PVA containing  $2.1 \times 10^{-4}$  M Cr(VI) and 5 mM phosphate buffer at pH 5.7. Irradiations are at various light intensities ( $I_0$ ). Inset: plot of the rate of Cr (VI) reduction as a function of incident  $I_0$ .

### 3.3.3 Effect of pH on Cr(VI) Reduction

Illustrated in Figure 3-7a is the dependence of  $\phi(-\text{Cr(VI)})$  on  $[\text{H}^+]$  for SPEEK/PVA solutions with pH values in the range of 5 and 9. The equivalent plot for solutions containing PVA but no SPEEK is shown in Figure 3-7b. As shown in Figure 3-7a, the photoreaction in SPEEK/PVA solutions containing  $1 \times 10^{-3}$  M Cr(VI) was most efficient at pH 5.7 with a quantum yield of 0.045. This is a higher efficiency than the  $\phi(-\text{Cr(VI)})$  value obtained at the same pH from the data of Figure 3-6, determined at a lower  $[\text{Cr(VI)}]$  of  $2.1 \times 10^{-4}$  M. These

results are consistent with the assumption that scavenging of  $\text{SPEEK}^\bullet$  by  $\text{O}_2$  affected the efficiency of the photoreduction; at higher  $[\text{Cr(VI)}]$  the metal ions outcompeted oxygen for the reducing radicals, thereby increasing  $\phi(-\text{Cr(VI)})$ . Further evidence of this behavior are the systematically higher reduction quantum yields depicted at  $5 \leq \text{pH} \leq 6$  in Figure 3-7a when  $[\text{Cr(VI)}]$  was increased from 0.32 to 1 mM.

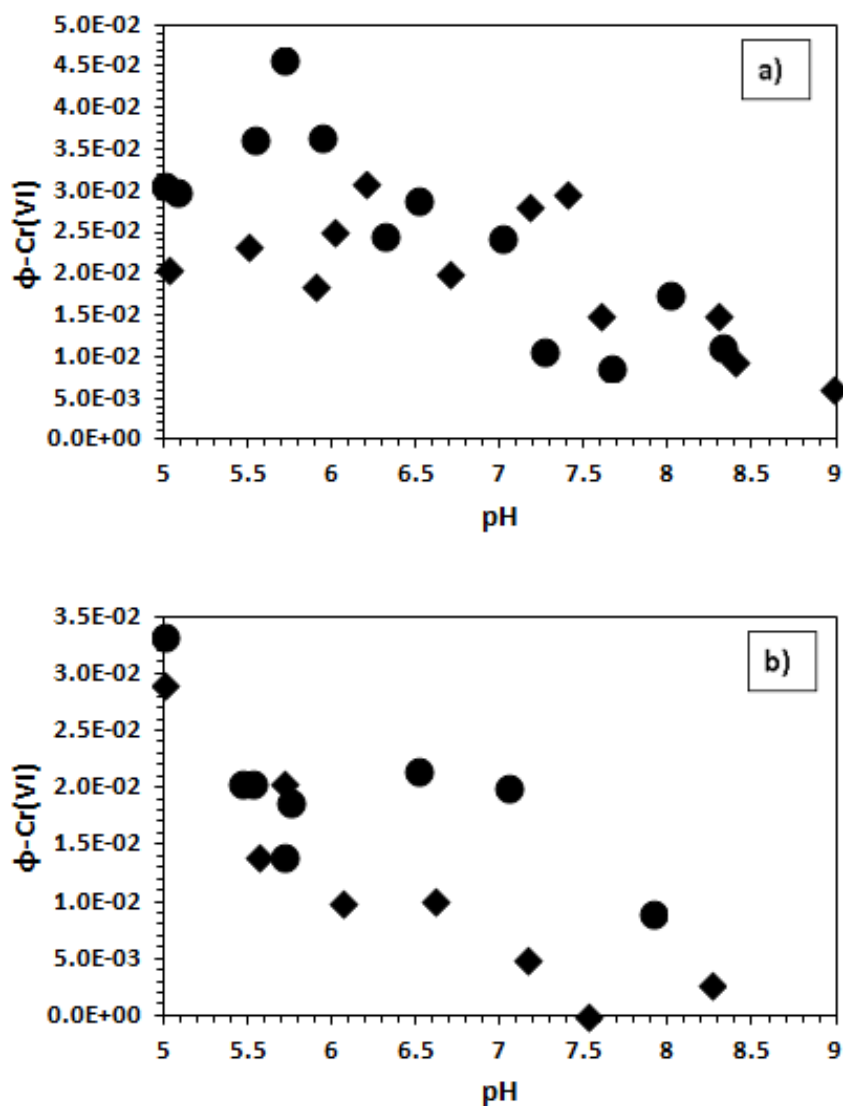


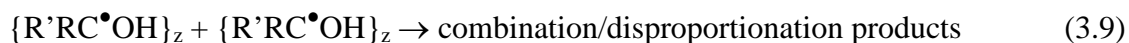
Figure 3-7. Quantum yield of Cr(VI) reduction dependence on the solution pH. Determinations of reduction rates were carried out using air-saturated, buffered (5 mM) solutions containing; a) 0.018 M SPEEK/ 0.36 M PVA with initial  $\text{Cr}^{6+}$  concentrations of  $3.2 \times 10^{-4}$  M (◆) and  $1 \times 10^{-3}$  M (●) and b) 0.36 M PVA with initial  $\text{Cr}^{6+}$  concentrations of  $3.2 \times 10^{-4}$  M (◆) and  $1 \times 10^{-3}$  M (●). ( $I_0 = 3.0 \times 10^{-5}$  M(hv)/s).

Another trend that is noticed in Figure 3-7a pertains to the gradual decrease of  $\phi(-\text{Cr(VI)})$  that occurred with increasing solution basicity and also the similar  $\phi(-\text{Cr(VI)})$  values obtained at  $\text{pH} > 6$  irrespective of  $[\text{Cr(VI)}]$ . Such evolution of the reduction efficiency with increasing  $\text{pH}$  is not unexpected since the standard redox potential for reaction 3.6 follows the Nernst equation,  $E = (1.35 - 0.138 \text{ pH}) \text{ V}$ , whereas the potential for reaction 3.8,



obeys the relationship,  $E = (1.48 - 0.158 \text{ pH}) \text{ V}$ .<sup>34</sup> As is the case with all  $\alpha$ -hydroxy radicals, the redox potential of  $\{\text{R}'\text{R}'\text{COH}\}_z$  is expected to increase with  $\text{pH}$  since the deprotonated form, the radical anion  $\{\text{R}'\text{R}'\text{CO}^-\}_z$ , is a stronger reducing agent than  $\text{SPEEK}^\bullet$ .<sup>22</sup> However, because of the stronger dependence of reactions 3.6 and 3.8 on  $[\text{H}^+]$  than for the ionization of  $\text{SPEEK}^\bullet$ , the net result is a decrease in the driving force for the reduction of  $\text{Cr(VI)}$  with increasing  $\text{pH}$ . The decrease in the thermodynamic driving for the  $\text{Cr(VI)}$  reduction with increasing basicity explains the decline of  $\phi(-\text{Cr(VI)})$  observed at  $\text{pH} > 6$  in Figure 3-7a.

Earlier work in our group has shown that in neutral systems containing  $\text{Ag}^+$  and  $\text{Cu}^{2+}$ , the quantum yield of the triplet excited state of SPEEK,  $^3\text{SPEEK}^*$ , reaches values between 0.04-0.056.<sup>19a</sup> Since, as shown in Chapter 2, each  $^3\text{SPEEK}^*$  forms 2 polyketone radicals, then the  $\text{SPEEK}^\bullet$  quantum yield is anticipated to be in the range of 0.08-0.112. However, some of the SPEEK radicals persist for several minutes at room temperature and the quantum yield determined experimentally,  $\phi_i(\text{SPEEK}^\bullet)$ , is 0.02.<sup>19</sup> The reason for the discrepancy in  $\phi_i(\text{SPEEK}^\bullet)$  is due to the decay of  $\text{SPEEK}^\bullet$  via dimerization and disproportionation processes that are typical of  $\alpha$ -hydroxy radicals. Those reactions are represented by the following equation,





According to equation 3.5 the irreversible reduction of Cr(VI) requires 3 SPEEK radicals, meaning that the quantum yield for SPEEK<sup>•</sup> that participated in the reaction amounts to 0.135. This yield is slightly higher than the expected value based on the earlier quantum yield for <sup>3</sup>SPEEK\*. Consequently, Cr(VI) is a more efficient scavenger for SPEEK<sup>•</sup> than O<sub>2</sub>, Ag<sup>+</sup> and Cu<sup>2+</sup>, which intercepted only between 40 and 80 % of the photogenerated SPEEK radicals.

The data presented in Figure 3-7a indicate a decrease of  $\phi(-\text{Cr(VI)})$  at pH = 5, a result that is not surprising given that the yield of H<sub>2</sub>O<sub>2</sub> decreases with increasing solution acidity.<sup>22</sup> Such an effect is understandable having in mind that the triplet excited state of benzophenone, <sup>3</sup>BP\*, undergoes quenching by H<sub>3</sub>O<sup>+</sup>; a similar proton-induced deactivation of <sup>3</sup>SPEEK\* explains the lower yields for both the O<sub>2</sub> and Cr(VI) reductions observed in acid solutions. In the case of Cr(VI) the increases in the driving force induced by lowering the pH is counterbalanced by the quenching effect that H<sub>3</sub>O<sup>+</sup> exerts. For this reason a maximum in  $\phi(-\text{Cr(VI)})$  was obtained in the pH range of 5 to 6 and not in neutral solutions as observed during the H<sub>2</sub>O<sub>2</sub> formation.

A different evolution of  $\phi(-\text{Cr(VI)})$  vs pH is depicted in Figure 3-7b for illuminations of solutions free of SPEEK. In such systems  $\phi(-\text{Cr(VI)})$  achieves a maximum value at pH = 5 close to the quantum yield obtained in the presence of SPEEK. The reduction efficiency remains about constant in the range of  $5.5 \leq \text{pH} \leq 6.5-7$  but decreases abruptly thereafter. Also, at both [Cr(VI)] the  $\phi(-\text{Cr(VI)})$  values are about 30-50 % lower than the corresponding quantum yields shown in Figure 3-7a for solution with SPEEK. These observation indicate that the photoreduction of Cr(VI) was significantly different in the presence and absence of SPEEK. Values of  $\phi(-\text{Cr(VI)})$  have reported for air-saturated PVA solutions in the pH range of 1.4 to 3.6 that contained 1 mM Cr(VI).<sup>35</sup> A trend similar to that shown in Figure 3.7b was reported with efficiencies that decreased with increasing pH. The highest quantum yield (0.022) was

determined at pH = 1.4, decreasing drastically to a value 20 times lower at pH = 2 and remaining constant thereafter. Such lower quantum yields probably are a consequence of the 20 times smaller [PVA] used in the previous study.

PVA films containing Cr(VI) are important holographic materials and the photochemical formation of images in these systems has been investigated extensively.<sup>36</sup> Generation of holographic images results from crosslinking of PVA chains and radicals of this polymer are frequently invoked as important intermediates in such processes. Such polyol radicals have been detected via ESR techniques during illumination of PVA films containing Cr(VI).<sup>35</sup> Hydrogen-atom abstraction from PVA yields  $\alpha$ -hydroxy radical of the polyol that are strong reducing agents.<sup>37</sup> If the Cr(VI) photoreduction proceeded via involvement of the  $\alpha$ -hydroxy radicals of PVA as reducing agents then similar results should have been obtained in solutions with and without SPEEK. The fact that significant differences were observed in Figures 3-7a and 3-7b clearly indicates that the reaction mechanism is different when light is absorbed by the  $\text{HCrO}_4^-$  ions as compared with the case of SPEEK acting as the sensitizer. A plausible mechanism for the photochemistry observed in the absence of SPEEK involves a two-electron oxidation of PVA by the excited Cr(VI) species as proposed previously.<sup>35</sup> In that mechanism the PVA radicals are no longer the key species that initiate the reduction of Cr(VI) as they are generated via a subsequent, non-photochemical reaction involving Cr(IV). Such a mechanism predicts a stronger dependence of the reduction quantum yield on solution pH given that the driving force provided by the reactivity of  $\alpha$ -hydroxy radical is not available to compensate for the increasingly less favorable conditions induced by increases in pH.

### 3.3.4 Cr(VI) Photoreduction in SPEEK/PVA Films

A viable application for SPEEK/PVA to be used in waste water treatment would be as a film that collects and filters out Cr(VI) by reduction to nontoxic trivalent chromium. A benefit of using SPEEK/PVA films for chromium waste water treatment is the swelling ability; an increase in surface area increases reaction site for Cr(VI) reduction. Film was immersed in air-saturated, buffered solution containing  $3.4 \times 10^{-4}$  M Cr(VI) equilibrated for 1 hour before commencing with illuminations. An aliquot was taken before exposure to 350 nm photons for the initial concentration of [Cr(VI)] and was measured by direct analysis of the solutions. Illumination yielded an optical signal with wavelengths of maximum absorptions at 256 and 350 nm with a broad shoulder at 450 nm that decayed slowly over a few hours.

Figure 3-8 shows the reduction of Cr(VI) in SPEEK/PVA film swollen in buffered solution containing  $3.4 \times 10^{-4}$  M Cr(VI). Quantifications of the remaining [Cr(VI)] in solution after illumination in film were carried out by direct analysis in 1 cm cells. The extinction coefficient for Cr(VI) was measured in SPEEK/PVA solutions to be  $1580 \text{ M}^{-1}\text{cm}^{-1}$  ( $\lambda_{\text{max}} = 350$  nm), which has a 1.2% error based on literature value obtained in aqueous solutions.<sup>38</sup> The data in Figure 3-8 clearly demonstrated the reduction of Cr(VI) in SPEEK/PVA film in the presence of air.

The inset shows a new species has formed from the photolysis of SPEEK/PVA film water-swollen in buffered Cr(VI) solution. This new species appears at 220 minutes after irradiation and has an optical maximum absorption at 290 nm with a small shoulder appearing at 237 nm. A similar signal has been obtained and identified as the superoxochromium(III) ion,  $\text{CrO}_2^{2+}$ , with an extinction coefficient of  $3100 \text{ M}^{-1}\text{cm}^{-1}$  ( $\lambda_{\text{max}} = 290$  nm).<sup>39</sup>

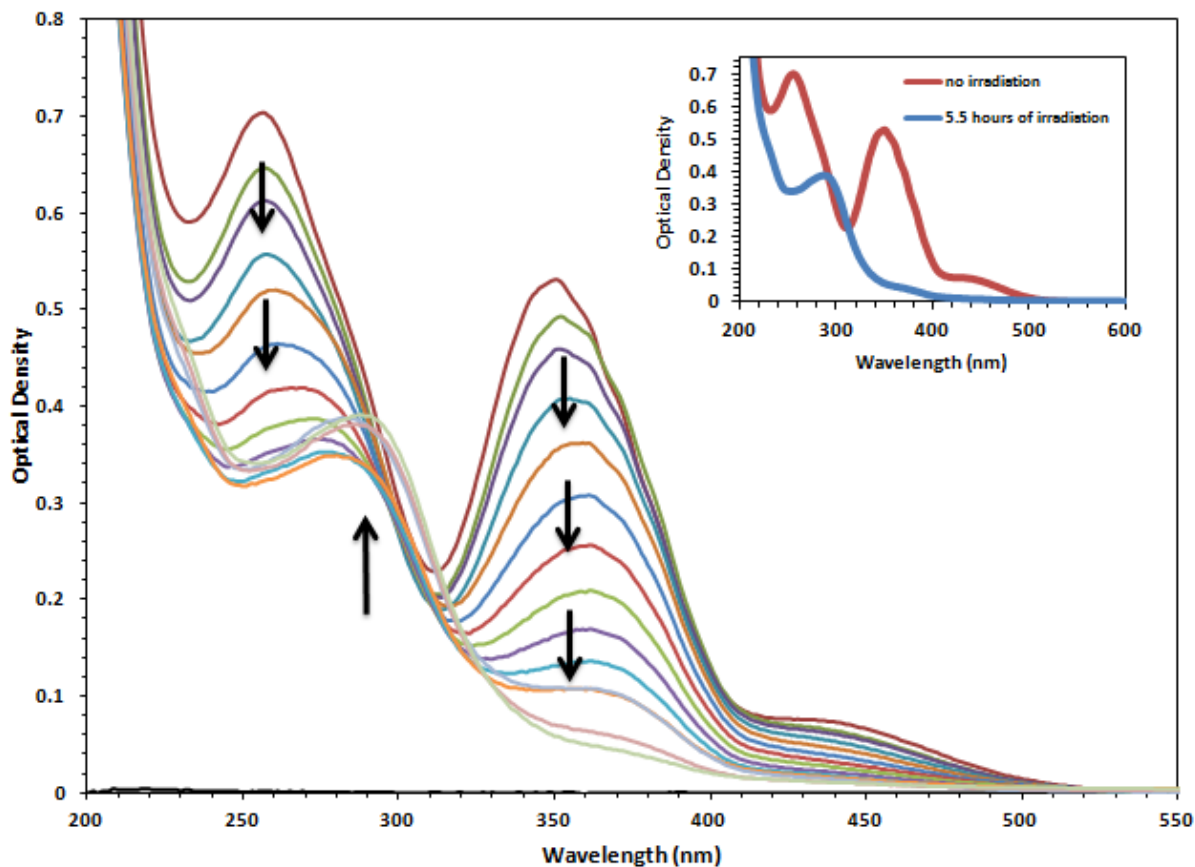


Figure 3-8. Spectra of photoreduction of Cr(VI) in water-swollen SPEEK/PVA Film. Irradiation of film was conducted in buffered solution of  $3.4 \times 10^{-4}$  M Cr(VI) with 350 nm photons with intensity of  $3 \times 10^{-5}$  M(hv)/s and pH was 5.7. [Cr(VI)] was detected by direct analysis of solution ( $l = 1$  cm). Film surface area was  $24 \text{ cm}^2$ . *Inset*: Comparison plot of the abs spectra of chromium solution before irradiation and 5.5 hrs after irradiation.

Formation of superoxochromium(III) was generated within the film and possibly diffused into solution. The stability of  $\text{CrO}_2^{2+}$  in air-saturated solutions continues for at least 30 minutes at room temperature before decomposing to Cr(III).<sup>39</sup> The  $\text{CrO}_2^{2+}$  generated in the film is stable for more than 24 hours in a closed vessel. Quantification of  $\text{CrO}_2^{2+}$  was calculated to be  $1.2 \times 10^{-4}$  M, which is approximately 1/3 of the initial Cr(VI) concentration. Results obtained from ICP analysis on the chromium solution is in agreement with spectrophotometric data. The remainder of chromium may exist as a complex bound within the film.

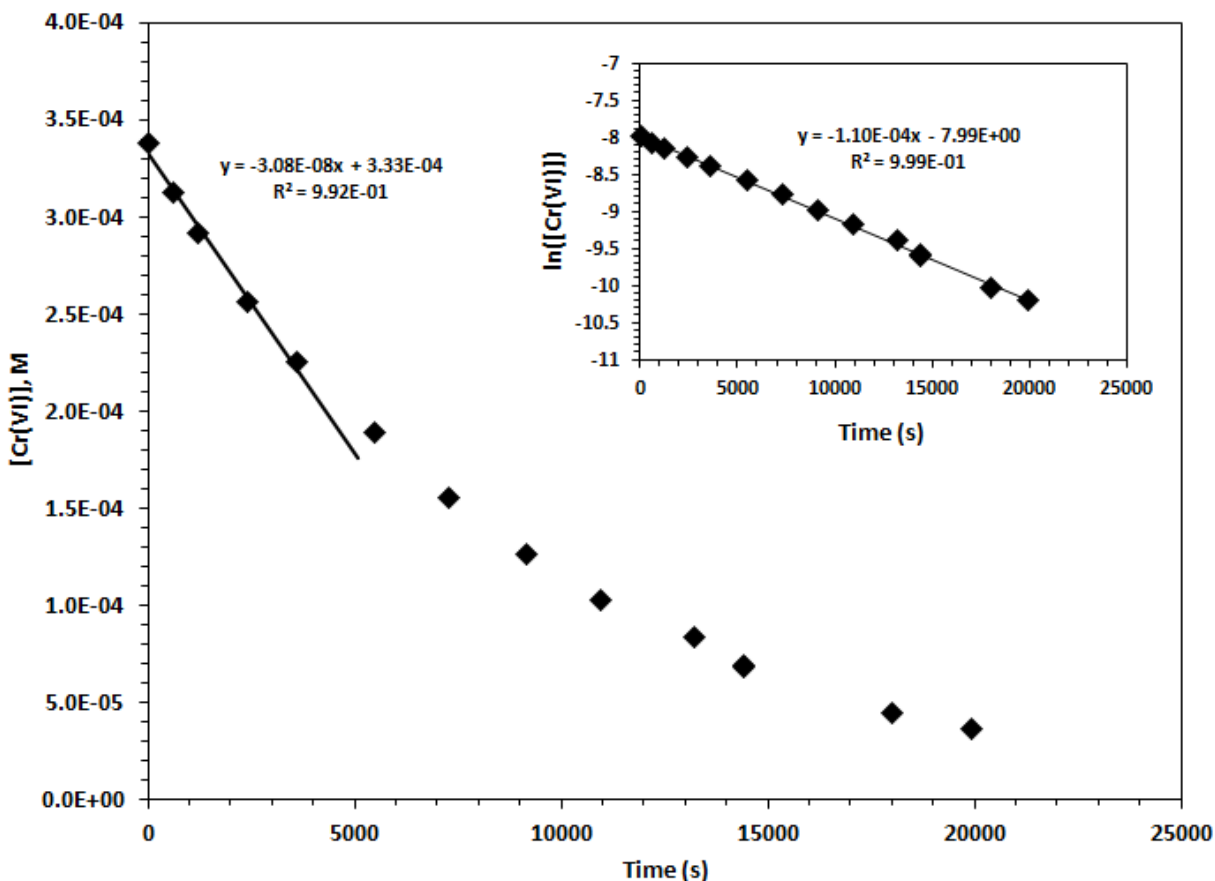


Figure 3-9. Photoreduction of Cr(VI) in swollen SPEEK/PVA Film. Irradiation of film was conducted in air-saturated, buffered solution of  $3.4 \times 10^{-4}$  M Cr(VI) with 350 nm photons ( $I_0 = 3 \times 10^{-5}$  M(hv)/s, pH = 5.7). [Cr(VI)] was detected by direct analysis ( $l = 1$  cm,  $\epsilon = 1580$  cm<sup>-1</sup>M<sup>-1</sup>). *Inset*: First order reduction plot.

Figure 3-9 shows the reduction process of Cr(VI) in SPEEK/PVA film, and the inset shows that the reduction is first-order in [Cr(VI)]. Unlike the zero-order reduction process seen in solutions of SPEEK/PVA, a different reduction process is observed in the films primarily due to the incorporation of  $\text{HCrO}_4^-$  is limited by the presence of negatively charged sulfonic groups in the polymer film. By obtaining the initial rate of reduction, the initial quantum yield of Cr(VI) reduction by SPEEK/PVA was acquired to be  $\phi_i(-\text{Cr(VI)}) = 0.47$ . The yield is ten times higher than that obtained in solutions of SPEEK/PVA. Because Cr(VI) requires 3 SPEEK• for fully

reduction to Cr(III), the quantum yield for the SPEEK● radicals scavenged by chromium is  $\phi(\text{SPEEK}\bullet) = 1.41$ . This means that Cr(VI) was able to scavenge more radicals than oxygen,  $\text{Ag}^+$  and  $\text{Cu}^{2+}$ .<sup>19a</sup>

### 3.4 Conclusions

Photoreduction of Cr(VI) in SPEEK/PVA films has demonstrated that the polymeric system has the potential to function as a means of treatment for contaminated water by collecting and/or reducing hexavalent chromium. Studies of the Cr(VI) reduction in polymeric solutions prove that the constant presence of SPEEK as a photoinitiator is more efficient with a zero order reduction process. Because the system is light-sensitive, the rate determining step is the photochemical process that generates SPEEK radicals, which was proven to be first order in respect of light intensity. The reduction yields dependence on pH is great, therefore a maximum quantum yield of Cr(VI) reduction was reached at pH 5.7. Though oxygen is a quencher of the reactive photoinitiator, reduction of Cr(VI) is still competitive and prevails.

## References

- 1) Stern, A.H. A Quantitative Assessment of the Carcinogenicity of Hexavalent Chromium by the Oral Route and Its Relevance to Human Exposure. *Environ. Res.*, **2010**, *110*, 798-807.
- 2) Reynolds, M.F.; Peterson-Roth, E.C.; Bessalov, I.A.; Johnston, T.; Gurel, V.M.; Menard, H.I.; Zhitkovich, A. Rapid DNA Double-Strand Breaks Resulting from Processing of Cr-DNA Cross-Links by Both MutS Dimers. *Cancer Res.*, **2009**, *69*, 1071-1079.
- 3) Vincent, J. B. Chromium: Celebrating 50 Years as an Essential Element? *Dalton Trans.* **2010**, *39*, 3787-3794.
- 4) Nguyen, A.; Mulyani, I.; Levina, A.; Lay, P.A. Reactivity of Chromium(III) Nutritional Supplements in Biological Media: An X-Ray Absorption Spectroscopic Study. *Inorg. Chem.* **2008**, *47*, 4299-4309.
- 5) Cetin, D.; Donmez, S.; Donmez, G. The Treatment of Textile Wastewater Including Chromium(VI) and Reactive Dye by Sulfate-Reducing Bacterial Enrichment. *J. Environ. Manage.*, **2008**, *88*, 76-82.
- 6) Losi, M.E.; Amrhein, C.; Frankenberger Jr., W.T. Environmental Biochemistry of Chromium. *Rev. of Environ. Contam. and Toxicol.*, **1994**, 13691-13121.
- 7) Choppala, G.; Bolan, N.; Seshadri, B. Chemodynamics of Chromium Reduction in Soil: Implications to Bioavailability. *J. Hazard. Mater.*, **2013**, *261*, 718-724.
- 8) Nordstrom, D.K. Hydrogeochemical Processes Governing the Origin, Transport, and Fate of Major and Trace Elements from Mine Wastes and Mineralized Rock to Surface Waters. *Appl. Geochem.* **2011**, *26*, 1777-1791.
- 9) Torras, J.; Buj, I.; Rovira, M.; de Pablo, J. Chromium Recovery from Exhausted Baths Generated in Plating Processes and Its Reuse in the Tanning Industry. *J. Hazard. Mater.*, **2012**, *209-210*, 343-347.
- 10) Legrini, O.; Oliveros, E.; Braun, A.M. Photochemical Processes for Water Treatment. *Chem. Rev.* **1993**, *93*, 671-698.
- 11) Mytych, P.; Stasicka, Z. Photochemical Reduction of Chromium(VI) by Phenol and Its Halogen Derivatives. *Appl. Catal. B: Environ.*, **2004**, *52*, 167-172.
- 12) Hug, S.J.; Laubscher, H.U. Iron(III) Catalyzed Photochemical Reduction of Chromium(VI) by Oxalate and Citrate in Aqueous Solutions. *Environ. Sci. Technol.*, **1997**, *31*, 160-170.
- 13) Mytych, P.; Karocki, A.; Stasicka, Z. Mechanism of Photochemical Reduction of Chromium(VI) by Alcohols and Its Environmental Aspects. *J. Photochem. Photobiol. A, Chem.*, **2003**, *160*, 163-170.



- 14) Liu, Y.; Hu, X.; Wang, H.; Chen, A.; Liu, S.; Guo, Y.; He, Y.; Hu, X.; Li, J.; Liu, S.; Wang, Y.; Zhou, L. Photoreduction of Cr(VI) from Acidic Aqueous Solutions Using TiO<sub>2</sub>-Impregnated Glutaraldehyde-Crosslinked Alginate Beads and the Effects of Fe(III) Ions. *Chem. Eng. J.*, **2013**, *226*, 131-138.
- 15) Cieslak-Golonka, M.; Daszkiewicz, M. Coordination Geometry of Cr(VI) Species: Structural and Spectroscopic Characteristics. *Coord. Chem. Rev.* **2005**, *249*, 2391-2407.
- 16) Michel, G.; Cahay, R. Raman Spectroscopic Investigations on the Chromium(VI) Equilibria Part 2: Species Present, Influence of Ionic Strength and CrO<sub>4</sub><sup>2-</sup>-Cr<sub>2</sub>O<sub>7</sub><sup>2-</sup> Equilibrium Constant. *J. Raman Spectrosc.*, **1986**, *17*, 79-82.
- 17) Alam, M.; Montalvo, R.A. Titania-Assisted Photoreduction of Cr(VI) to Cr (III) in Aqueous Media: Kinetics and Mechanisms. *Metall. Mater. Trans. B*, **1998**, *29B*, 95-104.
- 18) Djouider, F.; Aljohani, M.S. Application of Ionizing Radiation to Environmental Protection: Removal of Toxic Cr(VI) Metal Ion in Industrial Wastewater: Preliminary Study. *J. Radioanal. Nucl. Chem.*, **2010**, *28*, 417-423.
- 19) (a) Korchev, A.S., Shulyak, T.S., Slaten, B.L., Gale, W.F., Mills, G. Sulfonated Poly(Ether Ether Ketone)/Poly(Vinyl Alcohol) Sensitizing System for Solution Photogeneration of Small Ag, Au, and Cu Crystallites. *J. Phys. Chem. B*. **2005**, *109*, 7773-7745. (b) Korchev, A.S., Konovalova, T., Cammarata, V., Kispert, L., Slaten, L., Mills, G. Radical-Induced Generation of Small Silver Particles in SPEEK/PVA Polymer Films and Solutions: UV-Vis, EPR, and FT-IR Studies. *Langmuir*. **2006**, *22*, 375-384. (c) Korchev, A. S.; Bozak, M. J.; Slaten, B. L.; Mills, G. Polymer-Initiated Photogeneration of Silver Nanoparticles in SPEEK/PVA Films: Direct Metal Photopatterning. *J. Am. Chem. Soc.* **2004**, *126*, 10-11.
- 20) Marczenko, Z. *Separation and Spectrophotometric Determination of Elements*; Ellis Horwood Limited: West Sussex, England, **1986**.
- 21) Heller, H. G.; Langan, J.R. *J. Chem. Soc., Perkin Trans.*, **1981**, *2*, 341-343.
- 22) Little, B.K.; Lockhart, P.; Slaten, B.L.; Mills, G. Photogeneration of H<sub>2</sub>O<sub>2</sub> in SPEEK/PVA Aqueous Polymer Solutions. *J. Phys. Chem. A*, **2013**, *117*, 4148-4157.
- 23) Weckhuysen, B.M.; Wachs, I.E.; Schoonheydt, R.A. Surface Chemistry and Spectroscopy of Chromium in Inorganic Oxides. *Chem. Rev.*, **1996**, *96*, 3327-3349.
- 24) Knoesel, R.; Weill, G. Room-Temperature Phosphorescence of Poly(p-vinylbenzophenone) in Solution. *Polym. Photochem.* **1986**, *7*, 119-127.
- 25) She, S.; Zhou, Y.; Zhang, L.; Wang, L.; Wang, L. Preparation of Fluorescent Polyvinyl Alcohol Keto-Derivatives Nanoparticles and Selective Determination of Chromium(VI). *Spectrochim. Acta, Part A*, **2005**, *62*, 711-715.

- 26) Allen, T.L. Microdetermination of Chromium with 1,5-Diphenylcarbazide. *Anal. Chem.*, **1958**, *30* (3), 447-450.
- 27) Gilbert, A.; Baggott, J. *Essentials of Molecular Photochemistry*; CRC Press: Boca Raton, **1991**; Chapter 7.
- 28) Sedláč, M. In *Physical Chemistry of Polyelectrolytes*; Radeva, T., Ed.; Marcel Dekker: New York, **2001**, 1-58.
- 29) Cong, R.; Temyanko, E.; Russo, P. S.; Edwin, N.; Uppo, R. M. Dynamics of Poly(Styrene sulfonate) Sodium Salt in Aqueous Solution. *Macromol.* **2006**, *39*, 731-739.
- 30) Ledger, M. B.; Porter, G. Primary Photochemical Processes in Aromatic Molecules. Part 15.—The Photochemistry of Aromatic Carbonyl Compounds in Aqueous Solution. *J. Chem. Soc., Faraday Trans. 1* **1972**, *68*, 539-553.
- 31) Westheimer, F.H.; Novick, A. The Kinetics of the Oxidation of Isopropyl Alcohol by Chromic Acid. *J. Chem. Phys.*, **1943**, *11*(11), 506-512.
- 32) (a) Klaning, U. 1:1 Complexes of Acid Chromate Ion with Alcohols or Acetaldehyde. *Acta Chem. Scand.*, **1957**, *11* (8), 1313-1316. (b) Klaning, U. Chromic Acid Esters, A Correction. *Acta Chem. Scand.*, **1958**, *12* (3), 576-577.
- 33) van Niekerk, W.; Pienaar, J. J.; Lachmann, G.; van Eldik, R.; Hamza, M. A Kinetic and Mechanistic Study of the Chromium (VI) Reduction by Hydrogen Peroxide in Acidic Aqueous Solutions. *Water SA* **2007**, *33*, 619-626.
- 34) Niki, K.; Tanaka, A.; Yamada, A.; Itabashi, E.; Hartford, W. H. In *Encyclopedia of Electrochemistry of the Elements*; Bard, A. J., Ed.; Marcel Dekker: New York, **1986**; Vol. IX, part B, pp. 255-427.
- 35) Manivannan, G.; Changkakoti, R.; Lessard, R. A.; Mailhot, G.; Bolte, M. Primary Photoprocesses of Cr(VI) in Real-Time Holographic Recording Material: Dichromated Poly(vinyl alcohol). *J. Phys. Chem.* **1993**, *97*, 7228-7233.
- 36) (a) Barichard, A.; Israëli, Y.; Rivaton, A. Photocrosslinking in Dichromated Poly(acrylic acid) During Hologram Recording and Comparison with Dichromated Poly(vinyl alcohol). *J. Polym. Sci A*, **2008**, *46*, 636-642. (b) Djuoani, F.; Israëli, Y.; Frezet, L.; Rivaton, A.; Lessard, R. A.; Bolte, M. New Combined Polymer/Chromium Approach for Investigating the Phototransformations Involved in Hologram Formation in Dichromated Poly(vinyl alcohol). *J. Polym. Sci A*, **2006**, *44*, 1317-1325. (c) Bolte, M.; Israëli, Y.; Djuoani, F.; Rivaton, A.; Frezet, L.; Lessard, R. A. Hologram formation reconsidered in dichromated polyvinylalcohol: polymer cross-linking around chromium (V). In *Practical Holography XIX: Materials and Applications*. 2005, SPIE Vol. 5742, 195-204. (d) Pizzocaro, C.; Lafond, C.; Bolte, M. Dichromated

polyvinylalcohol: key role of chromium (V) in the properties of the photosensitive material. *J. Photochem. Photobiol. A*, **2002**, *151*, 221-228.

37) von Sonntag, C.; Bothe, E.; Ulanski, P.; Adhikary, A. Radical transfer reactions in polymers. *Radiat. Phys. Chem.* **1999**, *55*, 599-603.

38) Krumpoic, M.; Rocek, J. Three-Electron Oxidations. 12. Chromium(V) Formation in the Chromic Acid Oxidation of 2-Hydroxy-2-methylbutyric Acid. *J. Amer. Chem. Soc.*, **1977**, *99*, 137-143.

39) Scott, S.L.; Bakac, A.; Espenson, J.H. Oxidation of Alcohols, Aldehydes, and Carboxylates by the Aquachromium(IV) Ion. *J. Am. Chem. Soc.*, **1992**, *114*, 4205-4213.

## **IV. Kinetic Investigation on Photochemical Reduction of Cr(VI) Sensitized by SPEEK in the Presence of PVA**

### **4.1 Introduction**

The results presented in the previous chapter demonstrated that illumination with 350 nm photons of air-saturated solutions containing dissolved SPEEK and PVA polymers induced an efficient photoreduction of Cr(VI) species. Furthermore, reduction of Cr(VI) to Cr(III) species was also observed when aqueous solutions in contact with crosslinked SPEEK/PVA films were exposed to 350 nm light. Since SPEEK/PVA films swell in water, the Cr(VI) ions were able to diffuse into the water-swollen films and react with the highly reducing  $\alpha$ -hydroxy radicals of SPEEK that are generated when the polyketone is exposed to light in the presence of PVA.<sup>1</sup> The outcome of the photoreaction was complete reduction of both Cr(VI) ions, and also Cr(V) intermediates, to form species that resemble Cr(III) complexes. Most noteworthy was the very large quantum yield of Cr(VI) reduction that amounted to 0.47, which is 10 times the maximum value found at pH = 5.7 in air-saturated SPEEK/PVA solutions. These findings are remarkable since they suggest a possible utilization of SPEEK/PVA films as materials able to remove toxic Cr(VI) ions from contamination waters. Pollution of water by Cr(VI) ions is a worldwide problem and methods that can remove them from solutions are highly desirable.<sup>2</sup> Cr(VI) ions are contaminants that can be transported efficiently in aqueous solutions. In contrast, Cr(III) species are less toxic, and can be readily precipitated from aqueous solutions. Therefore, procedures for eliminating Cr(VI) toxicity usually involve reduction of this species to Cr(III).

Another unusual finding of the film experiment was that only 1/3 of the original amount of Cr(VI) was detected in solution presumably as a Cr(III) compound, indicating that most of the Cr species that resulted from the reduction process remained bonded to the polymer film.

Enough anionic sulfonic groups were present in the SPEEK chains of the film to bind all the formed Cr(III) ions under the assumption that three  $\text{SO}_3^-$  groups were needed per Cr(III) species. The fact that less than 100% of the Cr(III) was electrostatically bonded to the film suggests that coordination of these ions to the anionic groups of SPEEK may be a slow process. Nevertheless, the results are encouraging as they show that SPEEK/PVA films could function as light activated filters for the irreversible removal of Cr(VI) from solution. However, Cr(V) was the main product detected during the photoreduction of Cr(VI) in PVA films.<sup>3</sup> In addition, illumination of air-saturated  $\text{HCrO}_4^-$  solutions can result in an initial reduction to Cr(III) that is followed by re-oxidation to Cr(VI) induced by  $\text{O}_2$ .<sup>4</sup> Numerous studies on the thermal reductions of Cr(VI) in acid solution have indicated the transient formation of Cr(V) and Cr(IV) species.<sup>5-7</sup> Evidence has also been presented that these species are generated as intermediates during the solution photoreduction of Cr(VI) in the presence of alcohols and PVA.<sup>8-10</sup> Formation of long-living Cr(V) and Cr(IV) compounds is not desirable because they have been found to exhibit high toxicities similar to that of Cr(VI) species.<sup>11</sup>

The results shown in Chapter 3 indicated that SPEEK/PVA films exhibit promising properties as light-activated filters able to treat waste waters contaminated with Cr(VI) ions. However, an in-depth investigation of the reduction process was considered necessary to gather information about the mechanism for Cr(VI) photoreduction in SPEEK/PVA system and to determine the fate of possible Cr(V) and Cr(IV) intermediates. Earlier studies on the thermal reduction of Cr(VI) in acid solutions have shown that formation of Cr(III) can occur through several different mechanism.<sup>5</sup> A complex mechanism seemed also to be operative during the Cr(VI) photoreduction in acid 2-propanol.<sup>8,9</sup> Evidence that complex processes operated during the photoreduction of Cr(VI) in SPEEK/PVA solutions at  $\text{pH} = 5.7$  is presented in this chapter.

Experiments performed at different initial [Cr(VI)] and in degassed solutions resulted in enhanced quantum yields of Cr(VI) reduction. These results indicate that Cr(VI) species compete with O<sub>2</sub> for the α-hydroxy radicals of SPEEK. An estimate of the rate constant for the reaction of the SPEEK• with the Cr(VI) species was obtained from such a competition analysis of kinetic data obtained in the presence of oxygen. Electron paramagnetic resonance (EPR) spectroscopy was employed for the detection of Cr(V) and Cr(III). Finally, a mechanism was derived for the reduction of hexavalent chromium in air-saturated SPEEK/PVA solutions.

## 4.2 Experimental

Poly (vinyl alcohol), (PVA) 99+% hydrolyzed with an average molar mass of 8.9-9.8 x 10<sup>4</sup> g/mol and potassium phosphate monobasic were purchased from Sigma Aldrich. Potassium dichromate, potassium phosphate dibasic, and 1, 5-diphenylcarbazide was obtained from Fisher. Poly(ether ether ketone) (PEEK) was a gift from Evonik with an average molar mass of 4.5 x 10<sup>4</sup> g/mol. PEEK was received in sheets that were cut into strips, further grinded into a powder, and later dried in a vacuum oven at 100 °C for about 6 hours. Solutions of 30% w/v were prepared with the dried PEEK and H<sub>2</sub>SO<sub>4</sub>, and were stirred constantly at a temperature between 50-55 °C for several days. Collection of sulfonated PEEK used the same procedure as described before.<sup>1</sup> Solution preparations for SPEEK/PVA solutions were conducted as stated previously,<sup>1</sup> and the molarity for solutions containing PVA with no SPEEK was the same as that for solutions of SPEEK/PVA. Phosphate buffer solutions (5 mM) were prepared at the standard pH of 5.7 which was employed in all the photochemical experiments. Stock solutions of 2 x 10<sup>-3</sup> M and 0.125 M Cr(VI) were used to obtain the desired concentration of Cr(VI) via dilution. These concentrations

were determined by optical measurements performed on a Shimadzu UV-Vis 2501PC spectrophotometer by DPC method as described in Chapter 3.

Illuminations of air-saturated solutions were conducted under continuous stirring of solutions placed in a 3 mL optical beakers shown in Chapter 3. Gas-tight syringes from Hamilton were used to extract aliquots from the photolyzed solutions. Efforts to detect Cr(III) ions formed during illuminations of SPEEK/PVA solutions used a 10 cm optical cell shown in Figure 4-1.

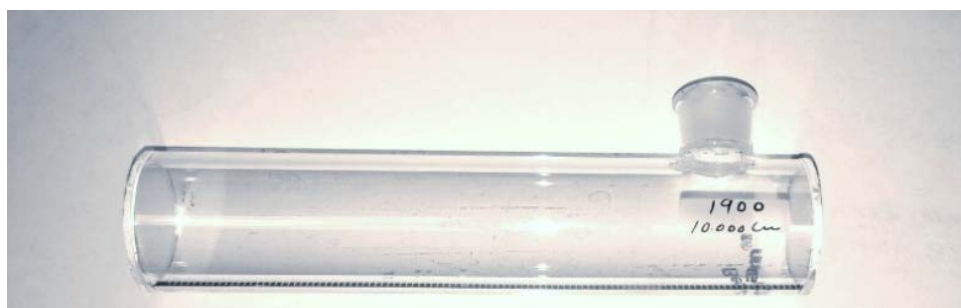


Figure 4-1. Image of the 10 cm quartz optical cell employed as illumination vessel during the detection of Cr(III) formed upon photolysis of SPEEK/PVA solutions.

Irradiations in the absence of air were conducted by means of a vessel that enabled degassing of the solutions, see Figure 4-2. The height of the main reservoir (6 mL) of the vessel was 13.4 cm with a wall thickness of 2.4 mm (O.D. = 1.5 cm). An Ace Thred #7 glass adapter with an electrode fitting cap was fused on top of the vessel. A glass side arm (1 cm wide), located on the top of the vessel was used to connect the reservoir to a Chem-Vac 0-4 high vacuum stopcock with a self-removing cap. The arm length measured from reservoir to the side opening was 11 cm. The freeze-pump-thaw procedure was employed to remove air from the polymeric solutions. This required slowly immersing the vessel into liquid nitrogen, then suctioning the air from the vessel, followed by closing the stopcock and thawing the solution to

room temperature. After thawing, the solution was back-filled with argon gas. This process was repeated three times. Aliquots of solution were withdrawn through the electrode-fitting cap by using gas syringes.



Image 4-2. Illumination vessel used for photolysis of air-free solutions. Degassing was accomplished via freeze-pump-thaw cycles.

Optical data were collected on Shimadzu UV-Vis 2501PC spectrophotometer and the illuminations were carried out inside a Rayonet 100 circular illuminator that generated photons with  $\lambda = 350 \pm 15$  nm by means of 16 RPR-3500A lamps; the light intensity ( $I_0$ ) was determined by using the Aberchrome 540 actinometer.<sup>12</sup> EPR analyses were conducted on Bruker EMX-6/1 X-Band EPR Spectrometer and were performed at 77 K. Typical instrumental conditions were as follows: center field, 3380 G; sweep width, 180 G; microwave power, 20dB; modulation frequency, 100 kHz; receiver gain,  $2 \times 10^4$ . Quantification of [Cr(VI)] employed in most cases



the DPC spectrophotometric method that results in an optical signal with  $\lambda_{\text{max}} = 545 \text{ nm}$  and  $\epsilon = 4.71 \times 10^4 \text{ M}^{-1} \text{ cm}^{-1}$ .<sup>13</sup> Both the DPC procedure and direct spectrophotometric detection of Cr(VI) signals exhibited a typical error of 8 %, but deviations of 30% were observed, which are typical of the concentrated SPEEK/PVA solutions.<sup>14</sup>

## 4.3 Results and Discussion

### 4.3.1 Reduction of Cr(VI) in Polymeric Solutions Free of Oxygen

As was shown in Figure 3.7a of Chapter 3, the reduction quantum yields, ( $\phi(-\text{Cr(VI)})$ ), in air-containing solutions of SPEEK/PVA increased at higher [Cr(VI)]. A reasonable explanation assumes that at low metal ion concentrations  $\text{O}_2$  was able to compete with Cr(VI) for SPEEK $\bullet$ , thereby decreasing the efficiency of the reduction process. The reason for such a decrease in efficiency is that reduction of oxygen by the polyketone radicals yields  $\bullet\text{O}_2^-$  and  $\text{HO}_2\bullet$ , which eventually form  $\text{H}_2\text{O}_2$ .<sup>14</sup> Most experiments were performed at  $\text{pH} > 5$ , which is the acidity region where  $\bullet\text{O}_2^-$  predominates given the  $\text{pK}_a$  value of 4.8 for  $\text{HO}_2\bullet$  radicals.<sup>15</sup> Radiation chemical experiments have shown that  $\text{HO}_2\bullet$  is able to reduce Cr(VI) whereas  $\bullet\text{O}_2^-$  is unable to serve as a reductant.<sup>16</sup> Thus, the lower yields of Cr(VI) reduction noticed in air-saturated solutions at low metal ion concentrations reflected significant scavenging of SPEEK $\bullet$  by  $\text{O}_2$ , leading to  $\bullet\text{O}_2^-$  radicals that do not participate in the reduction process. To test this hypothesis experiments were performed with air-free solutions; presented in Figure 4-3 are optical spectra recorded after mixing the DPC reagent with aliquots from photolyzed solutions containing Cr(VI), SPEEK, and PVA. As in the case of air-saturated solutions, the absorption centered at 545 nm decreased in intensity as the illumination progressed, indicating that Cr(VI) was photoreduced. Depicted in

the inset is a kinetic plot of [Cr(VI)] during the photoreaction. The results are analogous to those obtained in an air-containing solution containing a similar [Cr(VI)] shown in Figure 3-3.

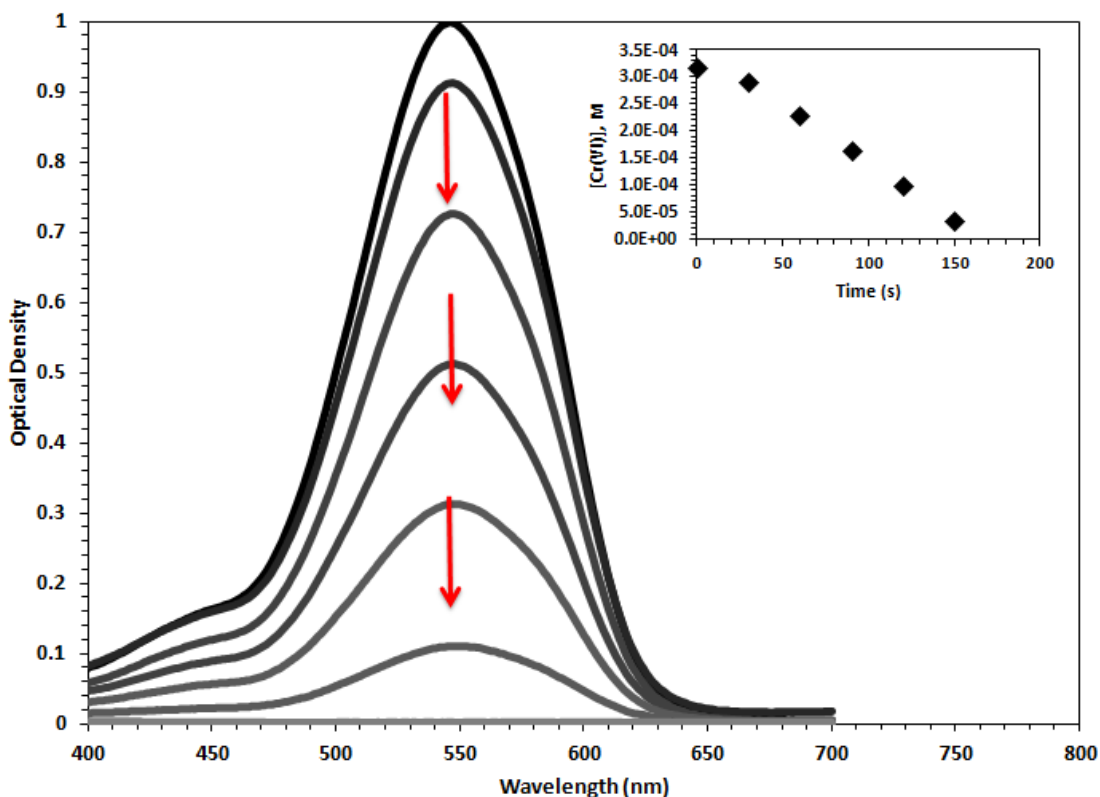


Figure 4-3. Optical spectra obtained after analysis with the 1,5-diphenylcarbazide (DPC) method on degassed, photolyzed solutions at pH = 5.7 containing 0.018 M SPEEK, 0.36 M PVA, and  $3.2 \times 10^{-4}$  M hexavalent chromium. Solution samples were diluted by a factor of 3 during the Cr(VI) assay. Top to bottom: samples irradiated with 350 nm light,  $I_0 = 3 \times 10^{-5}$  M(h $\nu$ )/s, for 0 min, 0.5, 1, 1.5, 2, 2.5 and 3 min. Inset: Plot of absorbance at 545 nm divided by  $\epsilon$  as a function of irradiation time ( $l = 0.2$  cm).

An important difference is that [Cr(VI)] decreased linearly with time throughout the illumination in the case of the air-saturated solution whereas in the absence of O<sub>2</sub> a linear decay of the metal ion concentration was noticed only after an initial period of practically no change. According to the data shown in the inset of Figure 4-3, the length of time with no significant change in [Cr(VI)] (denoted as the induction period) amounted to about 30 s. Another significant difference is that although the photoreaction followed a zero order rate law with respect to [Cr(VI)] in the

presence or absence of O<sub>2</sub>, a faster decrease in [Cr(VI)] was noticed when air was absent. This finding confirmed the notion that scavenging of SPEEK• by O<sub>2</sub> affected in a negative fashion the efficiency of the Cr(VI) photoreduction. The slope obtained from the linear decrease in metal ion concentration corresponded to the reduction rate, r(-Cr(VI)), which was employed to evaluate the quantum yield of reduction via the equation:  $\phi(-\text{Cr(VI)}) = r(-\text{Cr(VI)})/I_0$ .

Experiments conducted with air-free solutions containing several initial [Cr(VI)] yielded similar observations, relevant results are presented in Figure 4-4. An induction period was also

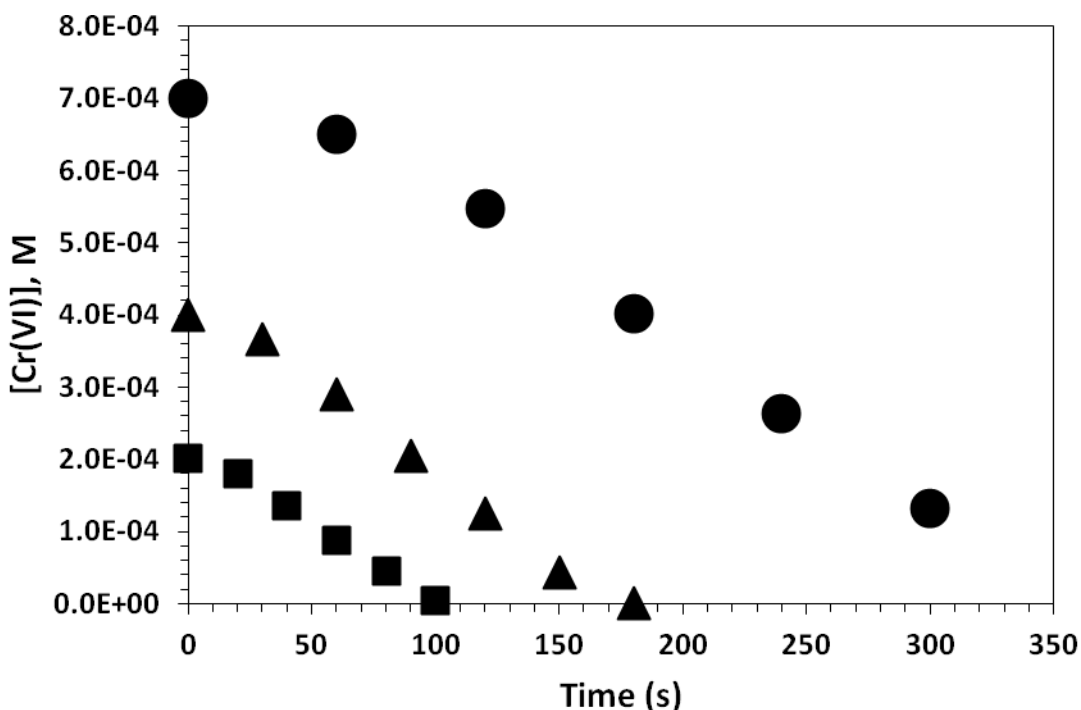
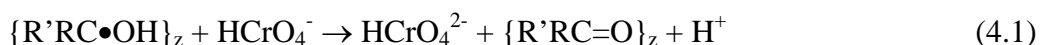


Figure 4-4. Photoreduction of Cr(VI) in degassed solutions buffered at pH = 5.7 with 5 mM of the phosphate buffer also containing 0.018 M SPEEK and 0.36 M PVA with [Cr(VI)]: 2 x 10<sup>-4</sup> M (■), 4 x 10<sup>-4</sup> M (▲), and 7 x 10<sup>-4</sup> M (●). Photolysis with 350 nm light, I<sub>0</sub> = 3 x 10<sup>-5</sup> M(hv)/s.

evident in each experiment followed by a linear decrease in [Cr(VI)]. Interestingly, similar slopes were obtained in all these experiments but longer induction periods resulted when the initial [Cr(VI)] increased. Occurrence of a period of small [Cr(VI)] change has been reported to

occur during the initial stage of the Cr(VI) reduction by oxalic acid.<sup>17</sup> Such phenomenon was attributed to the formation of a Cr(V) intermediate exhibiting optical properties very similar to those of Cr(VI). Consequently, any decrease in optical density due to the consumption of Cr(VI) was compensated by the absorption of the generated Cr(V). A similar transformation seems to result from the reaction of SPEEK• and Cr(VI),



where  $\{R'RC\bullet OH\}_z$  represents the SPEEK• radical and  $HCrO_4^{2-}$  corresponds to the generated Cr(V) species. The latter compound was detected as an intermediate in time resolved studies on the reduction of  $HCrO_4^-$  by  $\bullet CO_2^-$  radicals.<sup>18</sup> As was found in the earlier study,<sup>17</sup> both Cr(V) and Cr(VI) species exhibited fairly similar optical spectra.<sup>18</sup> An important issue is that the DPC spectrophotometric method yields the same optical spectrum when Cr(V) or Cr(VI) species are present in the solutions.<sup>13</sup> Therefore, the induction periods noticed in Figures 4-3 and 4-4 originated because most of the Cr(VI) initially reduced is transformed into a product ( $HCrO_4^{2-}$ ) that exhibit nearly the same optical properties upon reaction with DPC as those of the precursor. Such explanation requires the Cr(V) generated to be fairly stable at room temperature. Indeed, the disproportionation of Cr(V) required the presence of  $H^+$  ions to proceed efficiently and was not detected at  $pH > 5$ .<sup>18</sup> The fact that the induction periods lengthened with increased  $[Cr(VI)]$  seem to indicate that Cr(V) competed with Cr(VI) for the SPEEK• radicals.

Similar experiments were conducted in air-free solutions at pH 5.7 containing only PVA but no SPEEK and different initial  $[Cr(VI)]$ . As in the case of solutions with air presented in Chapter 3, the photoreduction of Cr(VI) initiated in the presence of PVA followed a first order

rate law. In most cases  $[\text{Cr(VI)}]$  decreased in a linear fashion with increasing illumination time during the first half-life of the reaction. Presented in Figure 4-5 are the corresponding linear

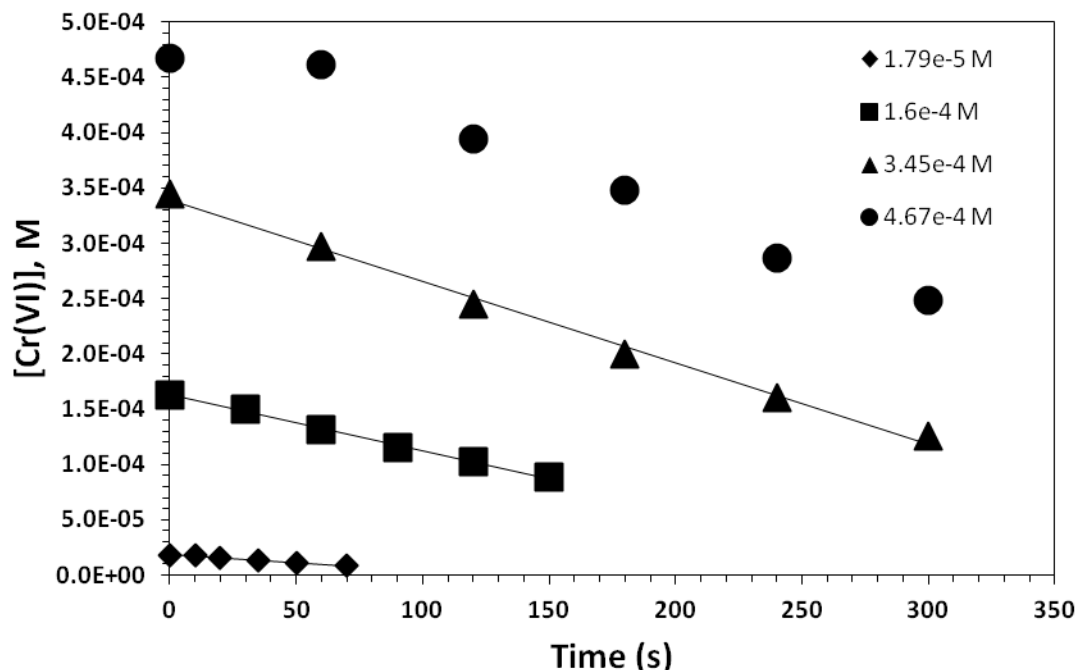


Figure 4-5. Initial rates of  $\text{HCrO}_4^-$  photoreduction in degassed 0.36 M PVA solutions free of SPEEK at various Cr(VI) initial concentrations. Illumination of solutions buffered at pH 5.7 with  $[\text{buffer}] = 5 \text{ mM}$  containing:  $\blacklozenge$   $[\text{Cr(VI)}] = 0.0179 \text{ mM}$ ;  $\blacksquare$   $[\text{Cr(VI)}] = 0.16 \text{ mM}$ ,  $\blacktriangle$   $[\text{Cr(VI)}] = 0.345 \text{ mM}$  and  $\bullet$   $[\text{Cr(VI)}] = 0.467 \text{ mM}$ , with 350 nm photons,  $I_0 = 3 \times 10^{-5} \text{ M(hv)/s}$ .  $[\text{Cr(VI)}]$  were determined using the DPC method.

plots; the slopes of the straight lines increased steadily with raising  $[\text{Cr(VI)}]$ . Initial rates of metal ion reduction were evaluated from the slopes, which served to calculate quantum yields for the photoreactions. Another interesting observation was that induction periods became evident only upon photolysis of solutions with  $[\text{Cr(VI)}] \geq 4.6 \times 10^{-4} \text{ M}$ . Also, the length of the induction periods increased with increasing metal ion concentration (data not included in the Figure).

Compared in Figure 4-6 are the quantum yields of Cr(VI) reduction in air-free solutions with and without SPEEK as a function of the metal ion concentration. An average  $\phi(-\text{Cr(VI)})$  of 0.06 was obtained in air-free SPEEK/PVA throughout the range of metal ion concentrations.

Hence, the Cr(VI) species were able to scavenge most of the available SPEEK• at all initial [metal ion] employed in the air-free experiments. Since the reduction of a Cr(VI) ion requires 3 reducing equivalents, the quantum yield of consumed polyketone radicals therefore equals 0.18.

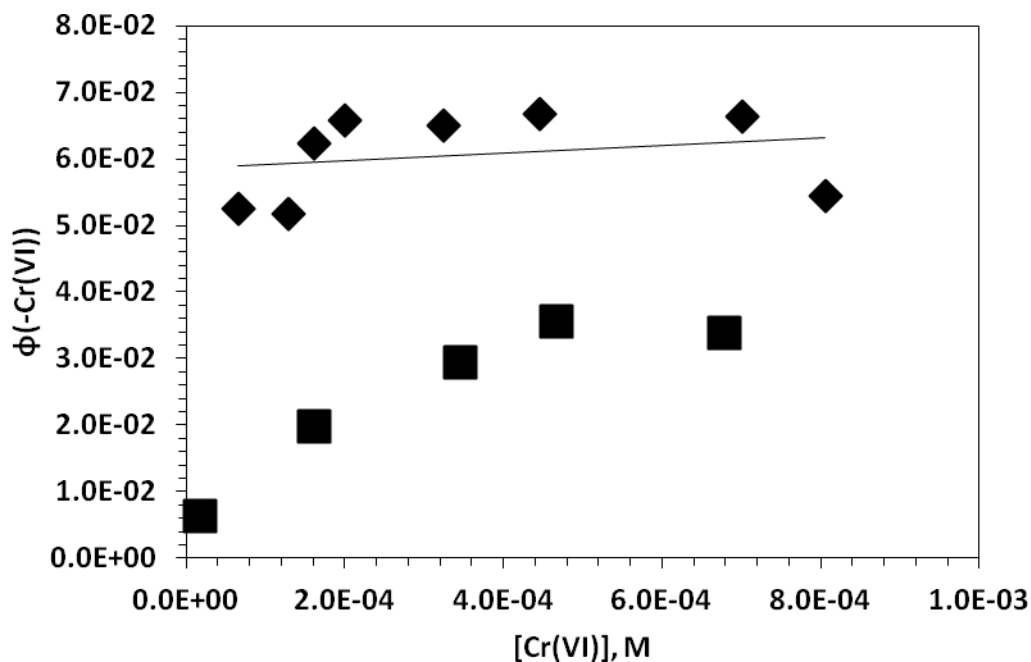


Figure 4-6. Comparison of quantum yields of Cr(VI) reduction in degassed solutions with 0.018 M SPEEK and 0.36 M PVA (◆), and solutions free of SPEEK with 0.36 M PVA (■) as a function of [Cr(VI)]. Irradiations conducted at pH = 5.7 with 350 nm light ( $I_0 = 3 \times 10^{-5}$  M(hv)/s); line is a guide to the eye.

This value is 2.5 times higher than the maximum yield (0.07) determined during reduction of  $\text{Ag}^+$  ions by SPEEK•.<sup>1b</sup> The average  $\phi(-\text{Cr(VI)})$  determined in the absence of  $\text{O}_2$  is about 30% higher than the maximum quantum yield obtained at pH 5.7 in solutions with air and  $[\text{Cr(VI)}] = 3.2 \times 10^{-4}$  M (see Chapter 3). Evidently, a significant fraction of the SPEEK radicals will not contribute to the reduction process in the presence of air at lower [Cr(VI)]. The results of Figure 4-6 also indicate that the photoreduction of Cr(VI) is significantly less efficient in the absence of SPEEK. Under these conditions,  $\phi(-\text{Cr(VI)})$  increased to a maximum of 0.036 at [Cr(VI)] of  $5 \times$

$10^{-4}$  M but this value is still 1.7 times lower than the average quantum yield determined in the presence of SPEEK. No further improvements in  $\phi(-\text{Cr(VI)})$  were noticed at higher concentrations of metal ion presumably because self-quenching of Cr(VI) becomes more probable.

#### 4.3.2 Effects of [Cr(VI)] on Reduction of Cr(VI) in Air-Saturated Polymeric Solutions

Illuminations of SPEEK/PVA solutions with varying initial concentrations of Cr(VI) were also conducted in the presence of air. Relevant zero-order kinetic plots for solutions with initial [Cr(VI)] of  $7.16 \times 10^{-5}$  M and  $2.84 \times 10^{-4}$  M are displayed in Figure 4-7a. Oxygen can compete with Cr(VI) for SPEEK• because the  $[\text{O}_2]$  in water amounts to  $2.6 \times 10^{-4}$  M.<sup>14</sup> As a result of the partial scavenging of the polyketone radicals by  $\text{O}_2$ , the reduction of Cr(VI) is relatively slow. Presented in Figure 4-7b are zero-order kinetic plots for results collected during illumination of air-saturated solutions of SPEEK/PVA containing  $1.2 \times 10^{-3}$  M and  $1.3 \times 10^{-3}$  M Cr(VI). Much faster reduction of Cr(VI) were achieved in these experiments given that the higher [Cr(VI)] enabled the metal ions to compete with  $\text{O}_2$  for the SPEEK radicals. An additional familiar feature of these plots is the appearance of an induction period lasting about 40 s in both cases. Equivalent experiments were performed with air-saturated solution containing only PVA and various initial metal ion concentrations. Linear plots of the initial kinetic data are shown in Figure 4-8. Slow reductions were observed in all these experiments and no induction period was evident in these experiments. Presented in Figure 4-9 is a comparison of the quantum yields of Cr(VI) reduction measured in air-saturated solution containing PVA with and without SPEEK. In both systems  $\phi(-\text{Cr(VI)})$  increased linearly with [Cr(VI)] up to a concentration of  $3.3 \times 10^{-4}$  M. The reduction quantum yield reached a maximum of 0.02 at  $5.7 \times 10^{-4}$  M Cr(VI) for

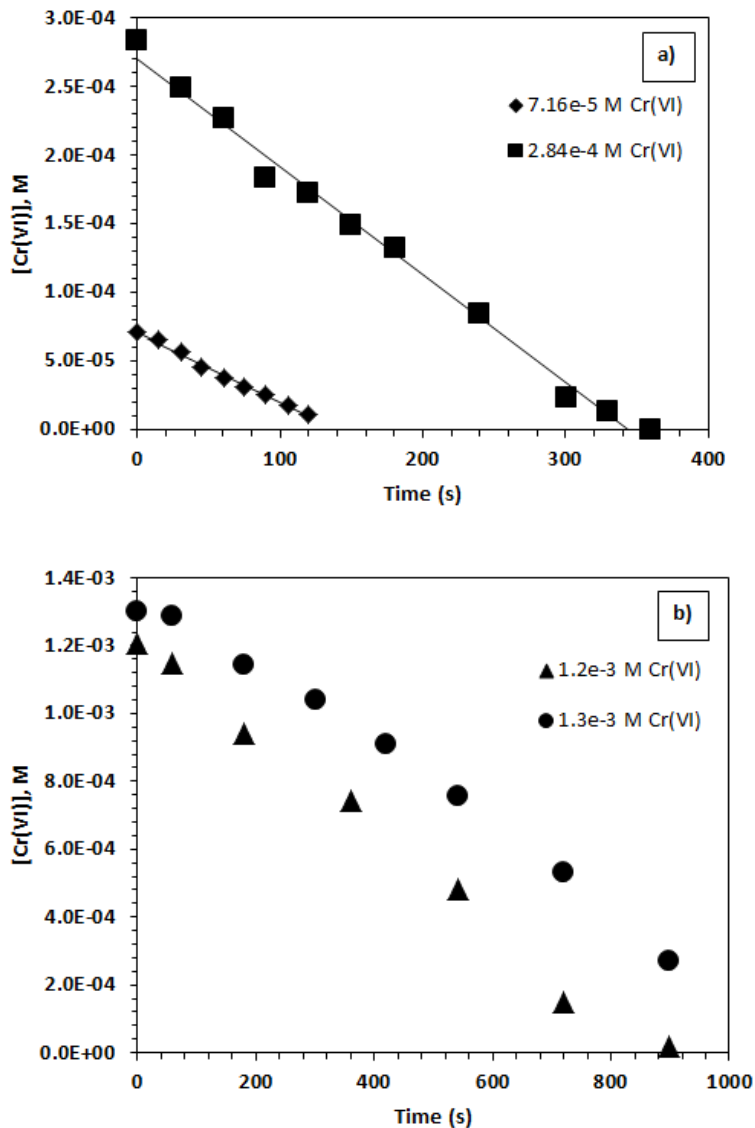


Figure 4-7. Photoreduction of  $\text{HCrO}_4^-$  in air-saturated, solutions of 0.018 M/0.36 M SPEEK/PVA buffered at  $\text{pH} = 5.7$  with 5 mM phosphate buffer. a)  $\blacksquare$   $[\text{Cr(VI)}] = 0.28 \text{ mM}$ ,  $\blacklozenge$   $[\text{Cr(VI)}] = 0.0716 \text{ mM}$ ; b)  $\bullet$   $[\text{Cr(VI)}] = 1.3 \text{ mM}$ ,  $\blacktriangle$   $[\text{Cr(VI)}] = 1.2 \text{ mM}$ . Samples irradiated with 350 nm photons with  $I_0 = 3 \times 10^{-5} \text{ M(hv)/s}$ ;  $[\text{Cr(VI)}]$  determined using the DPC method.

solutions without SPEEK but declined at higher  $[\text{Cr(VI)}]$ . Given that Cr(VI) is the chromophore in solutions without SPEEK, self-quenching of the excited metal ions is a possible explanation for the decline in  $\phi(-\text{Cr(VI)})$  at the higher Cr concentrations. On the other hand, the reduction quantum yield continued to increase at  $[\text{Cr(VI)}] > 3.3 \times 10^{-4} \text{ M}$  for solutions containing SPEEK.



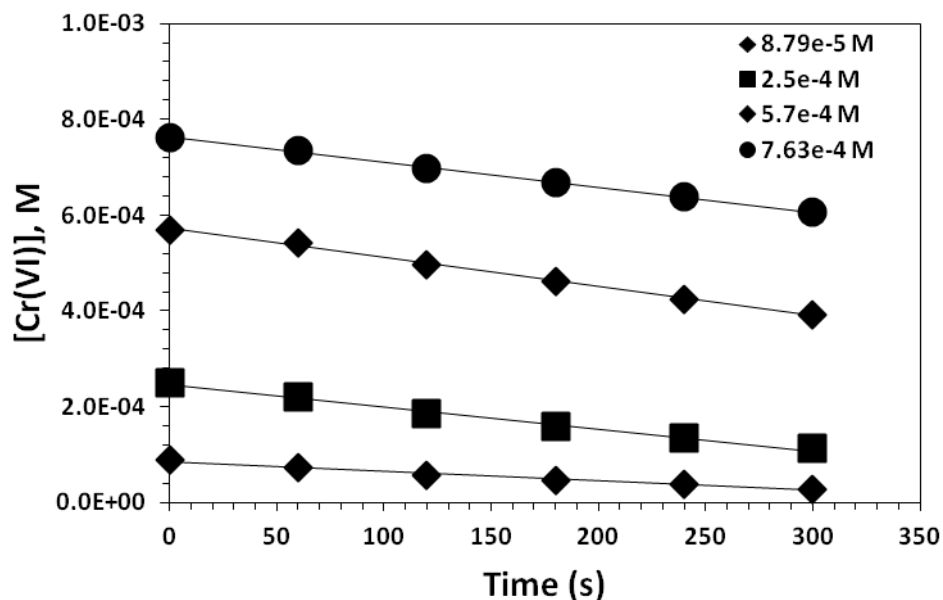


Figure 4-8. Determination of initial rates during the photoreduction of Cr(VI) in air-saturated solutions at pH = 5.7 with 0.36 M PVA with 5 mM buffer with 350 nm photons,  $I_0 = 3 \times 10^{-5}$  M(hv)/s. [Cr(VI)] were determined by direct analysis.

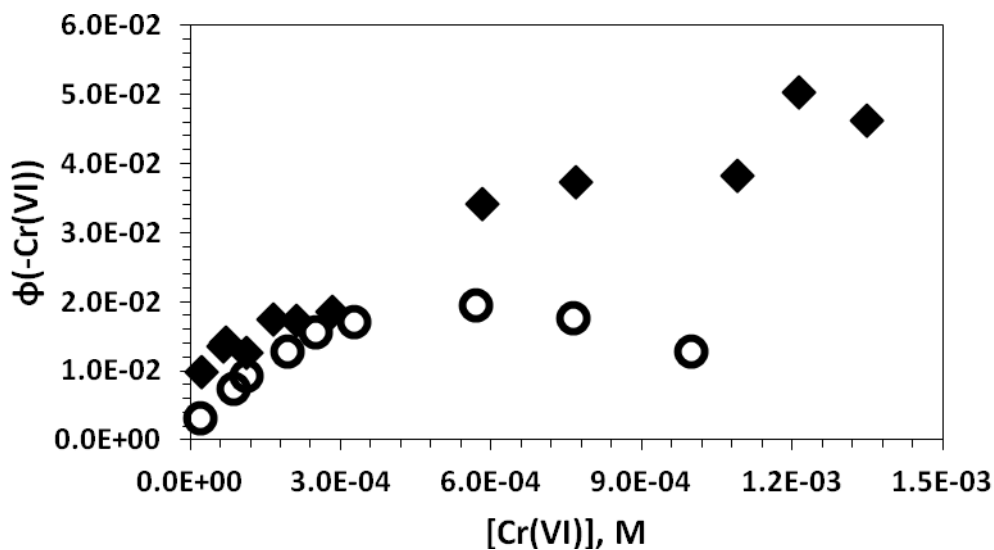
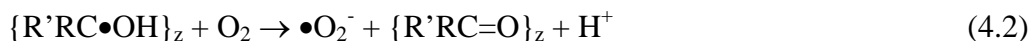


Figure 4-9. Comparison of quantum yield of Cr(VI) reduction in air-saturated solutions at pH = 5.7 of SPEEK/PVA (0.018 M/0.36 M) (♦) and solutions containing 0.36 M PVA but no SPEEK (○) as a function of [Cr(VI)]. Quantum yields for solutions without SPEEK were obtained from initial rates of reduction. Irradiations were conducted with 350 nm light,  $I_0 = 3 \times 10^{-5}$  M(hv)/s.

The linear increase of  $\phi(-\text{Cr(VI)})$  with increasing  $[\text{Cr(VI)}]$  exhibited by SPEEK/PVA solutions in Figure 4-9 is further support to the idea that Cr(VI) competed with oxygen for SPEEK•. Such competition involves reactions 4.1 and 4.2,



At pH = 5.7 the reduction of oxygen yields mainly  $\bullet\text{O}_2^-$  since  $\text{HO}_2\bullet$  radicals have  $\text{pK}_a = 4.8$ .<sup>15</sup>

Scavenging of SPEEK• by  $\text{O}_2$  decreases  $\phi(-\text{Cr(VI)})$  because  $\bullet\text{O}_2^-$  is unable to reduce Cr(VI).<sup>16</sup>

The fraction of radicals ( $f$ ) that react with chromate are given by:

$$f = (k_{4.1}[\text{Cr(VI)}][\text{SPEEK}\bullet]) / (k_{4.1}[\text{Cr(VI)}][\text{SPEEK}\bullet] + k_{4.2}[\text{O}_2][\text{SPEEK}\bullet]) \quad (4.3)$$

Division of this expression by the light intensity, the yield of Cr (VI) reduced is obtained

$$\phi(-\text{Cr(VI)}) = \phi(\text{SPEEK}\bullet) (k_{4.1}[\text{Cr(VI)}] / k_{4.1}[\text{Cr(VI)}] + k_{4.2}[\text{O}_2]) \quad (4.4)$$

Inversion of this equation yields:

$$1/\phi(-\text{Cr(VI)}) = 1/\phi(\text{SPEEK}\bullet) + \{k_{4.2}[\text{O}_2] / k_{4.1}\phi(\text{SPEEK}\bullet)\}(1/[\text{Cr(VI)}]) \quad (4.5)$$

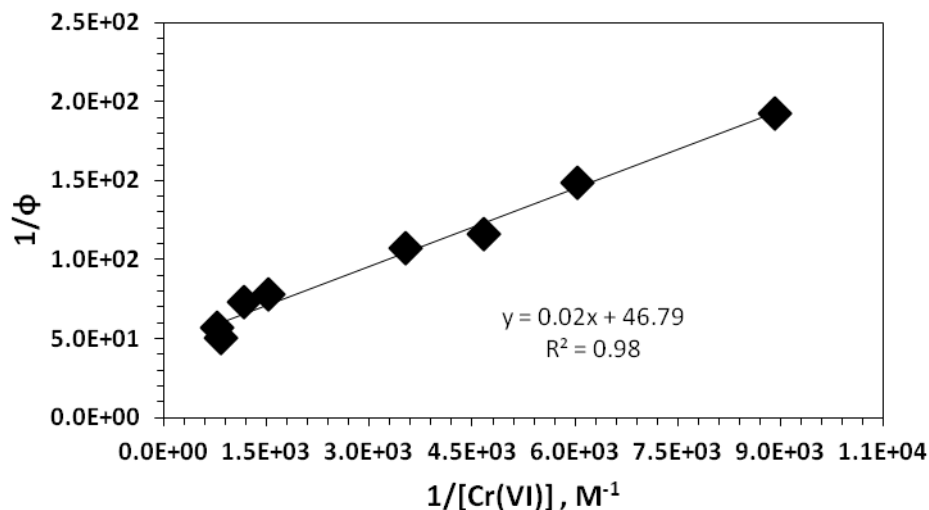


Figure 4-10. Double-reciprocal plot resulting from competition analysis of the yields of Cr (VI) reduction as a function of chromate concentration in air-saturated solutions buffered at pH = 5.7 with 0.018 M SPEEK and 0.36 M PVA. Illuminations were conducted with 350 nm light,  $I_0 = 3 \times 10^{-5} \text{ M(hv)/s}$ .

Figure 4-10 depicts a plot according to equation 4.5 of the results shown in Figure 4-9 for the SPEEK/PVA solutions. A reasonable straight line is obtained where  $1/\phi(\text{SPEEK}\bullet)$  corresponds to the y-intercept and the slope is equal to  $\{k_{4.2}[\text{O}_2]/k_{4.1}\phi(\text{SPEEK}\bullet)\}$ . The rate constant for the reduction of  $\text{O}_2$  by  $\text{SPEEK}\bullet$  is not known but this value is anticipated to be close to that of a typical  $\alpha$ -hydroxy radical such as  $(\text{CH}_3)_2\text{C}\bullet\text{OH}$ ,  $k_{4.2} = 4 \times 10^9 \text{ M}^{-1} \text{ s}^{-1}$ .<sup>19</sup> A value of  $\phi(\text{SPEEK}\bullet) = 0.02$  is calculated from the intercept, which is larger (but within experimental error) than the quantum yield of 0.014 obtained at  $\text{pH} = 6$  using steady-state measurements.<sup>14</sup> Using the slope together with  $\phi(\text{SPEEK}\bullet)$  and the selected  $k_{4.2}$  value yielded a rate constant for the reduction of  $\text{Cr}(\text{VI})$  by  $\text{SPEEK}\bullet$  equal to  $6 \times 10^8 \text{ M}^{-1} \text{ s}^{-1}$ . This value of  $k_{4.1}$  agrees well with rate constant for the reaction of  $\text{Cr}(\text{VI})$  with  $\bullet\text{CO}_2^-$ ,  $k = 1.2 \times 10^8 \text{ M}^{-1} \text{ s}^{-1}$ .<sup>18</sup>

A remaining issue pertains to the induction periods detected at high  $[\text{Cr}(\text{VI})]$  in solutions with and without air and also at lower  $\text{Cr}(\text{VI})$  concentrations in SPEEK/PVA solutions free of air. Inspection of the results shown in Figures 4-4 through 4-9 reveals that induction periods are always noticed in systems where the photoreduction of  $\text{Cr}(\text{VI})$  is fast, that is, under conditions that result in high quantum yields. In fact, the data shown in Figures 4-6 and 4-9 indicate that induction periods occurred in systems characterized by  $\phi(-\text{Cr}(\text{VI})) \geq 0.04$  irrespective of the presence/absence of SPEEK or air. Fast reduction of  $\text{Cr}(\text{VI})$  enables accumulation of  $\text{Cr}(\text{V})$ , resulting in only minor absorption changes due to the similar optical properties exhibited by both chromium species. Evidence that  $\text{Cr}(\text{V})$  species persist for long times was obtained in experiments where analysis of the photolyzed solutions were carried out immediately after light exposure and also after keeping them in the dark for different times. Irradiated samples aged in the dark for 1 or 2 hours exhibited lower optical signals (by about 20%) as compared with solutions analyzed right after illumination. A logical explanation for such observations is that

Cr(V) species formed from the photoreduction of Cr(VI) persisted for several hours at room temperature. In solutions containing low [Cr(VI)] part of the radicals reacted with the photogenerated Cr(V). However, in solutions with high [Cr(VI)] most of the radicals attacked Cr(VI) leading to an accumulation of Cr(V), resulting in an apparent induction period. The fact that induction periods were observed in the presence of air only at high [Cr(VI)] suggest that Cr(V) was somewhat susceptible to the attack of O<sub>2</sub>.

#### 4.3.3 Cr(V) EPR Study

Numerous studies have reported the detection of long lasting Cr(V) intermediates during the reduction of Cr(VI) by means of electron paramagnetic resonance (EPR).<sup>6,9-11,17</sup> Considering that Cr(V) species were suspected to play a role during the photoreduction of Cr(VI) in SPEEK/PVA systems, EPR analysis was performed on illuminated samples. For this purpose, degassed as well as air-saturated PVA solutions with and without SPEEK containing  $6 \times 10^{-4}$  M Cr(VI) were irradiated directly in EPR optical tubes for the length of time needed to achieve complete Cr(VI) reduction (as determined via the DPC spectrophotometric method). Exceptions were solutions without SPEEK, which were irradiated for shorter times. Presented in Figure 4-11a are ESR spectra recorded after photolysis of degassed PVA solutions in the presence and absence of SPEEK. An intense signal centered at 3395 G that is characteristic of Cr(V) was detected in the PVA sample illuminated in the absence of SPEEK. No such a Cr(V) signal was noticed in the sample irradiated in the presence of SPEEK. Instead a weak Cr(V) signal centered at 3350 G was noticed. Such difference is not surprising given that the sample with SPEEK was analyzed after all Cr(VI) was reduced, indicating that only small amounts of Cr(V) persisted at the end of the photoreaction.

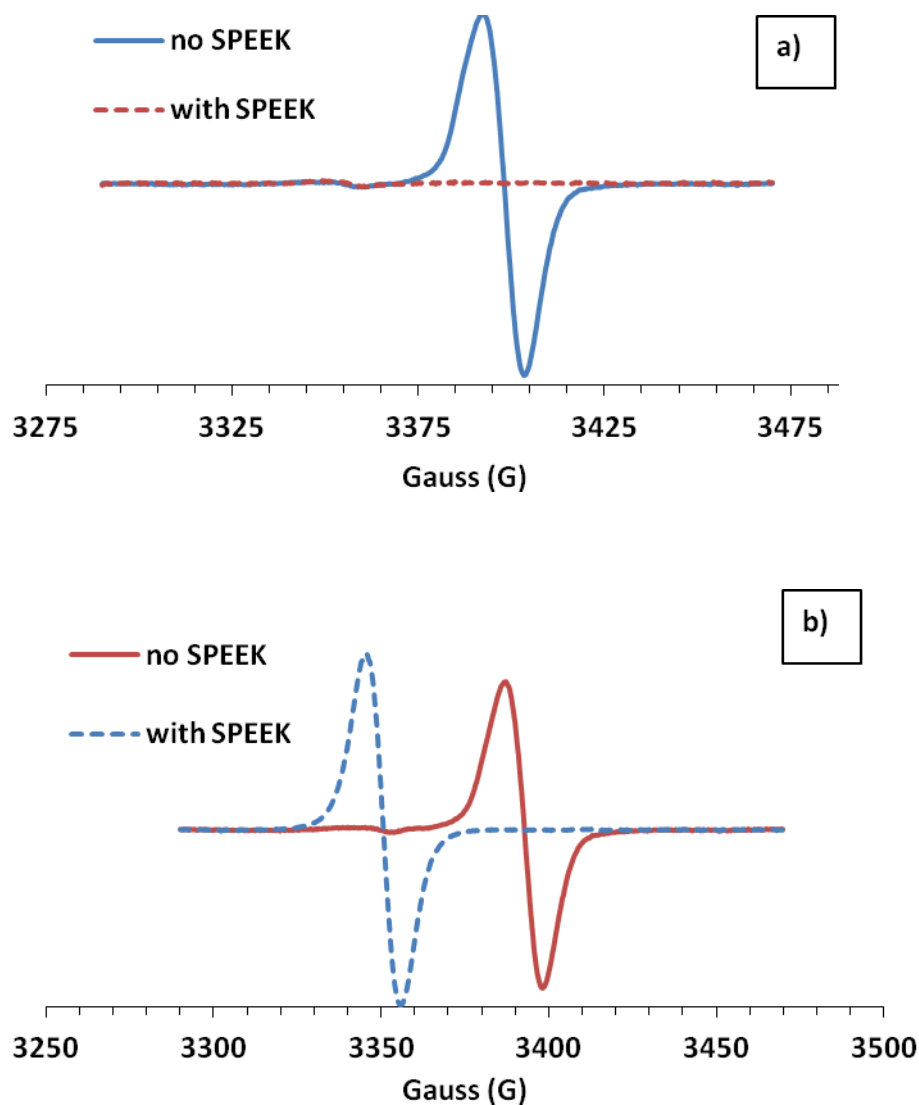


Figure 4-11. EPR spectra of Cr(V) signal in degassed polymeric solutions with and without SPEEK (a), and air-saturated solutions with and without SPEEK (b). In degassed solutions, samples were irradiated for 5 minutes; air-saturated solutions were exposed to light for 20 minutes.  $[\text{Cr(VI)}]_i = 6 \times 10^{-4} \text{ M}$ ,  $I_0 = 3 \times 10^{-5} \text{ M(hv)/s}$ .

Shown in Figure 4-11b are spectra recorded from air-saturated PVA solutions that were illuminated in the presence and absence of SPEEK. The Cr(V) signal centered at 3395 G was detected again in the solution photolyzed without SPEEK. An additional intense signal centered at 3350 G different signal was detected in the air-saturated containing SPEEK. The shift in signal

position suggests that a different Cr(V) species is formed in the presence of the polyketone. The EPR results confirmed that Cr(V) species were formed during the photoreduction of Cr(VI). In all experiments, the appearance of a broad and weak signal centered at 3350 G with a width of 3000 G was evidence for the presence of Cr(III).

#### **4.3.4 Formation of Cr(III) in SPEEK/PVA Solution**

Efforts to find evidence that Cr(III) formed during the reduction of Cr(VI) in air-saturated solutions of SPEEK/PVA utilized a 10 cm optical cell as photoreaction vessel, which also served a purpose in spectrophotometric analysis. This setup was used in attempts to detect Cr(III) directly by means of the extinction coefficient ( $144 \text{ M}^{-1}\text{cm}^{-1}$ ) at 600 nm for Cr(III) that was measured within 2% error of literature value.<sup>20</sup> Figure 4-12 shows the formation of the Cr(III) signal centered at 600 nm in SPEEK/PVA solutions containing air. Presented in the inset is the evolution of the optical signal of Cr(III) over time. The maximum signal is reached within 12 minutes of illumination, and remains constant. Formation of Cr(III) in SPEEK/PVA solution with  $3.2 \times 10^{-4} \text{ M}$  Cr(VI) reaches a maximum formation of  $7.7 \times 10^{-5} \text{ M}$ . This is only 24% of the initial concentration of Cr(VI). Less than 1/3 of Cr(VI) is reduced to the stable, non-toxic Cr(III). This implies that some intermediates are stabilizing in the polymeric solution.

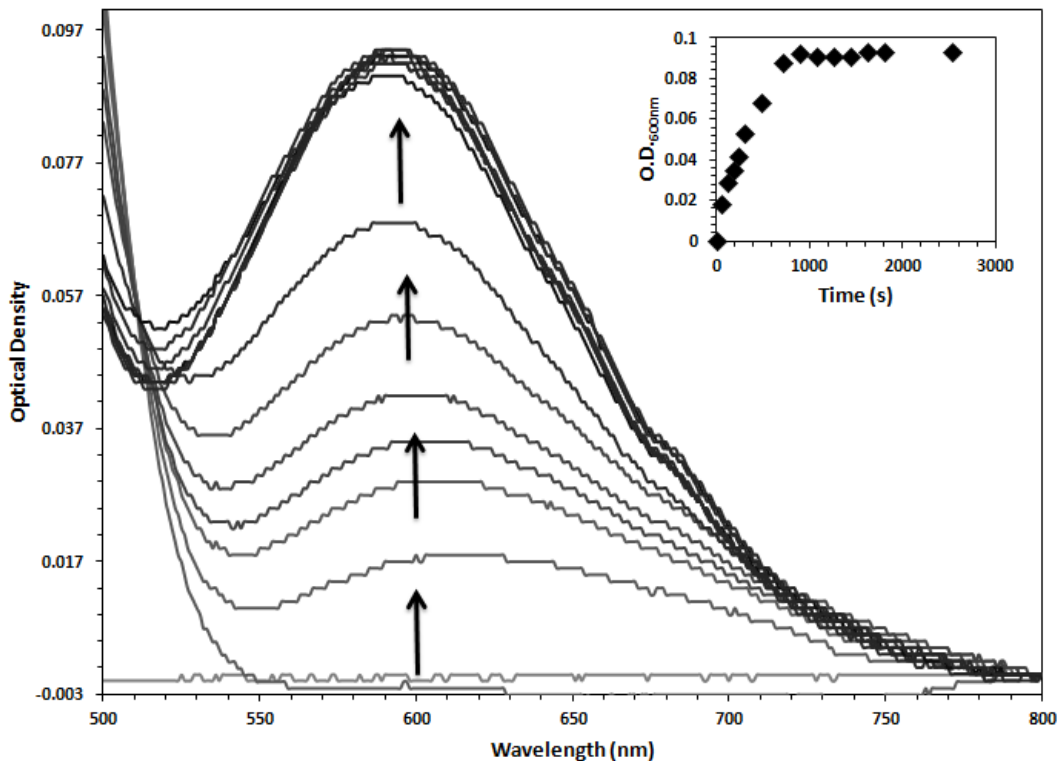
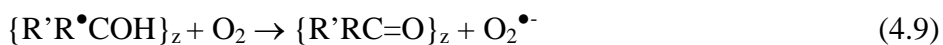
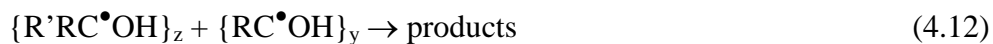
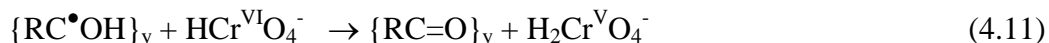
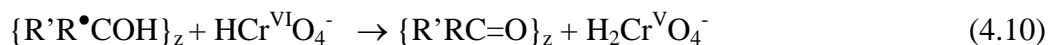


Figure 4-12. Optical measurements of the formation of Cr(III) in air-saturated solutions of 0.018 M SPEEK/0.36 M PVA with initial [Cr(VI)] of  $3.2 \times 10^{-4}$  M (pH = 5.7). Illumination times were 0, 1, 2, 3, 4, 5, 8, 12, 24, 27, 30, and 42 minutes ( $l=10$  cm,  $\epsilon = 144\text{M}^{-1}\text{cm}^{-1}$ ).  $I_0 = 3 \times 10^{-5}$   $\text{M}(h\nu)/\text{s}$ . Inset: Plot of evolution of signal at 600 nm.

#### 4.3.5 Mechanism for Chromium Reduction

Scheme 4-1 offers a possible mechanism of photoreduction of chromate in SPEEK/PVA solutions. Approximations will be made in order to derive a simplistic rate law for the reduction of Cr(VI).





**Scheme 4-1.** Mechanism of chromium photoreduction in air-saturated SPEEK/PVA solutions.

The photoexcitation of SPEEK is depicted in step 1, which is explained in more detail in Chapter 2. However, not shown is the emission and nonradiative decay of  $\{SPEEK\}_z^*$  to its ground state, or through intersystem crossing to form  $^3\{SPEEK\}_z^*$  shown in step 2. Fate of triplet-excited state of the polymer is quenched by either PVA or Cr(VI). A fast H-atom abstraction from PVA (step 3), modeled after  $^3BPK^*$  and 2-propanol with  $k = 2 \times 10^6 \text{ M}^{-1}\text{s}^{-1}$ , generates both SPEEK $\bullet$  and PVA $\bullet$  radicals. Reduction of oxygen by SPEEK $\bullet$  occurs in step 4. SPEEK $\bullet$  and PVA $\bullet$  radicals both reduce Cr(VI) in steps 5 and 6, respectfully. Step 7 illustrates radical termination by combination/disproportionation. Formation of Cr(III) eventually occurs via step 9.

In order to simplify the reduction mechanism, some assumptions have been made:

- 1) Reactions with superoxide radical were neglected, as well as, quenching by  $H^+$  and reduction of Cr(VI) via complexation with PVA.
- 2) Cr(VI) reduction occurs only by one-electron transfer.
- 3) Effective concentrations of reactive polymer groups are equal to molar concentrations of polymer units.
- 4) For simplification, the termination of radicals will be omitted.



According to Scheme 3-1, the steady-state concentrations of {SPEEK}\*<sub>1</sub>, {3SPEEK}\*<sub>1</sub>, SPEEK•<sub>1</sub>, and PVA•<sub>1</sub> are given by the following expressions:

$$[SPEEK^*] = \frac{\phi I_0 [SPEEK]}{k} \quad (4.14)$$

$$[{}^3SPEEK^*] = \frac{\phi I_0 [SPEEK]}{k_g [PVA]} \quad (4.15)$$

$$[PVA\bullet] = \frac{\phi I_0 [SPEEK]}{k_g [Cr(VI)] [PVA]} \quad (4.16)$$

$$[SPEEK\bullet] = \frac{\phi I_0 [SPEEK]}{k_7 [Cr(VI)]} \quad (4.17)$$

The photoreduction of Cr(VI) in solutions of SPEEK/PVA are determined by steps 7 and 8:

$$\frac{-d[Cr(VI)]}{dt} = k_5 [Cr(VI)] [PVA\bullet] + k_6 [Cr(VI)] [SPEEK\bullet] \quad (4.18)$$

$$= \left\{ \frac{2k_5 [Cr(VI)] + k_6 [O_2]}{k_4 [O_2] + k_g [Cr(VI)]} \right\} \times (\phi I_0 [SPEEK]) \quad (4.19)$$

The reduction of Cr(VI) is zero order in respect to [Cr(VI)].

#### 4.4 Conclusion

Further analysis of the reduction of Cr(VI) in air-saturated solutions of SPEEK/PVA were conducted by UV/Vis and EPR spectroscopy. Analysis of the optical signals indicated that an induction period was evident at the very early stages of the photoreduction. This induction period corresponded to a time length of apparent low change in [Cr(VI)], and was particularly evident in degassed solutions containing SPEEK, but only at high [Cr(VI)] in solutions without the polyketone. In air-saturated solutions, the induction period was only noticed at high [Cr(VI)] and not in solutions containing only PVA. Hence, the induction period existed in systems where Cr(VI) photoreduction occurred with the highest quantum yields. The induction period originates from the presence of a persistent Cr(V) species possessing optical properties analogous to those of the Cr(VI) precursor. Quantum yields were higher in degassed solutions which implied oxygen was inhibiting the reduction process of Cr(VI). However EPR studies showed that an usually unstable Cr(V) signal was present after complete reduction of Cr(VI) was reached which demonstrates the stability of the chromium intermediate in the presence of air. A different species of Cr(V) was present in SPEEK/PVA solutions than in PVA solutions. Formation of Cr(III) was less than the initial concentration of Cr(VI) which further prove the fact that chromium intermediates are stable and possibly bound to SPEEK. The simplified mechanism shows that the system is dependent on the constant formation of SPEEK radicals. Further analysis would need to be conducted on the formation of products generated to grasp a better insight on the mechanism concerning intermediates.

## References

- 1) (a) Korchev, A. S., Konovalova, T., Cammarata, V., Kispert, L., Slaten, B. L., Mills, G. Radical-Induced Generation of Small Silver Particles in SPEEK/PVA Polymer Films and Solutions: UV-Vis, EPR, and FT-IR Studies. *Langmuir*. **2006**, *22*, 375-384. (b) Korchev, A. S., Shulyak, T. S., Slaten, B. L., Gale, W. F., Mills, G. Sulfonated Poly(Ether Ether Ketone)/Poly(Vinyl Alcohol) Sensitizing System for Solution Photogeneration of Small Ag, Au, and Cu Crystallites. *J. Phys. Chem. B* **2005**, *109*, 7773-7745. (c) Korchev, A. S.; Bozak, M. J.; Slaten, B. L.; Mills, G. Polymer-Initiated Photogeneration of Silver Nanoparticles in SPEEK/PVA Films: Direct Metal Photopatterning. *J. Am. Chem. Soc.* **2004**, *126*, 10-11.
- 2) Barrera-Díaz, C. E.; Lugo-Lugo, V.; Bilyeu, B. A review of chemical, electrochemical and biological methods for aqueous Cr(VI) reduction. *J. Hazardous Mater.* **2012**, *223-224*, 1-12.
- 3) Pizzocaro, C.; Lafond, C.; Bolte, M. Dichromated polyvinylalcohol: key role of chromium (V) in the properties of the photosensitive material. *J. Photochem. Photobiol. A*, **2002**, *151*, 221-228.
- 4) Mytych, P.; Stasika, Z. Photochemical reduction of chromium(VI) by phenol and its halogen derivatives. *Appl. Catal. B* **2004**, *52*, 167-172.
- 5) Beattie, J. K.; Haight, Jr., G. P.; Chromium(VI) Oxidations of Inorganic Substrates. *Progress Inorg. Chem.: Inorganic Reaction Mechanisms*. Edwards, J. O., Ed.: New York, **1972**; Vol. 17, part II, pp. 93-145.
- 6) Wiberg, K. B.; Schäfer, H. Chromic Acid Oxidation of Isopropyl Alcohol. The Oxidation Steps. *J. Amer. Chem. Soc.* **1969**, *91*, 933-936.
- 7) Bakac, A. Mechanistic and Kinetic Aspects of Transition Metal Oxygen Chemistry. *Progress Inorg. Chem.* Karlin, K. H., Ed.: New York, **1995**; Vol. 43, pp. 267-351.
- 8) Mytych, P.; Karocki, A.; Stasicka, Z. Mechanism of photochemical reduction of Cr(VI) by alcohols and its environmental aspects. *J. Photochem Photobiol. A* **2003**, *160*, 163-170.
- 9) Klänning, U. K. Photoinduced Oxidation of Propan-2-ol by Acid Chromate. *J. Chem. Soc. Faraday Trans. 1* **1977**, *73*, 434-455.
- 10) Manivannan, G.; Changkakoti, R.; Lessard, R. A.; Mailhot, G.; Bolte, M. Primary Photoprocesses of Cr(VI) in Real-Time Holographic Recording Material: Dichromated Poly(vinyl alcohol). *J. Phys. Chem.* **1993**, *97*, 7228-7233.
- 11) Lay, P. A.; Levina, A. Action of Molecular Oxygen during the Reactions of Chromium(VI/V/IV) with Biological Reductants: Implications for Chromium-Induced Genotoxicities. *J. Am. Chem. Soc.* **1998**, *120*, 6704-6714.

- 12) Heller, H. G.; Langan, J. R. Photochromic Heterocyclic Fulgides. Part 3. The Use of (E)-a-(2,5-Dimethyl-3-furylethylidene) (isopropylidene)succinic Anhydride as a Simple Convenient Chemical Actinometer. *J. Chem. Soc., Perkin Trans. 2* **1981**, 341-343.
- 13) Allen, T.L. Microdetermination of Chromium with 1,5-Diphenylcarbazide. *Anal. Chem.*, **1958**, 30 (3), 447-450.
- 14) Little, B.K., Lockhart, P., Slaten, B.L., Mills, G. Photogeneration of H<sub>2</sub>O<sub>2</sub> in SPEEK/PVA Aqueous Polymer Solutions. *J. Phys. Chem. A* **2013**, 117, 4148–4157.
- 15) Bielski, B. H.; Cabelli, D. E.; Arudi, R. L.; Ross, A. B. Reactivity of HO<sub>2</sub>/O<sub>2</sub><sup>-</sup> Radicals in Aqueous Solution. *J. Phys. Chem. Ref. Data* **1985**, 14, 1041-1100.
- 16) Djouider, F.; Aljohani, M. S. Application of Ionizing Radiation to Environmental Protection: Removal of Toxic Cr(VI) Metal Ion in Industrial Wastewater: Preliminary Study. *J. Radioanal. Nuc. Chem.* **2010**, 285, 417-423.
- 17) Srinivasan, V.; Rocek, J. Formation of a Long-Lived Chromium(V) Intermediate in the Chromic Acid Oxidation of Oxalic Acid. *J. Amer. Chem. Soc.*, **1974**, 96, 127-133.
- 18) Buxton, G.V.; Djouider, F. Disproportionation of Cr(V) Generated by the Radiation-Induced Reduction of Cr(VI) in Aqueous Solution Containing Formate: A Pulse Radiolysis Study. *J. Chem. Soc., Faraday Trans.* **1996**, 92, 4173-4176.
- 19) Neta, P.; Grodkowski, J.; Ross, A. B. Rate Constants for Reactions of Aliphatic Carbon-Centered Radicals in Aqueous Solution. *J. Phys. Chem. Ref. Data* **1996**, 25, 709-1050.
- 20) Siefker, J.R.; Shah, R.D. Stability Constants and Molar Absorptivities for Complexes of Chromium(III) and Cobalt(II) with 2-Pyridylmethanamine. *Talanta*, **1979**, 26, 505-506.

## V. Conclusions

The results gathered in the present investigation demonstrate that  $\text{H}_2\text{O}_2$  is produced via illumination of SPEEK/PVA films swollen when in contact with aqueous solutions containing air. The kinetic data supports a mechanism in which a photochemical process that forms  $\alpha$ -hydroxy radicals of SPEEK dictates the rate of the peroxide formation. Photolysis of such systems results in quantum yields at least 5 times higher than previously found from analogous studies with solutions containing SPEEK and PVA. Additional corrections for the absorbed intensity of photons indicate that the quantum efficiencies are in the order of 0.2 in neutral solutions. Films containing SPEEK prepared from PEEK polymers made by Evonik are more efficient than films containing polyketone derived from a Victrex precursor, which was employed in the previous solution studies. Increases in the  $[\text{O}_2]$  induced by the presence of acetonitrile in the aqueous phase increases the efficiency of peroxide formation reaching quantum yields close to one. However, experiments with mixed solvents highlighted the role that film swelling by  $\text{H}_2\text{O}$  plays in the formation of peroxide since negligible peroxide photogeneration takes place for films free of liquid water. Therefore, preparation of SPEEK-based films useful as light-activated protective barriers will require the presence of a polymer component significantly more hygroscopic than PVA. In this way, swelling of the films could be accomplished via absorption of humidity from air.

Photoreduction of Cr(VI) in SPEEK/PVA films have demonstrated that the polymeric system has the potential to function as a means of treatment for contaminated water by collecting and/or reducing hexavalent chromium. Studies of the Cr(VI) reduction in polymeric solutions prove that the constant presence of SPEEK as a photoinitiator is more efficient with a zero order

reduction process. Because the system is light-sensitive, the rate determining step is the photochemical process that generates SPEEK radicals, which was proven to increase with increasing light intensity. The reduction yields dependence on pH is great, therefore a maximum quantum yield of Cr(VI) reduction was reached at pH 5.7. Though oxygen is a quencher of the reactive photoinitiator, reduction of Cr(VI) is still competitive and prevails.

Further analysis of the reduction of Cr(VI) in air-saturated solutions of SPEEK/PVA were conducted by UV/Vis and EPR spectroscopy. Analysis of the optical signals indicated that an induction period was evident at the very early stages of the photoreduction. This induction period corresponded to a time length of apparent low change in [Cr(VI)], and was particularly evident in degassed solutions containing SPEEK, but only at high [Cr(VI)] in solutions without the polyketone. In air-saturated solutions, the induction period was only noticed at high [Cr(VI)] and not in solutions containing only PVA. Hence, the induction period existed in systems where Cr(VI) photoreduction occurred with the highest quantum yields. The induction period originates from the presence of a persistent Cr(V) species possessing optical properties analogous to those of the Cr(VI) precursor. Quantum yields were higher in degassed solutions which implied oxygen was inhibiting the reduction process of Cr(VI). However EPR studies showed that an usually unstable Cr(V) signal was present after complete reduction of Cr(VI) was reached which demonstrates the stability of the chromium intermediate in the presence of air. A different species of Cr(V) was present in SPEEK/PVA solutions than in PVA solutions. Formation of Cr(III) was less than the initial concentration of Cr(VI) which further prove the fact that chromium intermediates are stable and possibly bound to SPEEK. The simplified mechanism shows that the system is dependent on the constant formation of SPEEK radicals. Further

analysis would need to be conducted on the formation of products generated to grasp a better insight on the mechanism concerning intermediates.